The use of inertial measurement units for the determination of gait spatio-temporal parameters

Patrick Esser

A thesis submitted in partial fulfilment of the requirements of Oxford Brookes University for the degree of Doctor of Philosophy

January 2011

Abstract

The aim of this work was to develop a methodology whereby inertial measurement units (IMUs) could be used to obtain accurate and objective gait parameters within typical developed adults (TDA) and Parkinson's disease (PD). The thesis comprised four studies, the first establishing the validity of the IMU method when measuring the vertical centre of mass (CoM) acceleration, velocity and position versus an optical motion capture system (OMCS) in TDA. The second study addressed the validity of the IMU and inverted pendulum model measurements within PD and also explored the inter-rater reliability of the measurement. In the third study the optimisation of the inverted pendulum model driven by IMU data was explored when comparing to standardised clinical tests within TDA and PD, and the fourth explored a novel phase plot analysis applied to CoM movement to explore gait in more detail.

The validity study showed no significant difference for vertical acceleration and position between IMU and OMCS measurements within TDA. Vertical velocity however did show a significant difference, but the error was still less than 2.5%. ICCs for all three parameters ranged from 0.782 to 0.952, indicating an adequate test-retest reliability.

Within PD there was no significant difference found for vertical CoM acceleration, velocity and position. ICCs for all three parameters ranged from 0.77 to 0.982. In addition, the reliability calculations found no difference for step time, stride length and walking speed for people with PD. Inter-rater reliability was found not to be different for the same parameters.

The optimisation of the correction factor when using the inverted pendulum model showed no significant difference between TDA and PD. Furthermore the correction factor was found not to be related to walking speed.

The fourth and final study found that phase plot analysis of variability could be performed on CoM vertical excursion. TDA and PD were shown to have, on average, different characteristics.

This thesis demonstrated that CoM motion can be objectively measured within a clinical setting in people with PD by utilizing IMUs. Furthermore, in depth gait variability analysis can be performed by utilizing a phase plot method.

Presentations, Publications and Patents relevant to thesis

The work contained in this thesis is that of the author. The following publications contain, in part, findings from the thesis or relevant findings discussed in the thesis that are the work of the author and collaborators.

Esser P, Collett J, Dawes H, Howells K. Inertial Sensing of Centre of Mass using Quaternions. *Journal of Sports Science (abstract)* 2008;26:71 - 72.

Esser P, Dawes H, Collett J, Howells K. IMU: Inertial Sensing of Vertical CoM Movement. *Journal of Biomechanics* 2009;42(2009):1578-81.

Elsworth C, Winward C, Sackley C, Meek C, Freebody J, **Esser P**, Soundy A, Barker K, Jones DH, Minns Lowe C, Paget S, Tims M, Parnell R, Patel S, Wade D, Dawes H. Supported community Exercise in people with Long-term Neurological Conditions (long-term neurological conditions): a phase II randomised controlled trial. *Clinical Rehabilitation* IN PRESS

Esser P, Dawes H, Collett J, Howells K, Maynard K. United Kingdom patent UK0823374.4 (*Applied for*)

Acknowledgements

Four years ago I was oblivious to what to do next in terms of my academic trajectory. I joined the Movement Science Group for my final working placement where I got the amazing opportunity to do an MPhil with transfer to PhD. Since than I've built measuring apparatus, applied it to humans, young and old, I've read into sensor technology, performed statistics and given presentations to a wide variety of people across Europe. Now, four years later, this thesis is the result. Of course this was not possible without the assistance and guidance of many peolple.

This work was carried out at the Human Performance Laboratory, Oxford Brookes University and at the Oxford Centre for Enablement, Nuffield Orthopaedic Centre NHS Trust. The work was funded by the Department of Health and a Wellcome Trust Technology Transfer grant.

First of all I want to thank all the participants for taking part in these studies during the past three years. Without your time, dedication and enthusiasm this work would not have been possible. I've met some fascinating people who made the scientific investigations both rewarding and enjoyable.

These research projects would not have been feasible without the support of the staff and patients at the OCE. I would like to thank the doctors, nurses, occupational and physiotherapists for their encouragement and support for this research. I would like to give a special mention to Derick Wade and Charlie Winward, whose clinical expertise were invaluable during the LIFE study which set me off onto this journey. Furthermore I can't forget the useful Friday morning Rivermead research meetings that took place at the OCE, which have been a constant source of advice, discussions and helpful clinical advice.

I'm grateful to all the people from the Movement Science Group at Oxford Brookes University. You guys and girls are not only colleagues but also friends. The cooperation amongst you all provides an invaluable source for technical assistance, innovative off the chart thinking, interesting debates and distractions. I will never forget the Friday chats and the interesting times we had outside working hours. I would especially like to thank Emad Al-Yahya, James Bateman, Thamar

Bovend'Eerdt, Andrea Dennis, Andy Meaney, Martyn Morris, Hannah Roper, and Elham Zareh for tolerating me during and making the workplace a second home.

I would also like to thank Kevin Maynard for his expertise within marketing which resulted in the patent application. You made me realize the other side of research which is commercially attractive for investors.

Furthermore I would like to say a big thank you to Hooshang Izadi whose expertise in statistical analysis has been an important aid to my work.

I would sincerely like to thank Ken Howells and Max Feltham for their invaluable input when writing up this work. Without their knowledge, experience and guidance this work would not have been published in its present form.

Most of all I would like to say a very big thank you to Helen Dawes and Johnny Collett who are both been extremely inspirational, enthusiastic and knowledgeable during this work. I feel that both have been exceptional supervisors and friends!

Ten slotte wil ik Marly en Andre Esser bedanken voor hun steun, luisterend oor en geduld tijdens mijn promotie traject. Het is altijd een heerlijk gevoel om even 'thuis' te komen. Bedankt pap en mam!

To all of you: thank you, bedankt, شكرا

Abbreviations

10MWT	Ten metre walking test
2D	Two dimensional
2minWT	Two minute walking test
3D	Three dimensional
a	Acceleration
ADC	Analog digital convertor
a_{gs}	Acceleration in global system
a_{os}	Acceleration in object system
au	Arbitrary unit
AWR	Angle random walk
a_z	Vertical acceleration
C	Capacitance
CGPM	Conférence générale des poids et mesures
cm	Centimetres
CNS	Central nervous system
CoM	Centre of mass
CoP	Centre of pressure
d	Step length
D_1	Excitatory dopamine receptors
D_2	Inhibitory dopamine receptors
DC	Direct current
DFT	Discreet Fourier transformation
DSP	Digital signal processing
ε	Error
EEG	Electroencephalogram
EMG	Electromyography
F	Force
F_c	Coriolis force
FFT	Fast Fourier transformation
FIR	Finite Impulse Response filter
f_{nyq}	Nyquist frequency
f_s	Sampling frequency
g	Gravitational constant

GI	Gait initiation
GP	Global pallidus
GPe	Global pallidus externa
GPi	Global pallidus interna
GRF	Ground reaction forces
h	vertical excursion
H&Y	Hoehn & Yahr scale
HCP	Hemiplegic cerebral palsy
Hz	Hertz
I	Moment of inertia
i,j,k	Complex numbers
ICC	Intra class correlation
ICF	International Classification of Functioning, Disability and Health
IIR	Infinite impulse response filter
IMU	Inertial measurement unit
k	Constant
K	Filter gain
kg	Kilogram
L	Leg length
m	Mass
M1	Primary motor cortex
MA	Motor activation
MDS	Movement disorder society
MI	Motor imaginary
MMSE	Mini mental state examination
MOA-B	Monoamine oxidase type B
MS	Multiple sclerosis
ms^{-1}	Metres per second
ms^{-2}	Acceleration
NICE	National Institute for Health and Clinical Excellence
O	Origin
OMCS	Optical motion capture systems
p	Position
PAR-Q	Physical activity readiness questionnaire
PD	Parkinson's disease

PDQ-39	Parkinson's disease Questionnaire 39
PMC	Pre-motor cortex
PN	Pontine nuclei
PRS	Physician rating scale
PSD	Power spectral density
Q	Charge
Q	Quaternion
$q0$	Quaternion scalar
$q1$	Quaternion scalar
$q2$	Quaternion scalar
$q3$	Quaternion scalar
r^2	Pearson's correlation
RMI	Rivermead mobility index
RMS	Root mean square
R_q	Quaternion rotation matrix
RRW	Rate random walk
RVGA	Rivermead visual gait assessment
s	Seconds
S1	Primary sensory cortex
SD_A	Standard deviation in / direction
SD_B	Standard deviation in \ direction
SI	Système International d'unités
SMA	Supplementary motor area
SN	Substantia nigra
SNr	Substantia nigra pars reticulata
SSW	Sit to stance to walk
SSWS	Self selected walking speed
STN	Subthalamic nucleus
STS	Sit to stance
t	Time
T	Torque
TDA	Typical developed adult
TUG	Timed up and go
U	Voltage
UK	United Kingdom

UPDRS	Unified Parkinson's disease rating scale
USA	United States of America
v	Velocity
VGAS	Visual gait assessment scale
WHO	World Health Organisation
$x_a(n)$	Analogue noise input
$x_d(n)$	Digitized noisy input
$y_d(n)$	Clean digital signal
β	Angle of phase plot plot
δt	Sampling interval
θ	Pitch
$\theta(t)$	White noise
θ_k	List of average data bins
σ^2	Allan deviation
σ^2_{Ω}	Allan variance
ϕ	Roll
ψ	Yaw
ω	Angular velocity
$\forall$	Ratio between SD_A and SD_B

Table of Contents

CHAPTER 1: INTRODUCTION **1**

1.1 GAIT **5**

1.1.1 GAIT CYCLE 6
1.1.2 MODELS OF GAIT 8

1.2 CENTRE OF MASS **12**

1.2.1 REFERENCE VALUE OF THE CENTRE OF MASS 13
1.2.2 LOCATION OF CENTRE OF MASS 13
1.2.3 MEASUREMENTS OF CENTRE OF MASS 15

1.3 GAIT SURVEY **16**

CHAPTER 2: MECHANICS **19**

2.1: INERTIAL MEASUREMENT UNITS **19**

2.1.1 ACCELEROMETERS 19
2.1.2 GYROSCOPES 21
2.1.3 MAGNETOMETERS 23
2.1.4 SENSOR FUSION 23

2.2: ORIENTATION OUTPUTS **24**

2.2.1 EULER ANGLES 24
2.2.2 QUATERNIONS 30

2.3: DIGITAL SIGNAL PROCESSING **33**

2.3.1 DIGITAL FILTERING 34
2.3.2 FREQUENCY ANALYSIS 36
2.3.3 ALLAN VARIANCE ANALYSIS 37
2.3.4 INTEGRATION AND DIFFERENTIATION 39

2.4: PRACTICAL APPLICATION **41**

2.4.1 TRANSPOSING ACCELERATION VECTORS FROM OBJECT TO GLOBAL SYSTEM 41
2.4.2 DOUBLE INTEGRATION PROCESS FROM ACCELERATION TO RELATIVE POSITION 42
2.4.3 FILTERING AND DE-DRIFTING 43

CHAPTER 3: IMU VALIDATION WITH OMCS **46**

3.1 RELEVANT PUBLICATIONS TO CHAPTER **46**

3.2 SUMMARY **46**

3.3 INTRODUCTION **46**

3.4 MATERIALS AND METHODS **47**

3.4.1 SUBJECTS AND EXPERIMENTAL DESIGN 47
3.4.2 DATA ANALYSES 48
3.4.3 STATISTICAL ANALYSES 49

3.5 RESULTS **50**

3.6 DISCUSSION **53**

CHAPTER 4: PARKINSON'S DISEASE **56**

4.1 SUMMARY **56**

4.2 PARKINSON'S DISEASE **56**

4.2.1 PATHOPHYSIOLOGY OF PARKINSON'S DISEASES 58
4.2.2 MOTOR CHARACTERISTICS OF PARKINSON'S DISEASE 59
4.2.3 NON-MOTOR CHARACTERISTICS OF PARKINSON'S DISEASE 61

4.2.4 Current diagnosis and treatment of Parkinson's Disease 61
4.2.5 Outcome measures in Parkinson's disease research 64
4.2.6 Gait outcome measurements in Parkinson's Disease 67

CHAPTER 5: IMU GAIT VALIDATION & RELIABILITY WITHIN PD 70

5.1 SUMMARY 70

5.2 INTRODUCTION 70

5.3 MATERIALS AND METHOD 71

5.3.1 Participants 71
5.3.2 Protocol 71
5.3.3 Statistical Analysis 72

5.4 RESULTS 73

5.4.1 Validity 73
5.4.2 Reliability 74

5.5 DISCUSSION 76

CHAPTER 6: ASSESSMENT OF SPATIOTEMPORAL MODELLING 78

6.1 SUMMARY 78

6.2 INTRODUCTION 78

6.3 MATERIALS AND METHOD 79

6.3.1 Participants 79
6.3.2 Protocol 80
6.3.3 Statistical Analysis 80

6.4 RESULTS 80

6.5 DISCUSSION 82

CHAPTER 7: NON LINEAR ANALYSIS APPLIED TO GAIT 84

7.1 SUMMARY 84

7.2 INTRODUCTION 84

7.3 MATERIALS AND METHOD 85

7.3.1 Theoretical exploration 88
7.3.2 Practical application 90

7.4 RESULTS 91

7.5 DISCUSSION 85

CHAPTER 8: GENERAL CONCLUSION 88

8.1 SUMMARY 88

8.2 INERTIAL MEASUREMENT UNIT TRACKING OF COM MOVEMENT 88

8.3 GAIT MODEL VALIDATION OF HUMAN GAIT 90

8.4 VARIABILITY ANALYSIS 92

8.5 LIMITATIONS OF THE PROPOSED STUDIES 93

8.6 FINAL REMARKS 94

9 REFERENCES 95

10 APPENDICES 122

10.1 UK PARKINSON'S DISEASE SOCIETY BRAIN BANK CLINICAL DIAGNOSTIC 122

10.2 QUESTIONNAIRES 123

10.2.1 BARTHEL INDEX 123
10.2.2 PARKINSON'S DISEASE QUESTIONNAIRE 39 (PDQ39) 124
10.2.3 RIVERMEAD MOBILITY INDEX 127

10.3 SINGLE CASE STUDY: STEP LENGTH VALIDATION IN PD 128

10.4 FLOW DIAGRAM LABVIEW8.5 129

10.4.1 PROGRAM BACKGROUND 129
10.4.2 OUTPUT PARAMETERS 131

10.5 RELEVANT PUBLICATIONS 131

List of Figures

Figure 1 Important factors within human movement showing the 5
Figure 2 Walking gait cycle as defined in clinical terms 6
Figure 3 mechanics of an inverted pendulum with *h* being the excursion of the Centre of Mass (CoM), *L* being the leg length measured from the anterior superior illiac spine to the tip of the medial malleolus. When using this model forward displacement can be derived using the model proposed by Zijlstra et al[72] where *d* equals the forward distance by for each step. *g* represents the gravitational acceleration and A_z represents the vertical acceleration. 10
Figure 4 The two major theories of gait with displaying the minimalisation of vertical excursion of the Centre of Mass in the a) '*six determinants of gait theory*' and b) '*Inverted Pendulum model*' both trying to reduce the energy consumption during walking. 11
Figure 5 *Mechanical MEMS (http://www.memx.com/)* 19
Figure 6 *MEMS triaxial accelerometer (http://archives.sensorsmag.com/)* 21
Figure 7 *A general outline of the fusion integration process* 24
Figure 8 3D rotations starting with roll defined as angle Θ followed by pitch defined as angle Φ and ended by yaw defined as angle Ψ 25
Figure 9 Inside mechanics of a gyroscope used in the Apollo 11 flight in 1969 27
Figure 10 Simple block displaying the analogue to digital conversion (ADC) combined with a simplified digital signal processing (DSP) filtering block according to Tan[128]. 33
Figure 11 Magnitude response shapes for the most commonly used filters with a stop and pass of the low pass band set at 250Hz and 200Hz respectively. The upper pass band pass and stop frequencies are set at 400Hz and 450Hz. 35
Figure 12 Simple example of a sinewave sampled at 128Hz (*grey solid line*) with additional uniform white noise filtered by a 2nd order, Butterworth low-pass filter with a cut-off frequency of 13Hz (*red striped line*). 35
Figure 13 FFT spectrum generated from a sine wave (217Hz, sample rate 1000Hz) divided over 250 frequency bins which show the real and imaginary part with peak amplitude response on frequency bin 54 and 196 which relates to 217Hz. 37
Figure 14 A possible log-log plot of Allan Deviation analysis results[142] 39
Figure 15 two different types of integrations shown on generated data. The graph on the left showing the standard 'area under the curve' numerical integration and right showing the integration process according to the Simpson's rule of integration taking the residue in account. Using Simpson's rule of integration results in a more accurate integration and therefore cleaner integral of distance over time. 40

FIGURE 16 VISIBLE SINGULARITIES WHEN USING EULER ANGLES WHERE THE PITCH (RED LINE) REACHES 90 DEGREES, WHERE THE YAW (GREEN LINE) AND ROLL (BLUE LINE) LOOSE THEIR DATA ACCORDINGLY. 42
FIGURE 17 EXAMPLE OF STANDARD NUMERICAL INTEGRATION COMPARED TO THE SIMPSON'S RULE OF INTEGRATION. BLUE THIN LINE SHOWING THE NUMERICAL INTEGRATION AND THE RED THICK LINE SHOWING THE SIMPSON'S RULE OF INTEGRATION WITH THE GREEN LINE INDICATING THE ERROR OVER A SMALL MEASUREMENT PERIOD. 43
FIGURE 18 FLOW DIAGRAM OF DOUBLE INTEGRATION WITH PARTS OF THE DIGITAL SIGNAL PROCESSING 44
FIGURE 19 REPRESENTATIVE DATA COLLECTED FROM A SUBJECT 3 WHO INITIATED THEIR GAIT AT T_0 AND WALKED OUT OF THE PRE-CALIBRATED FRAME OF THE OPTICAL MOTION CAPTURE SYSTEM AT $T=4$. GRAPHS ARE SHOWING RELATIVE POSITION, SPEED AND TRANSLATORY VERTICAL ACCELERATION FROM SUBJECT 3. THE BLUE DOTTED LINE REPRESENTS THE IMU, AND THE SOLID RED LINE REPRESENTS THE OMCS. THE ACCELERATION, SPEED AND POSITION ARE DE-DRIFTED USING THE DC ESTIMATE ACQUIRED BY USING THE HANNING WINDOW. THE DOTTED LINE REPRESENTS THE *OVERALL* ERROR WHICH IS CALCULATED AS THE DATA AT THE DIFFERENCE BETWEEN OMCS AND IMU AT T_N 52
FIGURE 20 CORRELATION BOX PLOT REPRESENTING THE SPEED IN THE ORTHOGONAL X AXES COMPARED WITH THE BIAS BETWEEN THE PEAKS OF THE IMU AND OMCS 53
FIGURE 21 COMMON CONCEPT OF PARKINSON'S DISEASE COURSE AND THE NEW DISEASE COURSE SUGGESTED BY LE ET AL[184] AND BARLOW ET AL[188] WHICH SHOWS THAT THE DISEASE STARTS AT A VERY EARLY AGE, PERHAPS EVEN DURING PRE OR PERINATAL PERIODS. (SOURCE LE ET AL[184], ETIOPATHOGENESIS OF PARKINSON DISEASE: A NEW BEGINNING?) 57
FIGURE 22 FRAMEWORK SET BY THE WORLD-HEALTH-ORGANISATION FOR THE INTERNATIONAL CLASSIFICATION OF FUNCTION, DISABILITY AND HEALTH TO STRUCTURE OUTCOME MEASURES IN PHYSIOTHERAPY EVALUATIONS 65
FIGURE 23 DATA FROM A REPRESENTATIVE PARTICIPANT, WALKING DURING THEIR STEADY WALKING PHASE (I.E. MIDDLE 10 METRE WALK) AT 1.13MS^{-1}, SHOWING RELATIVE POSITION, SPEED AND TRANSLATORY VERTICAL ACCELERATION. THE BLUE DOTTED LINE REPRESENTS THE IMU, AND THE SOLID RED LINE REPRESENTS THE OMCS. THE ACCELERATION, SPEED AND POSITION ARE DE-DRIFTED USING THE DC ESTIMATE ACQUIRED WITH A HANNING WINDOW[162]. THE GREEN DOTTED LINE REPRESENTS THE OVERALL ERROR BETWEEN THE TWO SYSTEMS WHICH IS CALCULATED AS THE DIFFERENCE BETWEEN OMCS AND IMU AT ANY TIME. 75
FIGURE 24 RELATIONSHIP BETWEEN THE INDIVIDUAL CORRECTION FACTOR AND WALKING ABILITY MEASURED AS WALKING SPEED. SHOWING PARKINSON'S DISEASE WHERE THE HORIZONTAL DOTTED LINE REPRESENTS THE STANDARD CORRECTION FACTOR OF 1.25 SET BY ZIJLSTRA ET AL. 81
FIGURE 25 SYMMETRY PLOT WITH COM EXCURSION$_I$ ON THE X-AXIS, COM EXCURSTION$_{I-1}$ ON THE Y-AXIS, COM EXCURSION OF 5.9±0.3CM WITH PHASE SHIFT OF 180DEGREES BETWEEN LEFT AND RIGHT STEP .... **ERROR! BOOKMARK NOT DEFINED.**

FIGURE 26 SINE WAVE MIMICKING NO STEP-TO-STEP VARIABILITY WITH A CONSTANT PHASE SHIFT OF 180 DEGREES, INDICATING *B*=45° 86

FIGURE 27 SHOWING THE NON-LINEAR ANALYSIS AND VARIABLES SD_A AND SD_B INDICATING THE STANDARD DEVIATIONS OF THE DATA CLOUD WITH β INDICATING THE ANGLE OF THE LEAST SQUARE FIT[130] 87

FIGURE 28 NON-LINEAR PLOTS BASED ON EQUAL SINE WAVES (FREQUENCY 10.1HZ, AMPLITUDE 5CM) WHILE BEING OUT OF PHASE BY 180^0 (A), 225^0 (B) 270^0 (C), 315^0 (D), 360^0 (E), 45^0 (F), 90° (G) AND 135^0 (H). IT BECOMES CLEAR THAT THE SINE WAVE PRODUCED DATA CLOUDS ROTATE AROUND THEIR OWN AXES (ANTI-CLOCKWISE) WITH CHANGE IN PHASE SHIFT........ 88

FIGURE 29 NON-LINEAR PLOTS BASED ON TWO SINE WAVES (FREQUENCY 10.1HZ, AMPLITUDE 5 AND 7CM) WITH DIFFERENT WHILE BEING OUT OF PHASE BY 180^0 (A), 170^0 (B) 360^0 (C) AND 90^0 (D). 89

FIGURE 30 NON-LINEAR PLOTS BASED ON THREE SINE WAVES (CONSTANT AMPLITUDE OF 5CM AND PHASE SHIFT OF 180°) REPRESENTING A CHANGE IN STEP LENGTH (A) AND STEP FREQUENCY (B) 90

FIGURE 31 REPRESENTATIVE GRAPHS WHERE THE TOP THREE SHOW TYPICAL GRAPHS OF PARTICIPANTS WITH PARKINSON'S DISEASE AND THE LOWER THREE REPRESENT TYPICAL GRAPHS FOR TYPICAL DEVELOPED ADULTS........ 84

List of Tables

TABLE 1 SYMBOL AND NAMES OF EULER ANGLES[2] 24
TABLE 2 MEAN DATA COLLECTED FROM IMU AND OMCS OVER 3 WALKS FOR EACH SUBJECT INCLUDING THE STANDARD DEVIATION CALCULATED OVER THE THREE WALKS........................ 50
TABLE 3 STEP TIME CALCULATED AS THE DIFFERENCE IN TIME BETWEEN TROUGHS OF POSITION MEASURED BY THE IMU AND OMCS 51
TABLE 4 ERROR BETWEEN INERTIAL MEASUREMENT UNIT AND OPTICAL MOTION CAPTURE SYSTEM DISPLAYED AS THE MEAN VALUE OVER 3 WALKSF BETWEEN SUBJECTS. 51
TABLE 5 RESEARCH OUTCOME MEASURES FOUND DURING THE SHORT PD REVIEW WITH PERCENTAGES AS SHOWN TAKEN FROM THE TOTAL AMOUNT OF REVIEWED PAPERS............... 68
TABLE 6 INDIVIDUAL, AVERAGE AND STANDARD DEVIATIONS OF DESCRIPTIVE MEASUREMENTS TAKEN OF AGE, HEIGHT, WEIGHT, BARTHEL INDEX, RMI AND TWO MINUTE WALKING TEST (2MWT).... 73
TABLE 7 CONCURRENT VALIDITY MEASUREMENTS SHOWING STEP TIME, STRIDE LENGTH AND WALKING SPEED FOR THE IMU AND OMCS SYSTEMS AND THE DIFFERENCES BETWEEN THE TWO SYSTEMS FOR INDIVIDUAL PARTICIPANTS AND AS A GROUP IN PERCENT. 74
TABLE 8 DATA COLLECTED BY EXPERT USER AND CLINICIAN 74
TABLE 9 CHARACTERISTICS FOR THE TYPICAL DEVELOPED ADULTS AND PARKINSON'S DISEASE. THE LEVEL OF IMPAIRMENT IN PD AS MEASURED BY BARTHEL INDEX (BI) IS DISPLAYED WITH THE ADJUSTED INDIVIDUAL CORRECTION FACTOR (γ) AND SEX IS INDICATED AS THE NUMBER OF MALES (M) TAKING PART. 81
TABLE 10 DESCRIPTIVE MEASUREMENTS SHOWING MEAN FOR BARTHEL INDEX (BI) AND PARKINSON'S DISEASE QUESTIONNAIRE (PDQ) FOR TYPICAL DEVELOPED ADULTS (TDA) AND PEOPLE WITH PARKINSON'S DISEASE (PD) WHERE AN ASTERIX SHOWS A SIGNIFICANT DIFFERENCE BETWEEN GROUPS ($p<0.05$). SEX IS INDICATED AS THE NUMBER OF MALES (M) TAKING PART. ....**ERROR! BOOKMARK NOT DEFINED.**
TABLE 11 OUTCOMES FROM NON-LINEAR METHOD APPLIED TO GAIT IN TYPICAL DEVELOPED ADULTS (TDA) AND PARKINSON'S DISEASE (PD) SHOWING THE ANGLE (β) OF THE LEAST SQUARE FIT WITH SD_A AND SD_B DESCRIBING THE STANDARD DEVIATIONS OF THE NON-LINEAR PLOT WITH RATIO $\forall$. AN ASTERIX INDICATES A SIGNIFICANT DIFFERENCE BETWEEN BOTH GROUPS......... 91

Chapter 1: Introduction

This chapter is primarily an overview of current gait measurement techniques, body reference points, gait models and the current use of gait measurements in clinical environments. The aim of this chapter was to explore the need for the development of a novel methodology whereby inertial measurement units (IMUs) could be used to obtain accurate and objective gait parameters within typical developed adults (TDA) and Parkinson's disease (PD).

Movement analysis has a long history. Aristotle (384-322 BC) studied animal movements and wrote his observations in the book 'De Motu Animalium'[1]. 2000 years later, Leonardo da Vinci (1452-1519) looked into the anatomical map of the human being. He studied the mechanical movement of the joints and limbs. Galileo Galilei (1564-1643) developed theories for the equilibrium in the joints even before Newton (1642-1727) published the laws of motion. Other key figures, like Bernoulli (1700-1782) and Euler (1707-1783) can be seen as founders of both the mechanical and biomechanical understanding of the world known today[2-4]

Many different disciplines use motion analysis to capture movement and posture of the human body. Increasingly researchers endeavour to obtain better understanding of the relationship between the human motor control systems and gait dynamics. Within sport science, movement analysis is used to increase efficiency and therefore performance. Within clinical gait analysis, medical professionals apply an evolving knowledge base in the interpretation of the walking patterns of impaired individuals for the planning of treatment protocols, e.g. orthotic prescriptions and surgical intervention, and to determine the extent to which an individual's gait pattern has been affected by an already diagnosed disorder.

The first analyses were done by eye, but with the development of photography the eye could be replaced by storing movements as pictures. Photographs were stacked on top of each other in order to make an animation of a movement. Muybridge, inventor of the zoopraxiscope and photographer, developed a technique of synchronising multiple cameras to capture a wide variety of movements. By spinning the zoopraxiscope he could create the first 'movement animations' of his time[2]. Etienne-Jules Marey improved this technique several times in cooperation with

Muybridge. The system was used by Marey in 1883 who correlated ground reaction forces with movement[5].

With the vast amount of motion analysis in the modern era, there are two main categories; kinesiological and biomechanical measurements. Kinesiology in motion analysis is mainly associated with anatomical, mechanical and the physiological basis of human movement based on qualitative measures such as surveys and questionnaires[6,7]. Several attempts have been made to develop a gait assessment scale to quantify the quality of gait in disabled people[11-13]. These scales mainly look into angular change while walking. Dickens et al reported low validity and repeatability of the Physicians Rating Scale (PRS) assessing gait in children with hemiplegic cerebral palsy (HCP)[8]. They concluded that the Visual Gait Assessment Scale (VGAS) did not show reliability for assessing sagittal plane hip motion in children with HCP, however useful data could be obtained for sagittal plane motion of the knee, ankle and foot[8]. Lord et al[9] however, developed a VGAS called the Rivermead Visual Gait Assessment (RVGA) which was intended for use with patients with neurological disease who present with impaired walking. They found that it was a valid and reliable way of assessing gait in patients with stroke (both uni- and bi-lateral) and Multiple Sclerosis (MS). Wolfson et al[10] showed a correlation between a VGAS and the risk of falling in elderly. Scales in the previous mentioned research were shown to be reliable and accurate[10]. However, visual analysis is subjective and the recording sensitivity is reliant on an individual assessor's opinion of the abnormality and its severity.

Biomechanical motion analysis can be divided in two subgroups; kinetics and kinematics[6]. Kinetic measurements provide information about how the movement is produced or maintained[6]. These analyses are hard to perform visually as they are related to forces that cause the motion which cannot be seen whereas only the effects can be seen. For kinetic measurements force plates are commonly used to measure the Ground Reaction Forces (GRF), Centre of Pressure (CoP) and calculated Centre of Mass (CoM) displacement[11]. As force plates are also limited in measurement volume and are relatively expensive, moveable force plates are often used to provide a cheaper and more flexible solution in terms of infrastructure and placement. Studies have shown a high intra class correlation coefficient indicating validity comparing fixed with moveable force plates, so moveable force plates can be used in a large number of measurements in different conditions[12].

Kinematics is mainly concerned with motion characteristics without taking the forces into account that cause the movement[4]. Biomechanical studies which use the kinematic approach are often carried out by using optical motion camera systems (OMCS) to determine the position of an object in a 3 dimensional calibrated space[13-15]. Within these systems there are two main groups widely used; passive and active marker systems. Systems such as VICON (Oxford, UK) are passive systems using infrared reflecting markers attached to the object to obtain kinematic data[14]. On the other hand active systems, such as the CODA (Codamotion, UK) system use light emitting LED diodes which are applied to the object to obtain similar kinematic data. Measurements of an OMCS are seen as being the gold standard[16]. Measurements are restricted to a calibrated area and therefore not always applicable in human locomotion, since only a few strides can be collected[17]. Outdoor experiments are also problematic with some systems as most optical camera systems use infrared reflective light. Recently however, the first optical motion capture system that has the abilities to measure in bright sunlight has been revealed by MotionAnalysis, (California, United States). It has been suggested that treadmills are often used to provide a solution for volume studies. Studies have been done looking at energy costs while walking on a treadmill in healthy humans[18] and in impaired patients[19 20] can to differ compared to overground walking.
Recently accelerometers have been used in movement analyses[21-23]. Billing et al reported an unobtrusive on-athlete instrumentation to measure GRF using insole accelerometers[24]. Recent developments utilizing Newton's second and third law provide GRF calculated from CoM acceleration measurements[24]. Light et al[25] used accelerometers to measure the skeletal transients on heel strike. Whenever a sensing axis deviates from the horizontal plane, a piezoresistant accelerometer will measure gravity as well as dynamic acceleration. An accelerometer positioned over the lower part of the back may be tilted due to curvature of the back. Postural alignment of the walking subject and inaccuracy in positioning of the instrument must be corrected for static gravity in order to assess true dynamic acceleration in gait[23 26 27]. This causes problems for the analyses as only the acceleration aligned to the axis in the accelerometers can be measured[17 23].

Research combining accelerometers with separate sensors like gyroscopes attached to the object show better results regarding analyses of a moving object[2 28]. This is due to the fact that the vectors of the object system can be transposed onto the axis of the global system. Luinge[29] measured body segment orientation with gyroscopes and accelerometers. These measurements led to the development a sensor fusion between gyroscopes and accelerometers.

New techniques allow sensors to be smaller and more accurate. These sensors can be relatively cheap. A sensor fusion like this is also known as an Inertial Measurement Unit (IMU)[29-32]. IMUs are more often used in industrial purposes, mainly to measure vibrations in a wide spectrum of applications. Pfau et al[17 33] has used IMUs on analyses of horses. More recently these IMUs have also been used in human movement analyses. Kavanagh et al[34] have used IMUs to measure upper body accelerations during walking by attaching an IMU with elastic bands to the head. Yack et al[35] measured the dynamic stability of elderly in walking. However, to obtain good reliable measurements methodological issues such as sampling rate and filters choices are critical and need to be adressed[27].

As shown above, there are many different ways to assess gait. However a survey of physiotherapists, reported that in clinical practice only 23.1% of respondents had actually had a patient assessed in a gait laboratory. Five main reasons for not using a gait assessment tool were lack of time (41.8%), budget constraints (38.8%), lack of space (28.4%), and a lack of awareness of and availability of any tool (both 27%)[36].

Toro et al[36] reported the five most important desired uses for gait assessment tool to be intervention (42.1%), to assist in the diagnosis of a gait abnormality (36.9%), to monitor patient progress (31.5%), to take a baseline assessment (31.2%) and to assist with orthotic prescription (9.4%).

1.1 Gait

Human movement is a complex phenomenon with many contributing factors which help to determine the quality of life[6]. Human movement is therefore important to understand to get an insight into quality of life and wellbeing of a person. More specifically gait assessments can provide valuable information. Interaction with a local or greater community, developmental skills such as communications and relationships with friends or family can all be dependent on human movement[37]. On the other hand there are also environmental factors involved, such as community mobility and type of work which can influence movement patterns[37]. Both these factors are influenced by somebody's physiological health. For example when suffering from cognitive or emotional disorders this has a big effect on community mobility affecting children[38] as well as elderly[39]. Spirduso et al[40] have mapped the most common aspects and the influences on human movement as a vicious cycle as shown below in Figure 1.

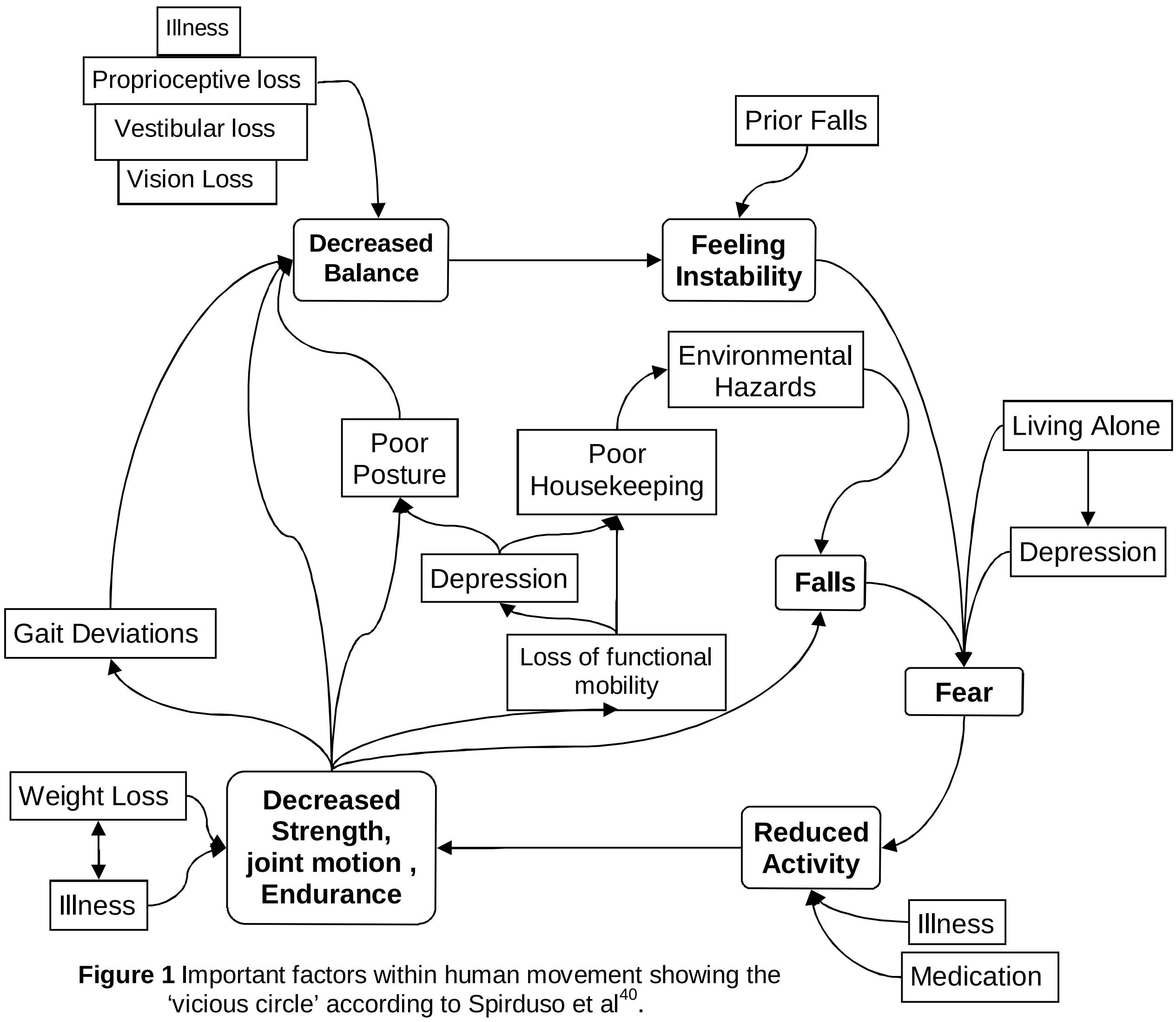

Figure 1 Important factors within human movement showing the 'vicious circle' according to Spirduso et al[40].

1.1.1 Gait cycle

Gait is a combination of various muscles, joints and bodily processes perfectly adjusted to each other working to propel the human body. Systems to arrange balance, power, control of movement and sensory systems need to react in an adequate manner to have a successful gait cycle. Leading robot laboratories in the world are trying to create a successful stand-alone robot that can imitate all these processes as smooth as human beings. The most and well known example is ASIMO made by Honda[41].

During the stance phase the energy is transferred from the swinging leg towards the stance leg which will prepare for toe-off. One gait cycle is defined by Perry[42] as '*the movements and events that occur between successive heel contacts of the same foot*'. The swing and stance phase are shown in Figure 2 normalised to their stride cycle as a percentage.

These phases can be divided in six main factors, being initial, heel and terminal contact as well as toe-off, foot-flat and heel-off[42].

Figure 2 Walking gait cycle as defined in clinical terms
Source: American Academy of Orthogonists & Prosthetics

Heel contact is the point in the gait cycle of initial contact where the heel touches the floor, also known as the loading phase[43]. During this period the force vector will be posterior of the knee and will move more towards the ankle when moving towards midstance[43]. This creates stability on the *'stance leg'*. Research by Woollacot[44 45] showed that in an eventual slip, the surface of the foot during heel strike increased the activity of the tibialis anterior and rectus femoris muscles indicating the continuous control of balance. Heel strike can also be seen as the starting point of the '*inverted pendulum model*' which will be explained in further detail in the next section.

During mid stance or foot flat the force vector moves anteriorly to the ankle and posterior to the knee and hip[43]. This phase occurs at around 12% into the gait cycle as displayed in Figure 2. Electromyography research by Matsusaka[46] revealed that during the mid stance the peroneus longus was more active during a greater force vector in mid stance and therefore concluded that mid stance plays a role in the control of medial-lateral balance in walking.

Finally during the terminal stance, also known as the toe off, the force vector will move posterior to the ankle. This cycle will repeat on the opposite leg until one gait cycle is completed. The time between the start to finish of one gait cycle is known as the stride time. When looking into one step (50% of a gait cycle) this known as the step time[42]. Besides the basic timing aspects the single phase can be determined as the point from where only one foot is in contact with the floor, which is equal to the swing phase of the opposite limb. It follows that the double stance phase is the remaining part of the step cycle. Measurements of these phases can be taken by means of foot switches[47 48], force sensors such as forceplates[49 50] or pressure soles[51] but also accelerometers[48], gyroscopes[52] and electromyography (EMG) measurements[53].

Aspects of a gait cycle can also be expressed in spatial and temporal factors. Spatial factors such as step length (distance between heel strikes on ipsilateral leg), stride length (summation of left and right step length) walking base (medio-lateral distance between left and right heel strike) and walking speed (metres per second) are the most used parameters[42]. The most used temporal aspects of gait are step time (time between heelstrikes on ipsilateral leg), cadence (measures as steps per minute), or step frequency (measured as steps per second)[42]. These parameters are often grouped together and labelled as spatio-temporal measurements of gait.

The ratio between step length and cadence, also known as the step factor and changes during development towards a *mature* gait. It has been shown by

Sutherland et al[54] in a study with 186 children ranging between the age of 1 and 7 years, that the step factor increases until the age of 4 after which the change in walking speed is more related to changes in limb length. These results are in agreement with Beck et al[55] who used a relative greater age range. Both studies also agreed that after the age of 5, changes in walking speed were more related to height than the step factor[54 55]. In elderly people it has been suggested that there is a decrease in step length[56]. Reductions up to 10% in step length after correction for leg length in healthy elderly compared to healthy younger people have been reported[56]. Maximum step length difference between young and older females of 40% have been reported by Schulz and colleagues[57]. This can be explained by different muscle strategies during gait as well as joint weaknesses in elderly participants as showed by Monaco et al[58 59]. Research by Beauchet et al[60] concluded that the reduction of stride length and increase in stance time were related to decreased walking speed.

Gait is a complex cycle with many variables. In order to understand gait better, models have been used to simplify gait. The main models and their use are explained in the next paragraph.

1.1.2 Models of gait

Gait is a cyclical movement which can be described with many models. The original '*six determinants of gait*' theory is often contradicted by simplified models such as *'inverted pendulum'* to '*multi-muscle*' models[61]. This section will discuss the commonly used theories and models to describe gait from a multilevel perspective.

The *'six determinants of gait'* were introduced in a classical paper by Saunders and Inman[61] in 1953. This theory rests on the effectiveness of an object moving in space in relation to Newton's first law of motion. This states that the least expenditure of energy can be mechanically achieved by a uniform motion in a straight line. In order to make motion of the CoM as uniform as possible over a straight line there are certain contributing determinants, the first determinant being *1)pelvic rotation*. When simplifying the lower limbs as being rigid pendulums in order to eliminate knee flexion it becomes visible that the centre of mass (CoM) is rising and falling in a sinusoidal manner. When there is no hip rotation the CoM excursion will be increased and will therefore subsequently increase energy consumption since there is an increase in muscular activation needed to raise the CoM[62]. With the introduction of pelvic rotation the CoM excursion can be reduced which will also reduce energy consumption. A study by Della Croce and colleagues[63] has shown that walking with pelvic rotation reduces energy consumption by 10%. Besides pelvic rotation, *2)pelvic tilt* plays a role in optimizing gait[61]. By tilting the pelvis the CoM pathway can be lowered and therefore optimized in terms of energy cost. However it has been shown that the range of motion of pelvic tilt does not affect gait efficiency, as proven by Joseph et al[64]. Another way to reduce CoM excursion is by *3)knee flexion during stance phase*. During normal gait the leg is extended at heel strike after which it flexes around 15 degrees during the stance phase. During toe off the leg is extended as well as the opposite limb which counts as roughly 40% of the gait cycle and is also known as '*double knee lock'.* Double knee lock meaning that both knees are fully extended. The three determinants above all reduce the excursion of the CoM. Pelvic rotation will elevate the extremities of the CoM trajectory whereas pelvic tilt and knee flexion will reduce the extremities.

The fourth and fifth determinants are focussed around the foot and knee. After heel strike the *4)foot acts as a lengthening of the leg*. During the transition phase from heel strike towards mid stance it controls the pathway and furthermore smoothen and lower the CoM pathway at the same time. During toe off rapid plantar flexion will extend the leg and therefore increase the speed of the CoM which will result in a decrease in metabolic cost and therefore better efficiency during walking. Equally the knee plays a vital more specific role as it will change *5)velocity of knee flexion* according to the CoM position in order to smooth the sinusoidal wave.

The sixth and last determinant explains how the efficiency of gait is based on *6)step width*. Humans prefer to walk at a step width of ~0.12L (where *L* is the leg length) as reported by Bauby and Kuo[65]. Metabolic cost increases at step width smaller than 0.10*L* (where L is the leg length) and the preferred step width (0.13*L* ± 0.03) was not significantly different from the minimum metabolic cost compared with the enforced 0.12*L* ± 0.05 step width nor 0.11*L* ± 0.01 as reported by Donelan[66]. According to the *'six determinants of gait'* theory, lateral change of the CoM reduces the excursion and makes the movement smoother[61]. To summarize, the '*six determinants of gait'* theory rests on the assumption that vertical and lateral excursion of the CoM is energetically costly and should be reduced.

The first simplified model of gait that has already been partly assumed by the first three determinants of gait is the pendulum model of gait. This model assumes that the leg is rigid by excluding the knee, ankle and foot. This model can be mathematically described as a pendulum with *L* being the length of the pendulum and *m* being the mass and fixed on a vertical circular path around support point *O* and having one degree of freedom can be seen as a simple pendulum[67]. This is the mechanical working of the inverted pendulum model used in most gait analysis[22 68-70]. The simple inverted pendulum is shown in Figure 3.

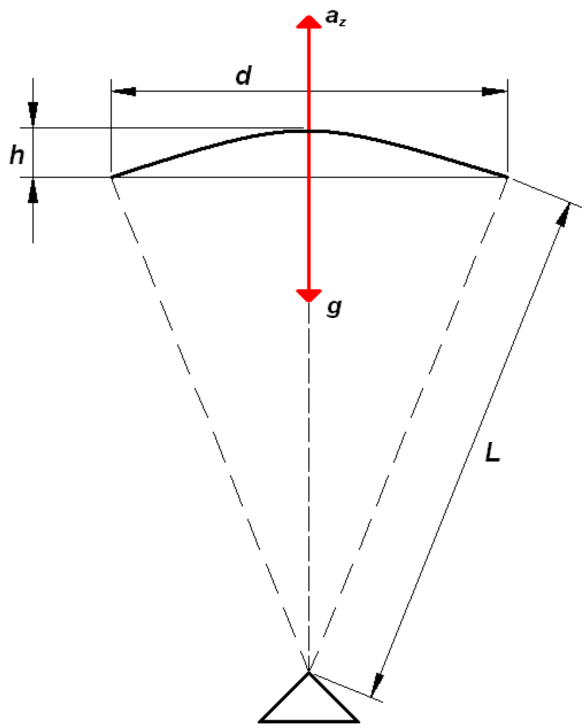

Figure 3 mechanics of an inverted pendulum with *h* being the excursion of the Centre of Mass (CoM), *L* being the leg length measured from the anterior superior illiac spine to the tip of the medial malleolus. When using this model forward displacement can be derived using the model proposed by Zijlstra et al[71] where *d* equals the forward distance by for each step. *g* represents the gravitational acceleration and a_z represents the vertical acceleration.

The mechanical definition of walking is that bipedal walking fits a mechanical description as an 'inverted pendulum', in which kinetic energy at the beginning of each stance phase translates into gravitational potential energy as the CoM rises to its highest point near mid-stance[62]. After mid-stance the potential energy is returned into kinetic energy as the CoM falls towards the end of stance[72-74].

In clinical gait analysis, mechanical energy is the gait variable which can derive the energetic walking cost of a patient's movement[75]. During mid-stance the potential energy should be returned to kinetic energy as the body falls during the second half of the inverted pendulum[72].

Knowing the characteristics of an inverted pendulum, the step length can be estimated by measuring the vertical excursion of the CoM (*h)* with the leg length (*L*) which can be described as:

$$d = 2\sqrt{2Lh - h^2} \quad (1.1.1)$$

Research showed that a correction factor is needed for healthy subjects, which is set at 1.25 due to a 25% underestimation of step length[71 76]. This underestimation can be mainly explained by the missing length of the foot, as it lengthens the pendulum and therefore increases step length *d*. Models such as the ‘*foot rocker’*l can potentially model the effects of the foot on gait which are based on a pivot system of the heel, ankle, forefoot and toe rocker to preserve energy[42]. The inverted pendulum model proposes that if the stance leg acts like an inverted pendulum it reduces the energy cost more than during the *‘six determinants of gait’* theory[77]. Both the *six determinants of gait* and the *inverted pendulum model* are shown in Figure 4.

Figure 4 The two major theories of gait with displaying the minimalisation of vertical excursion of the Centre of Mass in the a) ‘*six determinants of gait theory’* and b) *‘Inverted Pendulum model’* both trying to reduce the energy consumption during walking.
Source: Kuo 2007, *The six determinants of gait and the inverted pendulum analogy: A dynamic walking perspective*

As explained above the correction factor of 1.25 can be more accurately estimated by introducing a model proposed by Gonzalez et al[78]. They have proposed that during double stance the CoM is still moving forward. This forwards movement can be calculated as

$$d_{ds} = Kp \quad (1.1.2)$$

Whereby p is the length of the foot and K the propotial constant. K has been estimated as 0.83 by Han et al[79] and 0.67 by Schmid et al[80]. These factors (imagine a EUR shoe-size 45 = 29cm) relate to an addition of 24.1cm (when using K=0.83) or 19.4cm (when using K=0.67). By combining the inverted pendulum model with the double stance displacement as

$$d_t = d + d_{ds} \tag{1.1.3}$$

The total forward distance (d_t) can be determined. However, instead of calculating the double stance displacement this can be replaced by a correction factor γ as used throughout this thesis. As with a step length of 0.77m, the double stance model would relate to a correction of the single stance output by 23.8%=100-(0.77/(0.77+0.241)*100%) when using K=0.83 and 20.1%=100-(0.77/(0.77+0.194)*100%) when using K=0.67.

Recent work by Alvarez et al[81] however addressed the forward movement of the CoM by placing an IMU on each foot. They developed a method, combining the gyroscope output in the sagittal plane with the acceleration in x- and z-axis, which allowed them to measure horizontal displacement without having the uncertainty of the correction factor when using the inverted pendulum model.

Throughout this work the inverted pendulum model has been chosen. The aim of this thesis was to develop an easy to use method to derive accurate spatio-temporal gait parameters which would included the least amount of measurements and technical challenges for the end user. Over the next chapters the validation of the inverted pendulum will be looked at as well as the determination of the correction factors belonging to typical developed adults and Parkinson's disease.

1.2 Centre of Mass

Human gait and is essential for an independent life. Any abnormalities in gait could result in a decrease of mobility and therefore a decrease in health and social life and perhaps change in emotional status[6]. Gait is controlled by a 'vicious circle' of internal and external influences[6] as seen in Figure 1. Therefore it is crucial that gait can be understood, defined and accurately analysed in a quick and cost effective way.

1.2.1 Reference value of the Centre of Mass

Centre of Mass (CoM) is an important aspect of human locomotion. CoM can be defined as being "the point through which, for all orientations of a body, the resultant of the gravitational forces acting upon particles in the body pass" as reported by Dempster in 1955[82]. CoM is used as a reference point to measure gait dynamics[83]. Research dating back to 1876 by Marey utilized CoM movement in order to perform gait analysis[84]. Measurement devices were primitive but effective for the time; they normally did not contain more than a wooden frame with a kymograph. Cavagna et al[62] reported in 1963 that measurements of the displacement of the CoM represents between 60-70% of the total mechanical work done in walking. Furthermore recent studies demonstrate that CoM displacement can be used to determine gait parameters such as step-frequency and time[85 86].

Researchers have developed a range of methodologies for calculation of CoM displacement during walking. Some of the methods utilize kinematic data acquired from markers that are placed on the body, and others utilize kinetic data acquired from force platforms[83]. A simple kinematic method is placing a *single marker* on the sacrum which represents the projected CoM[87], whereas a more sophisticated method is done by the *segmental analysis method* which involves multiple markers which are integrated with anthropomorphic models to calculate segmental CoM positions. Accelerometers have also been used as an alternative kinematic method by Pfau et al[17 33] to estimate CoM displacement in quadrupedal gait.

Furthermore techniques as described by Gard et al[83] use anthropomorphic data from standard tables to determine mass fractions of segmental locations of centres of mass.

1.2.2 Location of Centre of Mass

The location of CoM was first estimated by Harless in 1860 by using cadavers[88]. By dissecting the cadavers into 18 segments, he was able to weigh the segments. The mass and CoM of the body segments were then measured or estimated using sensitive scales and balance plates. The specimens were beheaded criminals, with an unknown amount of blood loss, for which the weight cannot be accounted.

Braüne et al[89] followed up Harless in 1891 by using cadavers of German soldiers who died due to suicide. To avoid blood loss, they kept the bodies frozen throughout the research. They dissected the bodies as previously described, but instead of using balance plates, they drilled three thin rods into the segments. The point of the crossover of the three external fixed planes, perpendicular onto each other,

corresponded to the CoM of that segment[82 89]. This research was generally accepted and therefore used as a standard for more than over half a century[31].
With the introduction of more advanced measurement systems researchers were able to determine the location of the CoM in more detail. There are currently two methodological approaches in order to determine whole body CoM location being a kinetic and kinematical approach.

When Herbert Elfmann invented the first force plate in 1934, a new kinetic method of deriving the CoM arose[90 91]. CoM could be reviewed and balance of whole bodies could be measured in living people. As stated in his paper in 1938 where he explained the physics regarding his force plate: '*although designed for the investigation of movement, this apparatus can also be used for the more traditional measurement of the position of the center of gravity when the body is stationary*.'[91].
Dempster[82] defined the CoM as '*The point through which, for all orientations of a body, the resultant of the gravitational forces acting upon particles in the body pass*.'

For kinetic measurements force plates are embedded in the floor of a gait laboratory in the path of the participant. From the force signals that arise when the participant walks over the designated force plate, acceleration vectors can be derived in three dimensions by using Newton's second law which can be described as:

$$F = ma \tag{1.1.4}$$

where the mass (*m*) undergoes an acceleration (*a*) that has the same direction of the force (*F*). However during the integration process, to obtain the CoM location, opportunities for errors will be introduced. The general integration processes will be explained in chapter 2.3.4. The advantages of this method are that there are no markers needed and it does not rely on anthropometric estimates and therefore avoids the errors associated with a segmental kinematic approach[92]. However , the method is prone to error related to stride length variation as participants need to step fully on the force plates without deviating from their normal gait[92 93]. Therefore the force platform measurements can be unrepresentative of the participants' gait[93]. In addition problems are associated with pathological and children's gait as their step length may result in a *double strike* on the same platform[92].

The kinematic segmental method has been suggested as the '*gold standard*´ for CoM displacement measurements[16]. This method relies on a model considering the head, arms and trunk as one segment where the lower limb are made up of thigh, shank and foot segments[94]. For each of the segments the CoM is calculated based on data collected from cadavers[31]. Three dimensional whole body CoM can be derived using motion capture systems during locomotion. The major inaccuracies associated with the kinematic method are the reference data for segmental CoM positions which may not be accurate for the morphology of the test participant[94]. Furthermore error may be introduced by skin movement and incorrect positioning of markers used.

Using the methods above, the whole body CoM is often taken from the 4th lumbar vertebra[62 95], better known as the *projected CoM*. Auvinet et al[96] confirmed that the 3rd Lumbar region is a sufficient approximation of the CoM during normal walking. It has been demonstrated by Kerrigan et al[87] that the projected CoM motion can be estimated anywhere between the sacrum and the 4th lumbar vertebra. Lundberg[97] reported in 1996 that the fascia over the spinious processes is relatively rigidly fixed to the bone, and thus skin movement will follow bone movement more closely than many others regions. This area is close to the location of the 4th lumbar vertebra and suffers from minimal skin movement during walking[98].

1.2.3 Measurements of Centre of Mass

As mentioned before CoM can be used to measure several aspects of gait. Peak-to-peak amplitude of the CoM vertical displacement is often referred to as *vertical excursion* or *vertical displacement*. Researchers have reported the vertical displacement of the CoM to be 4-5cm for healthy adults at their self selected walking speed[61]. However, as reported by Saini et al[93], vertical CoM displacement obtained from kinetic and kinematic methods show a significant difference. Gard and Childress[99] have shown that CoM excursion is underestimated when using force platforms. In comparison, CoM excursion has been overestimated during faster walking speeds using the sacral marker method[83].

Different problems arise when measuring CoM with force platforms in human gait. As reported by Donelan in 2001, footsteps in heavy subjects are difficult to trace back to their origin of first contact[66]. Measuring the CoM in children was proven to be difficult due to their short step length, resulting in a double heel strike on the force platforms; this same problem was found in adults with pathological gaits[92]. When using force platforms it can be assumed that deriving the position of the CoM is accurate, as the CoM is not dependent on accurate marker placement[83].

Vertical CoM displacement can be used to estimate mechanical energy changes[100-102], work[62 68 72], to describe symmetry[103-105] and as an indicator as overall quality of gait[61]. Mechanical energy is the gait variable which can validate the energetic state of the disorder of patient's movement[75].

It has been shown that energy fluctuations in the Centre of Mass (CoM) during treadmill walking in humans are not equivalent to ground walking[18]. Ground reaction force have been showed to be significantly different[106]. The same research concludes that forces in mid- and late-stance are different to humans walking overground. Furthermore joint kinematics and metabolic rate have shown to be different when walking on a treadmill[107 108]. So for optimal gait mechanics overground walking will provide more valid data.

1.3 Gait Survey

In order to gain in insight into the required gait parameters as perceived by clinicians a questionnaire was setup via "SurveyMonkey" (http://www.surveymonkey.com) where questions related to gait analysis were derived from a previous study by Toro et al[36] in 2003. Questions were asking about the type of gait analysis and required gait parameters that would be useful during their daily clinical routine. The results of this survey were taken in account during the development of the gait analysis tool described in this work. Thirty specialist physiotherapists with a background in neurological rehabilitation were targeted throughout the United Kingdom of who 16 responded.

Of all respondents 70% were currently doing at least one kind of objective measurement regarding gait. The remaining 30% did not do any gait measurements but indicated they wish they could.

None of the responses indicated they did perform gait analysis on a majority of patients, while they did confirm that gait analysis was needed according to the NICE guidelines[109]. The top four reasons for not doing the analysis were lack of time, budget restraints, wrong equipment and no available space, which is in agreement with results found by Toro et al[36].

The respondents indicated that they were interested in measuring the following gait parameters: Effort (56%), Symmetry (43%), Smoothness (37.5%) and Cadence

(31%). They indicated that there was no currently available equipment which could provide these measures in their clinical setting.

The survey respondents were asked if there were any other gait parameters that they wanted to use, 42% answered positively. The three main suggestions were the quality of movement, the activity at specific joint angles and an overall objective measurement regarding ratios within walking (for example normal distributed gait parameters linked to age, height, weight and gender).

All survey respondents expressed interest in a method that gave an objective measure for the previously mentioned gait parameters that was quick, valid and reliable. 75% of the survey respondents indicated such a tool would add clinical value in the rehabilitation of patients in particular patient groups suffering from neurological conditions. Survey respondents indicated patients with orthopaedic problems (43.5%), musculoskeletal problems (37.5%) and elderly with gait deficits (31%) could also benefit.

Finally, clinicians taking part were asked for any open comments regarding the current gait analysis used in their clinic. The following answers were typical and representable for this group:

- Most indicated the main problems with gait analysis are due to cost and time to do analysis
- One clinician reported that for gait analyses they had to travel about one hour by car to be at a gait laboratory in order to obtain objective gait parameters. (There is only one clinical gait laboratory in Oxfordshire)
- Another participant acknowledged the importance of gait analyses, however she mentioned due to the lack of technical knowledge their mobile camera system hadn't been used in the last 3 years

The results from Toro et al[36] were confirmed by these findings, pointing out that there is a clinical need for a cheap, small and quick device to describe clinical gait parameters (walking speed, effort, symmetry, smoothness and cadence) in an objective way.

From this chapter it can be concluded that current gait measurement tools are relatively expensive, difficult to use and not accessible to clinicians. Gait analysis in a clinical setting could provide valuable information about someone's wellbeing and disease progression.

This thesis sets out to develop a tool which can provide an objective outcome measurement of spatio-temporal aspects of gait which is accessible and easy to use for clinicians. In addition this work sets out to derive spatio-temporal aspects of gait in an accurate and reliable manner, as measured by a single body reference point.

Chapter 2: Mechanics

This Chapter explores the sensory technology and mechanics used throughout this thesis. It focuses on the sensors in inertial measurement units and relevant parts of digital signal processing needed in order to drive gait models as described in Chapter 1. At the end of this chapter, the main methodological approach with regards to the digital signal processing of inertial measurement unit data will be described.

In less than 20 years, MEMS (micro electro-mechanical systems) technology has gone from an interesting academic exercise to an integral part of many common products. MEMS structures are not only electronic such as processors, but also mechanical. This includes a wide spectrum ranging from cog wheels (Figure 5) to pressure switches. MEMS technology is used in normal day to day products, for example airbags, accelerometers, television screens and disposable medical devices[110].

Figure 5 *Mechanical MEMS (http://www.memx.com/)*

2.1: Inertial Measurement Units

Sensor fusions between accelerometers, gyroscopes and magnetometers in an algorithm are used as inertial measurement units (IMU). In the next paragraphs these systems will be treated separately to discuss their functioning in more detail.

2.1.1 Accelerometers

A single axis accelerometer consists of a mass, suspended by a spring in a housing. Springs work according to Hooke's law. Hooke's law states that a spring will undergo a restoring force which is proportional to the distance it has been expanded[111]. Therefore we can write:

$$F = kx \qquad (2.1.1)$$

where k is a specified constant of the spring, x equals the expanded distance. Another physical principle is Newton's second law[112]. It states that the force operating on a mass which is being accelerated will have amplitude

$$F = ma \qquad (2.1.2)$$

where m equals the mass in *kg* and a equals the acceleration in m/s^2. Combining these two laws we can write:

$$F = kx = ma \qquad (2.1.3)$$

This tells us that an acceleration a will cause the mass to be displaced by:

$$x = \frac{ma}{k} \qquad (2.1.4)$$

In order to measure in multiple axes, this system needs to be duplicated along all required axes.

Development of MEMS technology allows accelerometers to become smaller and be more accurate. Dataflow can still be obtained, but less accurately by using Hooke's Law in MEMS technology as mechanics are replaced by digital components. Figure 6 shows a MEMS triaxial accelerometer by Hitachi Metals. In comparison to the accelerometer described before, there is still a mass involved and a housing which is vacuum sealed[113]. Polysilicon springs suspend the MEMS structure above the substrate such that the body of the sensor (also known as proof mass) can move around in the x and y axis. Around the four sides of the proof mass, there are 32 radial fingers. These fingers are positioned between plates that are fixed to the substrate. Each finger and a pair of fixed plates generate a capacitor. In this way the displacement of the proof mass can be measured by the difference in capacitance.

Capacitance can be written as a function of the amount of charge stored between plates which hold a potential difference in Volts. We can write that:

$$C = \frac{Q}{U} \qquad (2.1.5)$$

Where C is the capacitance in Farads, Q equals the charge in Coulomb and U equals the potential difference in Volts.

__Figure 6__ MEMS triaxial accelerometer (http://archives.sensorsmag.com/)

In reality there are two main issues concerning the accuracy of measurements. First of all is the error of the acceleration measurements. All MEMS acceleration sensors are critically damped, otherwise a sudden movement would cause them to resonate. Besides, the sensor cannot distinguish between vibration and real movement. These can be separated by using digital filters which can distinguish frequencies within movements as a result of vibrations known as noise.

2.1.2 Gyroscopes

Gyroscopes are used to measure angular motion or change. There are two main categories, mechanical and optical gyroscopes. Within these two categories there are many different gyroscopes available for specific purposes. The first rotating gyroscope was built by Leon Foucault in 1852. His gyroscope emerged from an investigation of the rotation of the earth and consisted of a rapidly rotating disk with very heavy rim, mounted in low-friction gimbals. His theory was that if the earth would turn beneath the gyroscope, it would maintain its position in space. Due to torque in the gimbals which created extra friction, it was difficult to observe[114]. Leon Foucault is seen as the inventor of the gyroscope, but in 1817 Johann von Bohnenberger invented the '*Bohnenberger's machine*' which consited of three movable gimbals, but a non-rotating ball in the middle[115].

Mechanical gyroscopes operate on the basis of conservation of angular momentum by sensing the change in direction of an angular momentum[2 31]. According to Newton's second law, the angular momentum of a body will remain unchanged unless it is acted upon by a torque[112]. The fundamental equation describing the behaviour of the gyroscope is:

$$\tau = \frac{dL}{dt} = \frac{d(I\omega)}{dt} = I\alpha \qquad (2.1.6)$$

Vector τ is the torque on the gyroscope with an angular momentum L. Scalar I is its momentum of inertia, vector ω is its angular velocity and α stands for its angular acceleration.

Gimballed gyroscopes or laser gyroscopes are too expensive to be practical and too large in size to use in human movement analyses. With the introduction of MEMS technology, vibrating gyroscopes are used to replace mechanical gyroscopes. Vibrating MEMS gyroscopes have advantages as they are small in size, inexpensive and low in power consumption. This makes them ideal to combine in small sensors and apply them in human movement tracking. As the earth is moving, any vibrating element will be undergoing the Coriolis effect. The Coriolis effect was first described by Gaspard-Gustave Coriolis in 1835. For example, taking the plane from Europe straight towards the south will give a deflection to the east, as the earth keeps on turning. However, this is only when the Coriolis effect is not taken into account. The Coriolis effect is caused by the Coriolis force which appears in the equation of motion of an object in a rotating frame of reference[116]. This force creates a second vibration when rotating a MEMS vibrating gyroscope in a rotating frame, of which the rate of turn measured in angular velocity ω can be measured. The Coriolis force is given by:

$$F_c = -2m(\omega \times v) \qquad (2.1.7)$$

Where m equals mass and v the momentary speed of the mass relative to the object to which it is attached. One of the most dramatic and visible results of the Coriolis force is the centrifugal force in cyclones. Due to the linear movement of the differences in the pressure zones, and the deviation at the equator to the east and west, high and low pressure areas can collide which could create a potential origin for hurricanes.

Gyroscope's outputs mostly used are Euler angles and Quaternions in order to describe orientation of the sensor. These two outcome measurements, their advantages and disadvantages will be discussed at a later stage in this section.

2.1.3 Magnetometers

Magnetometers determine the direction and or strength of the earth's magnetic field. Carl Friedrich Gauss (also known from the Gaussian distribution), published a paper in 1832 with a device that could measure the strength of the earth magnetic field[117]. The device worked on the fundamental assumption that every body, in which magnetic flux occurs, always contains an equal amount of north and south flux[117]. Bear in mind that there are two main types of magnetic bodies: firstly materials such as soft iron, immediately change the north and south flux under the influence of a slight external force. Once the force decreases and returns to the default force, such bodies return to their previous magnetic state. In contrast materials such as tempered steel remain in the changed state even after the external force deceases[117] [118]. When measuring the earth's magnetic field, measurements of the second sort of magnetic bodies is meant.

In order to measure the angular change in magnetic bodies of the second kind, we can assume that all the different parts can be described as $dm = 0$ where *dm* stands for the element of free magnetism in a particle. When measuring in a three fixed plane, perpendicular to each other *x,y* and *z* flux can be designated as *xdm* = *X*, *ydm* = *Y* and *zdm* = *Z* . Since under the assumption that *k* refers to an arbitrary constant magnitude, *(x-k)dm* = *X* [117]. From these relations, by using the equation (2.1.8) it is possible to determine the earth's magnetic field vector ($\vec{V}$).

$$\vec{V} = (x\cos\alpha + y\cos\beta + z\cos\gamma)dm \tag{2.1.8}$$

2.1.4 Sensor Fusion

Moore's law, which describes the decreasing size of electronics over time, plays an important role in predicting the future regarding cost and size within MEMS[32]. Sensor fusion is the combination of sensory data to obtain a more reliable and accurate single outcome measure than the combined sensors can produce individually.

The sensor used in this work uses *Kalman* sensor fusion between a tri-axial accelerometer, tri-axial gyroscope and tri-axial magnetometer. These systems are commercially available (Xsens, Enschede, the Netherlands, and Philips Pi-Node, Eindhoven, the Netherlands). The Kalman fusion between sensors remains a black box of which the specifications are unclear but has to be similar to Figure 7.

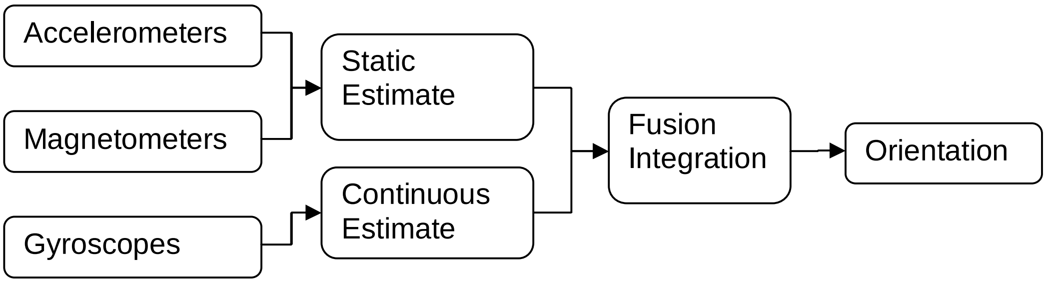

Figure 7 *A general outline of the fusion integration process*

In this case, the magnetometers are used to correct drift caused by the gyroscope. However, the influence of iron influences the local magnetic field which is measured by the magnetometers which on its turn affects the orientation output of the gyroscope. The sensor fusion in the IMUs used in this research creates the possibility to acquire accurate orientation within human movement.

2.2: Orientation Outputs

As mentioned before gyroscopes measure angular change or motion. The outputs of the gyroscopes (and Kalman fusion) are combined into two parameters, the Euler angles and the quaternions. Both outputs are explained in the next sections.

2.2.1 Euler Angles

The term Euler angle is used for any representation of 3 dimensional (3D) rotations decomposed into 3 separate angles[119]. When thinking about rotations, using the same algebras for 2D rotations is common. Euler angles can be seen as angles used in 2D rotations. But within 3D rotations, using a rotation matrix, many more aspects need attention.

Euler angles are commonly used in the aviation and engineering industry but also in astronomy. They are mainly applied in devices that rely on gyroscopes, as Euler angles are one of the raw outputs of a gyroscope. Each sector has its own terms for the Euler angles. Table 1 shows the term in combination with the symbol of the Euler angles.

Table 1 Symbol and names of Euler angles[2]

Rotation order	Airplane	Telescope	symbol	angular velocity
1	Attitude	Elevation	ϕ	Pitch
2	Bank	Azimuth	θ	Roll
3	Heading	Tilt	ψ	Yaw

Starting off with the 2D rotations using a 2D orthogonal matrix, the transformation of Cartesian coodinates by

$$\begin{bmatrix} x' \\ y' \end{bmatrix} = \mathbf{M}_2(\phi)\begin{bmatrix} x \\ y \end{bmatrix} = \begin{bmatrix} \cos\phi & -\sin\phi \\ \sin\phi & \cos\phi \end{bmatrix}\begin{bmatrix} x \\ y \end{bmatrix} = \begin{bmatrix} x\cos\phi - y\sin\phi \\ x\sin\phi + y\cos\phi \end{bmatrix} \tag{2.2.1}$$

(Basic 2D rotations with orthogonal matrix M_2 setup for a rotation with angle *θ*)

The 2x2 matrix M_2 is written in the form shown in equation(2.2.2) with the properties as shown in equation(2.2.3) and equation(2.2.4)

$$\mathbf{M}_2(\phi) = \begin{bmatrix} A & -B \\ B & A \end{bmatrix} = \begin{bmatrix} \cos\phi & -\sin\phi \\ \sin\phi & \cos\phi \end{bmatrix} \tag{2.2.2}$$

(Matrix M_2 described as a 2x2 matrix with variables *A* and *B*)

$$det\mathbf{M}_2 = A^2 + B^2 = 1 \tag{2.2.3}$$

(Determinant of matrix M_2 in fuction of variables *A* and *B*)

$$\mathbf{M}_2 \cdot \mathbf{M}_2^T = \begin{bmatrix} A^2 + B^2 & 0 \\ 0 & A^2 + B^2 \end{bmatrix} = \begin{bmatrix} 1 & 0 \\ 0 & 1 \end{bmatrix} \tag{2.2.4}$$

(The balance on both sides of the 2D rotation matrix M_2)

When looking into a 3D rotation, many more aspects should be taken in mind. Figure 8 shows what happens to *x,y,z*-axis and their vectors in corresponding planes while performing a 3D rotation. When writing M_2 as a 3D orthogonal matrix, it results in matrix *R*.

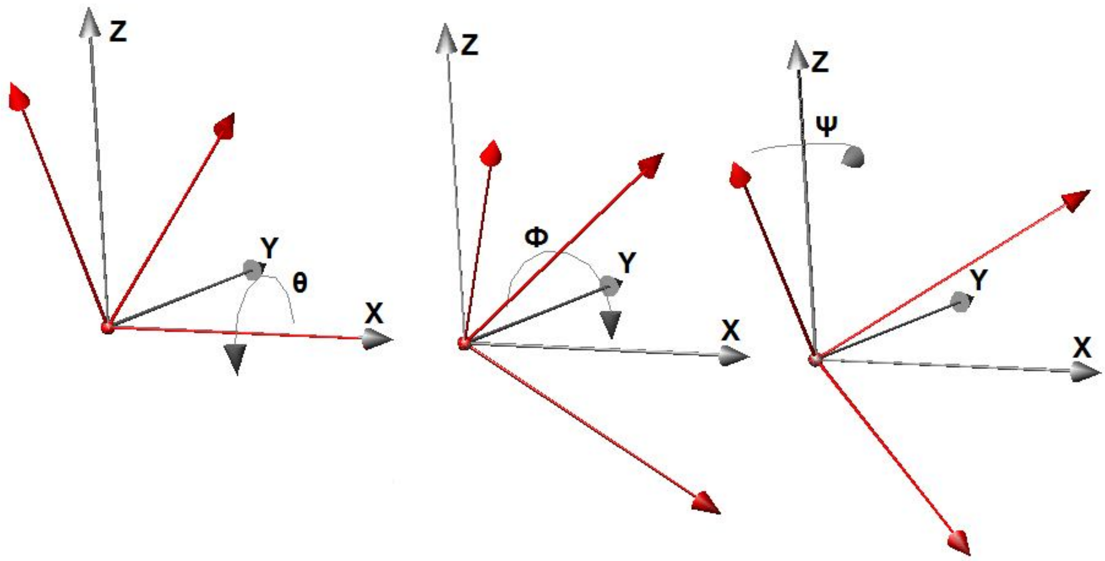

Figure 8 3D rotations starting with roll defined as angle θ followed by pitch defined as angle Φ and ended by yaw defined as angle Ψ

3 dimensional (3D) rotations can be divided into single dimensional rotations. They emerge in a specific order, depending on order of rotation. When following the rotations in Figure 8, angles for each rotation can be determined starting with the rotation around the x-axes with angle θ. This rotation can be defined as matrix R_X

$$R_y(\theta) = \begin{bmatrix} \cos\theta & 0 & -\sin\theta \\ 0 & 1 & 0 \\ \sin\theta & 0 & \cos\theta \end{bmatrix} \tag{2.2.5}$$

(R_X in Euler angles)

The rotation around the x-axes is followed by a rotation around the y-axes with angle ϕ will result in the rotation matrix R_Y defined as:

$$R_x(\phi) = \begin{bmatrix} 1 & 0 & 0 \\ 0 & \cos\phi & \sin\phi \\ 0 & -\sin\phi & \cos\phi \end{bmatrix} \tag{2.2.6}$$

(R_Y in Euler angles)

Following the two rotations, there is a rotation around the z-ax with angle Ψ. This can be defined in a rotation matrix defined as R_Z:

$$R_z(\psi) = \begin{bmatrix} \cos\psi & \sin\psi & 0 \\ -\sin\psi & \cos\psi & 0 \\ 0 & 0 & 1 \end{bmatrix} \tag{2.2.7}$$

(R_Z in Euler angles)

The order of rotation also determines the order of multiplying. In this example there is the matrix multiplication or $R_X R_Y R_Z$ which results in rotation matrix $R_{X,Y,Z}$:

$$R_{x,y,z} = \begin{bmatrix} \cos\theta\cos\psi & \cos\theta\sin\psi & -\sin\theta \\ \sin\phi\sin\theta\cos\psi - \cos\phi\sin\psi & \sin\phi\sin\theta\sin\psi + \cos\phi\cos\psi & \sin\phi\cos\theta \\ \cos\phi\sin\theta\cos\psi + \sin\phi\sin\psi & \cos\phi\sin\theta\sin\psi - \sin\phi\cos\psi & \cos\phi\cos\theta \end{bmatrix} \tag{2.2.8}$$

($R_{X,Y,Z}$ in Euler angles)

This rotation matrix can be used to transform vectors from the object system to the global system. The result will be V_{OG} defined as:

$$V_{OG} = R_{X,Y,Z} \cdot \begin{bmatrix} X_O \\ Y_O \\ Z_O \end{bmatrix} \tag{2.2.9}$$

(V_{OG} in Euler angles)

Where V_{OG} stands for the transposed vectors X, Y and Z from the object system into the global system.

2.2.1.1 Mechanical gimbal lock

Euler angles are relatively easy to understand, easy to represent and can be visualised. However they can suffer from singularities of which one important one is called ‘gimbal lock’. Gimbal is a term used in the structures from a gyroscope (Figure 9), it forms a single ring around an axle within the gyroscope on which the stable member turns. Gimbal lock is a loss of one degree of freedom in 3D space. When a plane rotates 90 degrees (or 270 degrees) from its initial position in the y-axis, the gimbal rings of the x and z axis align to each other. When the plane would move into the x or z axis, it would still give the same reading for both axes.

Figure 9 Inside mechanics of a gyroscope used in the Apollo 11 flight in 1969
Source: http://history.nasa.gov/

One of the most familiar gimbal lock problems happened during the Apollo 11 flight in 1969. They encountered the problem of losing one degree of freedom just before reconnecting the lunar excursion module to the command module but managed to get out of the gimbal lock with some minor corrections.

2.2.1.2 Mathematical gimbal lock

The gimbal lock explained above, is purely mechanical. There is also a possibility of going into mathematical gimbal lock. The Euler angle sequence *xyz* can be used to show where this problem arises.

In the rotation matrix from equation(2.2.8) and that *Φ, θ* and *Ψ* represent rotation about the *x*, *y* and *z* axes. As mentioned earlier, to create this singularity called gimbal lock in the *xyz* sequence, there must be a rotation around the *y*-axis to align the *z* and *x* axes. Bear in mind that if $\theta = \frac{\pi}{2}$ the resulting rotation matrix would result

$$R_{X,Y,Z}(\phi,\frac{\pi}{2},\psi)=\begin{bmatrix} 0 & 0 & -1 \\ \sin\phi\sin\theta\cos\psi-\cos\phi\sin\psi & \sin\phi\sin\theta\sin\psi+\cos\phi\cos\psi & 0 \\ \cos\phi\sin\theta\cos\psi+\sin\phi\sin\psi & \cos\phi\sin\theta\sin\psi-\sin\phi\cos\psi & 0 \end{bmatrix}$$

(2.2.10)

(Rotation matrix $R_{X,Y,Z}$ with $\theta = \pi/2$)

Considering *Φ* being *0* and *Ψ* being a random angle within the range of 1 to 360 degrees, equation(2.2.8) will result in:

$$R_{X,Y,Z}(0,\frac{\pi}{2},\psi)=\begin{bmatrix} 0 & 0 & 1 \\ -\sin\psi & \cos\psi & 0 \\ \cos\psi & \sin\psi & 0 \end{bmatrix} \quad (2.2.11)$$

(Rotation matrix $R_{X,Y,Z}$ with *Φ = 0 and Ψ being an arbitrary angle)*

When turning into the different axis with *Ψ* being *0* and *Φ* being a random angle within the range of 1 to 360 degrees, equation(2.2.8) results in:

$$R_{X,Y,Z}(\phi,\frac{\pi}{2},0)=\begin{bmatrix} 0 & 0 & 1 \\ \sin\phi & \cos\phi & 0 \\ \cos\phi & -\sin\phi & 0 \end{bmatrix} \quad (2.2.12)$$

(Rotation matrix $R_{X,Y,Z}$ with *Ψ = 0* and ɵ being an arbitrary angle)

When replacing the Φ with - Φ, the equation(2.2.12) results in:

$$R_{X,Y,Z}(-\phi,\frac{\pi}{2},0)=\begin{bmatrix} 0 & 0 & 1 \\ -\sin\phi & \cos\phi & 0 \\ \cos\phi & \sin\phi & 0 \end{bmatrix} \qquad (2.2.13)$$

(Rotation matrix $R_{X,Y,Z}$ with $\Psi = 0$ and -ɵ being an arbitrary angle)

Looking at the equations (2.2.11), (2.2.12), (2.2.13) notice that $R_{X,Y,Z}(-\phi,\frac{\pi}{2},0)=R_{X,Y,Z}(0,\frac{\pi}{2},\psi)$ and results in a single loss of one degree of freedom. Mathematical gimbal lock often occurs in program code which results in sudden loss of control and or signal[120].

In order to resolve this problem quaternions were considered in order to transpose the acceleration vectors from the object to the global system. Quaternions and the use of quaternions will be discussed in the next section.

2.2.2 Quaternions

Quaternions are commonly used to represent rotations. Quaternions were introduced by Sir William Hamilton in 1844 at a conference at the Royal Irish Academy[121]. According to the story, Sir William Hamilton walked along the canal in Dublin on the 16th of October 1843 when he found the solution to use complex numbers into higher dimensions as shown in equation (2.2.14)[121]. Quaternion algebra can be used in rotations of rigid bodies in 3 dimensional (3D) space[122]. Rotations through quaternions are used in many applications such as virtual reality[120], aerospace engineering[28] and orbital mechanics. This is mainly due to the fact that quaternions require less time than any other representations in calculations and are not affected by singularities[123].

$$i^2 = j^2 = k^2 = ijk = -1 \tag{2.2.14}$$

(Fundamental formula of quaternion algebra by Hamilton, 1844
where *i, j,* and *k* represent complex numbers)

Quaternion comes from the Latin word *Quaternio* which means ‘A set of four’. The combined operation of *Scalar* and *Versor* requires four numbers: one for scale, one for angle and two for orientation (common plane)[122].

Vector and scalar mathematics form the basis of quaternion multiplication. A vector is defined as a line segment with a starting point and direction. When a vector has a starting point in point A, the direction of the vector x will lead to a unique point B. Hamilton introduced an equation (2.2.14) looking at the relationship between two vectors in the same way that a vector represents the relationship between two points. When quaternions are applied to a vector, they create a unique new vector with a new length and direction.

A vector is defined by a fixed length and a variable orientation, however a quaternion is defined by a fixed relative length, and a variable relative orientation[124].

A scalar is defined as the ratio between the lengths of two parallel vectors $\vec{A}$ and $\vec{B}$. It presents the relative length of one vector with respect to the other. The scalar in programming language has been replaced by the term *real part*.

A quaternion is an operator that changes the orientation and length of a vector as:

$$\vec{A} = Q \lozenge \vec{B} \tag{2.2.15}$$

(Quaternion (Q) representing a Geometrical Quotient of two vectors *A* and *B with the quaternion operator noted by ◊)*

The definition in equation (2.2.15), is specified into vector and scalar changes. Following up (2.2.14) and knowing that a quaternion exists out of a scalar and three vectors (one for angle and two for orientation) we can write:

$$\begin{aligned} q &= q_0 + \vec{q} \\ & q_0 + iq_1 + jq_2 + kq_3 \end{aligned} \qquad (2.2.16)$$

(Quaternion displayed as the function between one scalar (q_0) and three vectors ($q_1 q_2 q_3$) multiplied according to the Hamilton's formula ***i***, ***j,*** and ***k***)

where q_0, q_1, q_2, and q_3 are real valued numbers and ***i***, ***j***, and ***k*** are the standard orthonormal basis and can be written as $\mathbb{R}$ **2 124 125**. Hamilton's fundamental formula for quaternion algebra is not complete without going into the complete multiplications:

$$\begin{aligned} k &= ij = -ji \\ i &= jk = -kj \\ j &= ki = -ik \end{aligned} \qquad (2.2.17)$$

(Remaining fundamentals for quaternion algebra by Hamilton 1844)

Knowing a single quaternion equation (2.2.16), quaternion multiplication can be done. A multiplication between the quaternions *p* and *q* is defined as:

$$\begin{aligned} pq &= (p_0 + ip_1 + jp_2 + kp_3)(q_0 + iq_1 + jq_2 + kq_3) \\ &= p_0q_0 + ip_0q_1 + jp_0q_2 + kp_0q_3 \\ &\quad + ip_1q_0 + i^2 p_1q_1 + ijp_1q_2 + ikp_1q_3 \\ &\quad + jp_2q_0 + jip_2q_1 + j^2 p_2q_2 + jkp_2q_3 \\ &\quad + kp_3q_0 + kip_3q_1 + kjp_3q_2 + k^2 p_3q_2 \end{aligned} \qquad (2.2.18)$$

(Result of a quaternion multiplication between *p* and *q*)

Looking into Hamilton's rule for quaternion algebra equation (2.2.17) there is a way to simplify the multiplication shown in equation (2.2.18).

$$\begin{aligned} pq &= p_0q_0 - (p_1q_1 + p_2q_2 + p_3q_3) + p_0(iq_1 + jq_2 + kq_3) + q_0(ip_1 + jp_2 + kp_3) \\ &\quad + i(p_2q_3 - p_3q_2) + j(p_3q_1 - p_1q_3) + k(p_1q_2 - p_2q_1) \end{aligned}$$

(2.2.19)

(Result of quaternion multiplication *p* and *q* according to Hamilton's rule for quaternion algebra)

2.2.2.1 Quaternions and rotations

As seen earlier in the Euler angle Section 2D rotations with an arbitrary value *ɵ* in the easiest way can be written in a 2D matrix Called M_2 and thus:

$$\begin{bmatrix} x' \\ y' \end{bmatrix} = \mathbf{M}_2(\phi)\begin{bmatrix} x \\ y \end{bmatrix} = \begin{bmatrix} \cos\phi & -\sin\phi \\ \sin\phi & \cos\phi \end{bmatrix}\begin{bmatrix} x \\ y \end{bmatrix} = \begin{bmatrix} x\cos\phi - y\sin\phi \\ x\sin\phi + y\cos\phi \end{bmatrix} \quad (2.2.20)$$

(Basic 2D rotations with orthogonal matrix M_2 setup for a rotation with angle *ϕ)*

Quaternions can also be written as a function of Euler angles in radians[119 124 125]. Pitch is displayed in equation(2.2.21), roll in equation (2.2.22)and yaw in equation(2.2.23). To convert these formulas to degrees they have to be multiplied by $180/\pi$.

$$\phi = \tan^{-1}\frac{2q_0q_1 + q_2q_3}{1-2(q_1^2+q_2^2)} \quad (2.2.21)$$

(Pitch [ϕ] in a function of quaternions)

$$\theta = \sin^{-1}(2(q_0q_2 - q_3q_1)) \quad (2.2.22)$$

(Roll [θ] in a function of quaternions)

$$\psi = \tan^{-1}\frac{(2q_0q_3 + q_1q_2)}{1-2(q_2^2+q_3^2)} \quad (2.2.23)$$

(Yaw [Ψ] in a function of quaternions)

This unique aspect creates the possibility to use quaternions which are not affected by singularities, to transform them to Euler angles when needed. It combines the two together into a new dimension. To refer back to Pitch Roll and Yaw, please see Figure 8.

As shown before in section 1.3.1 the Euler angle method suffers from singularities. Therefore quaternions might offer another opportunity to transpose vectors from the object onto the global system. A 4x4 rotation matrix $R_{(q)}$ consisting of quaternions has been used throughout this thesis and is shown in equation (2.2.24)

$$\mathbf{R}_{(q)} = \begin{bmatrix} (q_0^2+q_1^2-q_2^2-q_3^2) & (2q_1q_2-2q_0q_3) & (2q_1q_3+2q_0q_2) & 0 \\ (2q_1q_2+2q_0q_3) & (q_0^2-q_1^2+q_2^2-q_3^2) & (2q_2q_3-2q_0q_1) & 0 \\ (2q_1q_3-2q_0q_2) & (2q_2q_3+2q_0q_1) & (q_0^2-q_1^2-q_2^2+q_3^2) & 0 \\ 0 & 0 & 0 & (q_0^2+q_1^2+q_2^2+q_3^2) \end{bmatrix} \quad (2.2.24)$$

(Matrix $R_{(q)}$ expressed as a function of quaternions)

Using a matrix multiplication between the translatory acceleration vectors, the transformation between the object and global system can be made. Therefore we can write equation (2.2.25), where $a_{(gs)}$ is the global translatory acceleration, and $a_{(os)}$ is the translatory acceleration in the object system.

$$a_{gs}\left(\ddot{x},\ddot{y},\ddot{z}\right)=a_{os}\begin{bmatrix}x\\y\\z\end{bmatrix}\cdot\mathbf{R}_{(q)}\left(\boldsymbol{q}_0,\boldsymbol{q}_1,\boldsymbol{q}_2,\boldsymbol{q}_3\right) \qquad (2.2.25)$$

2.3: Digital Signal Processing

Digital processing is the processing of signals by digital means[126]. Historically analogue signal processing goes back to early electrical engineering and can still be found in simple radios, and televisions. However, digital signal processing circuits are currently replacing analogue processing in devices such as MP3 players, mobile phones and internet modems which allow the systems to become smaller, more energy efficient and robust[126].

A very important part of digital processing is digital filtering. With systems becoming smaller and therefore more sensitive to the surrounding environment, filtering becomes an essential step in creating new systems. In order to establish which *frequencies* in the signal are noise (i.e. movement artefact, power net frequency) frequency analysis has to precede the actual filtering process. Filtering processes are commonly processed according to Figure 10 where $x_a(n)$ refers to the analog noisy signal which becomes transformed by an analogue-to-digital convertor (ADC) to $x_d(n)$ which is the noisy digital signal. The next block is the actual digital signal processing (DSP) block which performs the necessary frequency analysis and appropriate digital filtering[127].

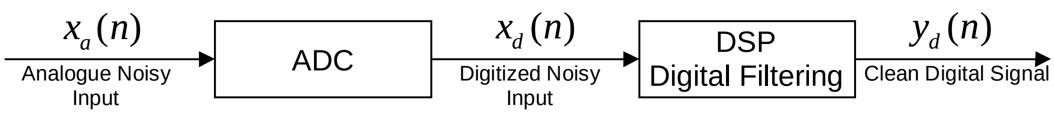

Figure 10 Simple block displaying the analogue to digital conversion (ADC) combined with a simplified digital signal processing (DSP) filtering block according to Tan[127].

The next two short paragraphs will explain the basics and effects of the combination of frequency analysis and digital filtering.

2.3.1 Digital Filtering

Digital filters can be divided in two primary types into, the Infinite Impulse Response (IIR filters) and the Finite Impulse Response filters (FIR filters). FIR filters are also known as recursive filters, as the output is only calculated from current and previous input values. IIR filters on the other hand use the output in addition to input values which rely on previous output values, so there is a feedback within the filter[128]. Using this feedback system an IIR filter requires less memory and calculations than a similar FIR filter[129]. However, IIR filters introduce another aspect of noise into the signal and are often hard to implement in existing applications[128 129]. FIR filters have more advantages as they can be easily designed, simple to implement on existing systems and when not using a feedback system, FIR filters run on less memory, which makes them faster and therefore introduce less noise[128 129].

Sampling theorem states that a continuous-time signal can be reconstructed from discrete, equally spaced samples if the sampling frequency is at least twice that of the highest frequency in the time signal[128]. The sampling frequency is well established and known as $f_s = \frac{1}{\delta t}$ where δt indicates the sampling interval. According to the sampling theorem, the highest frequency that the filter can process is called the Nyquist frequency (f_{nyq}) and can be calculated by using equation(2.3.1)

$$f_{nyq} = \frac{1/\delta t}{2} \tag{2.3.1}$$

Sampling frequencies within gait research performed by using optical motion capture systems range between 50Hz in slow walking[130] up to 100Hz in walking[18 131]. Accelerometers in gait generally have a sampling frequency of 100Hz[71 132].

A filter often used in gait research is the Butterworth filter[71 76 131 133 134] also known as a maximally flat magnitude filter as, the bandpass is mathematically as flat as possible. The specific bandpass for the most common filters are displayed in Figure 11, in which different magnitude responses are shown[129]. The effect of a 2nd order, Butterworth low-pass filter with a cut-off frequency of 13Hz is shown in Figure 12.

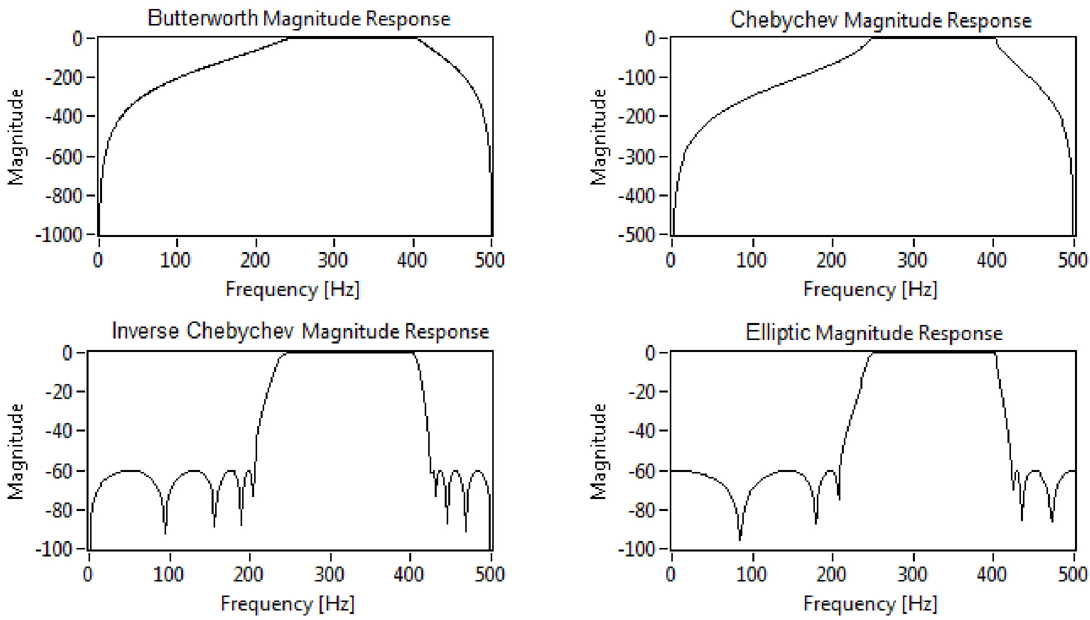

Figure 11 Magnitude response shapes for the most commonly used filters with a stop and pass of the low pass band set at 250Hz and 200Hz respectively. The upper pass band pass and stop frequencies are set at 400Hz and 450Hz.

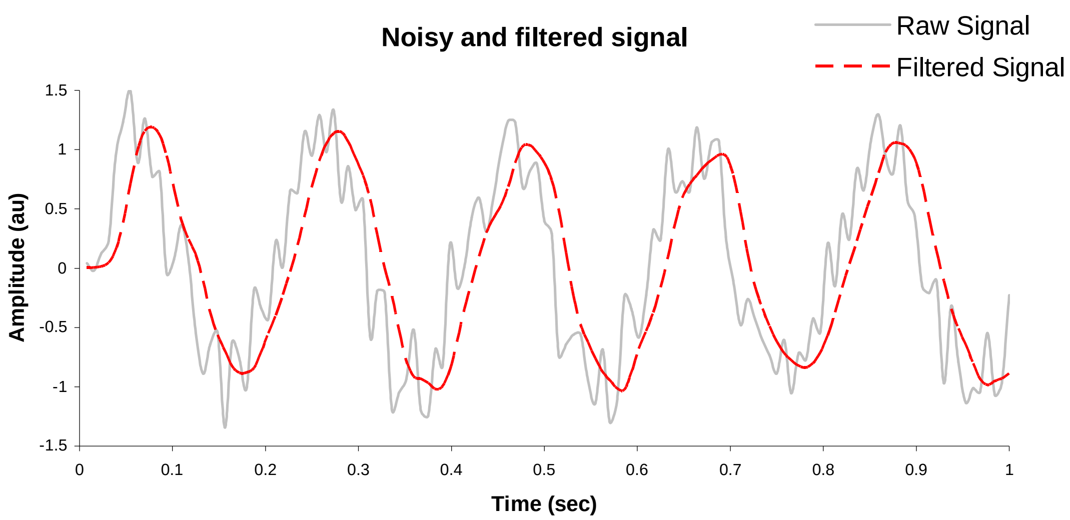

Figure 12 Simple example of a sinewave sampled at 128Hz (*grey solid line*) with additional uniform white noise filtered by a 2nd order, Butterworth low-pass filter with a cut-off frequency of 13Hz (*red striped line*).

The order of digital filtering can be defined as the number of previous inputs used to calculate the current output[126]. Formula (2.3.2) shows a zero order filter.

$$y_n = x_n \tag{2.3.2}$$

Filters can be either act as an amplifier (K>1), attenuator (0<K<1) or inverting amplifier (K<1) as shown in formula (2.3.3):

$$y_n = Kx_n \tag{2.3.3}$$

The order of a filter can be defined as the maximum delay in samples used in creating each output sample[135]. Equation (2.3.4) shows what different order filters look like with respect to their amplification function where the first function if a zero order filter, the second function is a first order filter and the third function is a j-order function:

$$\begin{aligned} y_n &= K_0 x_n \\ y_n &= K_0 x_n + K_1 x_{n-1} \\ y_n &= K_0 x_n + \ldots + K_j x_{n-j} \end{aligned} \tag{2.3.4}$$

By an increase of order within a filter, the cut-off bands are steeper as more previous points are being selected and processed during the filtering process. It also creates a minimal offset (delay) that increases with an increasing order, which becomes apparent in Figure 12.

2.3.2 Frequency Analysis

In order to determine the frequency of a certain signal, a frequency analysis has to be performed. An easy example to explain the use of frequency analysis in combination with filtering is audio sampling. Expensive video cameras have the ability to eliminate the noise caused by the wind touching the microphone by active frequency analysis and filtering. When performing a frequency analysis on this signal containing both signal and noise, it becomes apparent in which frequency bins the actual signal and noise is. In this example of wind a high-pass filter needs to be applied (cutting the low frequencies out of the signal) of about 200Hz[136]. Within walking depending on the research question the general accepted sample frequency is 100-120Hz[18 71 131 132 137 138]. Taking f_{nyq} in mind the maximal frequency is about 50Hz within walking. An example of a Fast Fourier Transform (FFT) analysis is displayed in Figure 13.

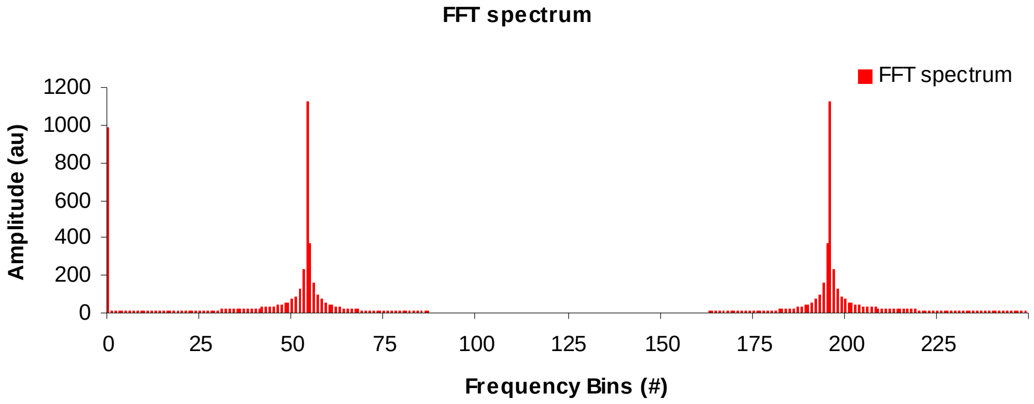

Figure 13 FFT spectrum generated from a sine wave (217Hz, sample rate 1000Hz) divided over 250 frequency bins which show the real and imaginary part with peak amplitude response on frequency bin 54 and 196 which relates to 217Hz.

Discreet Fourier Transform (DFT) analysis is another method to determine frequency responses with in a signal. This however requires more time to process as more operators ($N^2 Log_2(N)$) are included than in a Fast Fourier Transformation (N^2) but will result in a higher resolution of the frequency spectrum[128].

2.3.3 Allan Variance analysis

One way to notice noise, as it is a short time variation in the output, is to look at the peak-to-peak output variation or the standard deviation of the output while the sensor is at rest. These measurements will be in degrees per second ($^0/s$).
Noise can also be defined as a function of frequency and be detected by using a Fast Fourier Transform (FFT) or power spectral density (PSD) analysis. The output of this analysis is often $^0/s/\sqrt{Hz}$ or $(^0/s)^2/Hz$. Depending on the application of a sensor long term measurements error can be expressed in $^0/hr$ and short term in $^0/s$.

Allan variance is a time domain analysis technique originally developed to study frequency stability of oscillators[139]. In the Allan Variance, unknown variables in the known data are assumed to be generated by noise of a specific character. It defines five noise terms known as the quantization noise, angle random walk, bias instability, rate random walk, and rate ramp[140].

Quantization noise occurs at the start of the measurement within the first few seconds before noise of different spectra start to disturb the signal[127]. Quantization noise related to the rounding of analogue numbers when using an analogue-digital convertor is shown in Figure 10. Angle random walk (AWR) is the initial (white) noise that can be measured at start of a measurement, that is directly applicable to angle calculations over a relative short duration[141]. It has been proven that the white noise $(\theta(t))$ increases in linear fashion over time as $\theta(t) = \varepsilon \cdot t$ where ε is the error over time *t* (Thong et al[142]). Since an angular rate sensor measures the rotation rate about its sensitive axis, the output of a rate sensor will be a signal proportional to $^0/hr$. Bias instability is the minimal and most stable part of the Allan variance often measured in $^0/\sqrt{hr}$. This point determines the best given stability for the gyroscope tested and represents the integrity of the MEMS sensor. This could be dependent on temperature sensitivity as well as measurement (validated) and operating (maximum and minimum detectable values) range[143]. Sensors like the Xsens (Enschede, Netherlands) have internal temperature sensors which correct for variation in temperature automatically. Bias instability is always influenced in direct current devices by Flicker Noise, also known as pink noise[127]. These noises exist due to 'impurities' within the electrical systems, which use for example transistors or conductors. When the measurement duration is prolonged there will be an increase in Allan variance which is known as the rate random walk (RRW)[144].

Time series with *n* samples obtained from a sensor can be divided in a certain sample time with duration δt between data points. Taking a constant sample frequency clusters can be created by taking $\delta t, 2\delta t_0, ...m\delta t_0$ where $m < (n-1)/2$. In this way averages of the sum of each cluster can be calculated[140]. Allan variance can be defined as the two-sample variance of the data cluster averages as a function of cluster time[140]. A possible log-log plot is shown in Figure 14.

Allan variance (σ_Ω^2) as a function of logarithmic time intervals (δt) with number of samples (*n*), with data recorded length (*m*) and as a sum of list of average bins (θ_k) is estimated as follows[140]

$$\sigma_\Omega^2(\delta t) = \frac{1}{2\delta t^2 (n-2m)} \sum_{k=1}^{n-2m} (\theta_{k+2m} - 2\theta_{k+m} + \theta_k)^2 \qquad (2.3.5)$$

In order to determine the characteristics of the underlying noise processes the Allan deviation (σ^2) is plotted as a function of δt on a log-log scale[141]. It follows that

$$\sigma^2(\delta t) = \sqrt{\sigma^2_\Omega(\delta t)} \tag{2.3.6}$$

Different types of random process cause slopes with different gradients to appear on the plot, as shown in Figure 14.

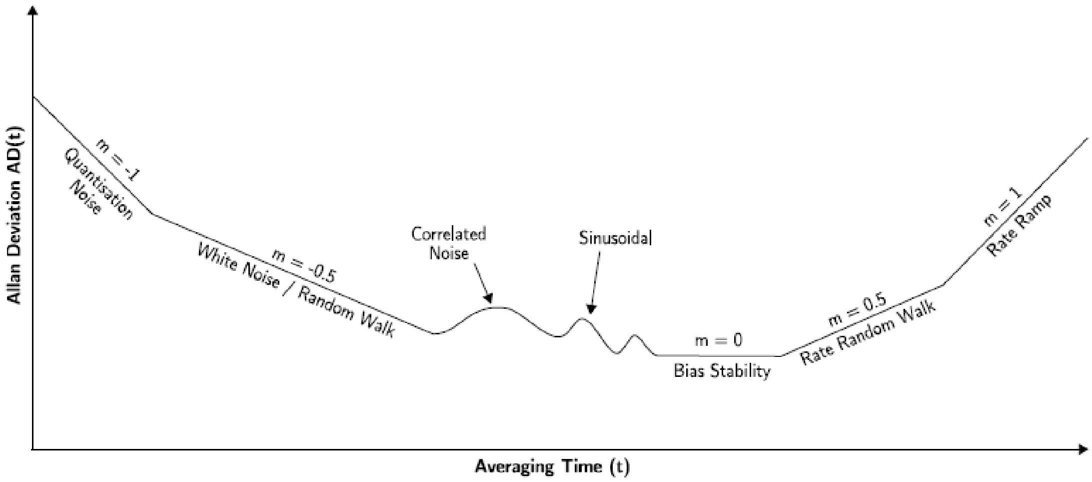

Figure 14 A possible log-log plot of Allan Deviation analysis results[141]

An attempt to perform the Allan deviation analysis on the IMU sensor (MTx, Xsens, Netherlands) failed due to the masses of data and the limitations of own written software (LabVIEW 8.5, National Instruments, Ireland) which required more memory than available. Woodman[141] performed similar analysis in 2007 on these sensors. Results from this study were used to model the drift over durations and to compare the sensors performance against simulated theoretical results. It was found that the first 60 seconds of a measurement are affected by white noise. It was concluded that these sensors could not be used for Inertial Navigation Systems since long term accuracy was impossible to achieve[141].

2.3.4 Integration and differentiation

In order to track the movement of an object in space, the position is needed. Hence accurate integration is needed. The raw output of an accelerometer is acceleration. Acceleration can be expressed as the change of speed over time and be displayed according to the SI (le Système International d'unités[145]) unit as ms^{-2}. The most commonly known form of acceleration is the local gravitational constant (*g*). This constant is averaged globally and equals approximately $9.81ms^{-2}$ as documented in 1901 by the 3rd Conférence Générale des Poids et Mesures (CGPM)[146].

There are several forms of integration. An example of the most commonly known integration is displayed in equation (2.3.7)

$$\int x^n dx = \frac{1}{n+1} x^{n+1} + C \tag{2.3.7}$$

The formula displayed above however cannot be used within numerical integration. One of the possibilities of integration with numerical values is Simpson's rule of Integration which calculates a definite integral[128]. Simpson's rule of integration is displayed in equation (2.3.8). Figure 15 shows the difference between the two integrals shown in equation (2.3.7) and (2.3.8).

$$y_i = \frac{1}{6} \sum_{j=o}^{i} (x_{j-1} + 4x_j + x_{j+1}) \Delta t \tag{2.3.8}$$

It has been shown by Thong et al[142] and Farell and Borth[147] that the standard deviation of the measured position due to acceleration noise, in the absence of drift and initialization errors, increases as $t^{1.5}$, where t is the integration time. Therefore de-drifting signals in their static phase is a commonly accepted method to reduce the drift and therefore increase the accuracy of double integration[148].

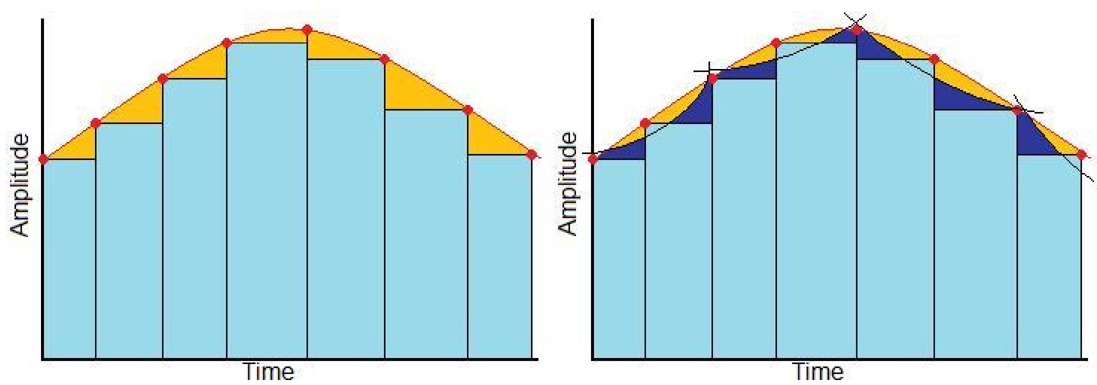

Figure 15 two different types of integrations shown on generated data. The graph on the left showing the standard 'area under the curve' numerical integration and right showing the integration process according to the Simpson's rule of integration taking the residue in account. Using Simpson's rule of integration results in a more accurate integration and therefore cleaner integral of distance over time.

It is worth pointing out that the integration effect is not always deterious. For instance, if the vibration is perfectly symmetric, then the integration effect can actually diminish the error by cancelling out the deviations[149]. Unfortunately these circumstances can only be obtained in perfect laboratories conditions. Overall, error in the measurements will cause the accumulation of speed and distance errors very quickly over a short period of time which can last up to 15 seconds in static state, and less than 5 seconds in dynamic state[150].

This approach to integration has been chosen throughout the methodology of this thesis since the combination of filtering and integration (as shown in the next Chapter) resulted in the most accurate integrals of acceleration to speed and position.

As well as integration there is also differentiation. Differentiation can be defined as the *'rate of change'* of one quantity against another[151]. Error due to rounding will appear within numerical differentiation. This has been formed into a mathematical formula by Kranzer[152] in 1963 and used as a basis to develop more difficult algorithms by current research[153] [154]. Within this aspect differentiation will always be referred to the rate of change of a derivative of distance over time, of which the most commonly used units are displacement [m], velocity [ms^{-1}] and acceleration [ms^{-2}].

2.4: Practical Application

This section will discuss the practical application and outcome measurements from the different digital processing applications as decribed above. Data shown in this section is real data collected by an IMU (MTx, Xsens, Netherlands) applied over the projected CoM during self selected walking in typical developed adults. The aim of this paragraph is to show and justify why certain methods have been chosen above others in order to derive accurate relative vertical position of the projected CoM.

2.4.1 Transposing acceleration vectors from object to global system

As described in Chapter 2.2 there are two main orientation outputs that result from measurements taken from the IMU (MTx, Xsens, Netherlands). Both have their advantages and disadvantages which are mentioned throughout Chapter 2.2.1 and 2.2.2. The aim of this first approach was to explore the Euler angle output in order to rotate the acceleration vectors from the object to global frame by means of the rotation matrix displayed in equation (2.2.8).

Results have shown that they suffer from singularities which could affect measurements taken during walking. A visible example is shown in Figure 16**Error! Reference source not found.** where a subject takes a couple of steps while the trunk tilts over 90 degrees, causing mathematical Gimbal lock.

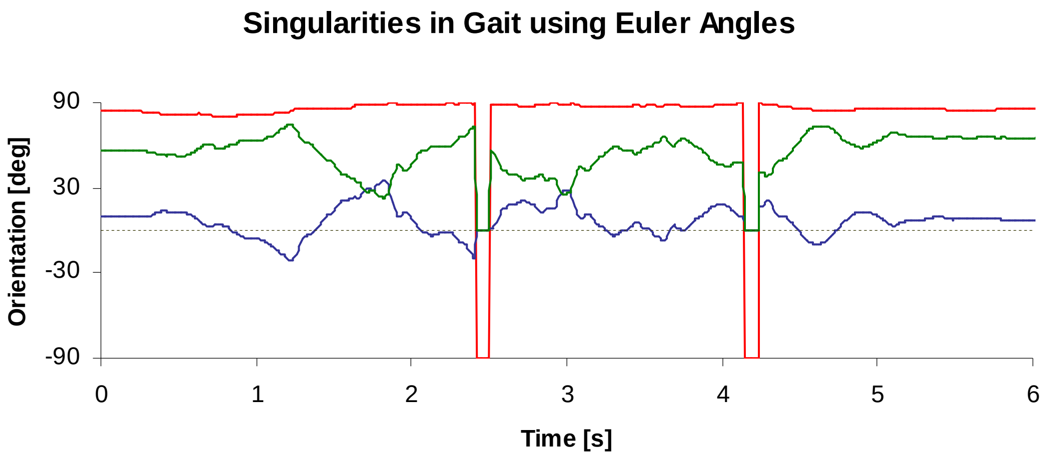

Figure 16 Visible singularities when using Euler angles where the pitch (red line) reaches 90 degrees, where the yaw (green line) and roll (blue line) lose their data accordingly.

Based on these results quaternions have been chosen throughout this work instead of Euler angles as they do not suffer from these singularities. Quaternions at the same time have the benefit that they require less processing power[124] which resulted in less time required to transpose the accelerations from the object to global system.

2.4.2 Double integration process from acceleration to relative position

Another utilized raw output of the IMU measurements is acceleration. As acceleration itself can't be utilized within the gait models proposed in Chapter 1.1.2 double integration of the signal is needed. Within LabVIEW 8.5 there were about 83 general integration methods available. Each could be specified by changing, for example, the integration width, initial and final condition and point-by-point integration. Adjusting these factors will change the outcome of the integration significantly. Therefore the aim of this stage was to explore the effects of different means of integration on the effect of the integral of acceleration.

A typical short sampling integration, according to numerical and Simpson's rule of integration, is shown in Figure 17**Error! Reference source not found.** showing signals from a reference point of real life data over 3.5 seconds. It becomes apparent that there is a short sign wave drift in the position signal which was also reported by

Woodman[141]. It is important to mention that over short time integrations the error is relatively small but will increase by $t^{1.5}$, as mentioned earlier.

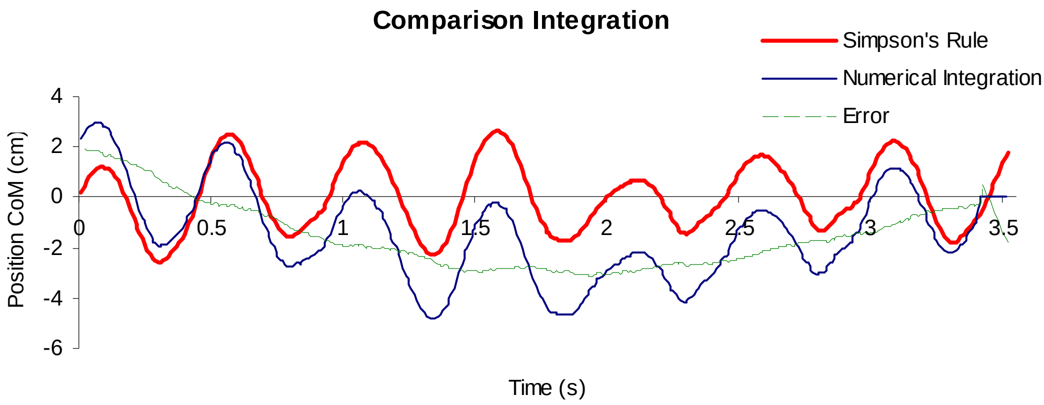

Figure 17 Example of standard numerical integration compared to the Simpson's rule of integration. Blue thin line showing the numerical integration and the red thick line showing the Simpson's rule of integration with the Green line indicating the error over a small measurement period.

These results show that numerical integration is introducing drift in the signal over a short duration of time which increases the error when compared to the Simpson's rule of integration. These results are in agreement with Chapter 2.2.3.

2.4.3 Filtering and de-drifting

As mentioned before, integration alone without additional DSP would cause the signal to drift. The aim of this section was to determine if commonly used filters found in the literature review would suit DSP when processing IMU data.

From literature it was decided to use a Butterworth Filter (4th order, cut-off frequency of 25Hz) which is commonly used throughout biomechanical movement research. Figure 18 shows a practical example of an applied 4th order Butterworth Filter on vertical, un-transposed, gravity corrected acceleration data as recorded by the MTx (Xsens, Enschede) on a typical developed adult. It becomes visible when looking at the difference between the raw and filtered data, that the peak amplitudes of the raw data are suppressed after filtering. Furthermore the offset (as mentioned in Chapter 2.3.1) becomes visible. Fast Fourier Transform analysis showed that with these settings all (unwanted) frequencies below 25Hz were removed from the raw signal.

Therefore it was accepted that a Butterworth filter could be used to filter the vertical acceleration before and between the integration steps.

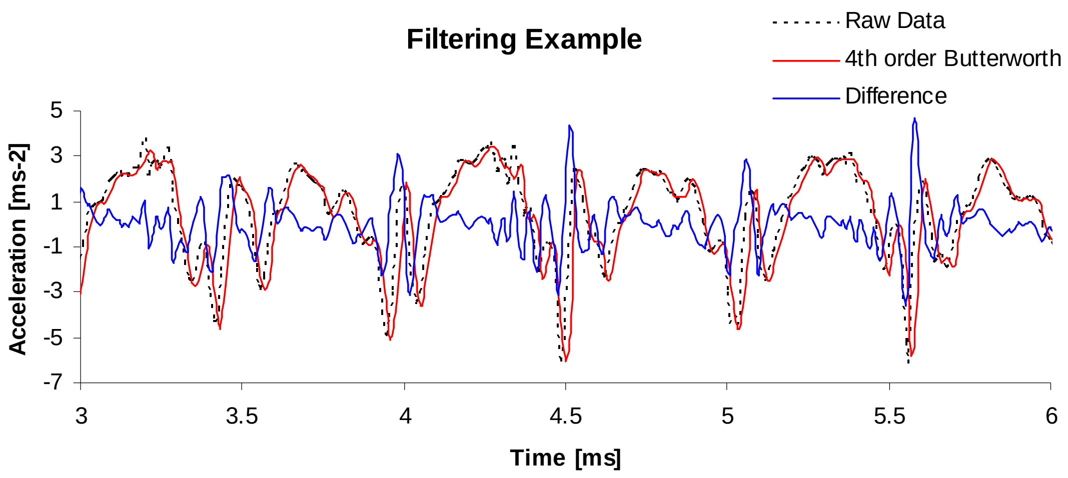

Figure 18 Applied example of 4th order Butterworth Filter on a section of vertical un-transposed but gravity corrected acceleration data over a 10 metre walk in typical developed adults. The dashed line (black) shows the raw data, the red line shows the filtered data with the blue line indicates the difference after filtering.

Additionally by combining the filter with the use of a Hanning spectral analysis (as discussed in Chapter 2.2.3) as an active filter, slow frequency drift can be detected and subtracted. The flow diagram for double integration including DSP throughout this thesis happens according to Figure 19.

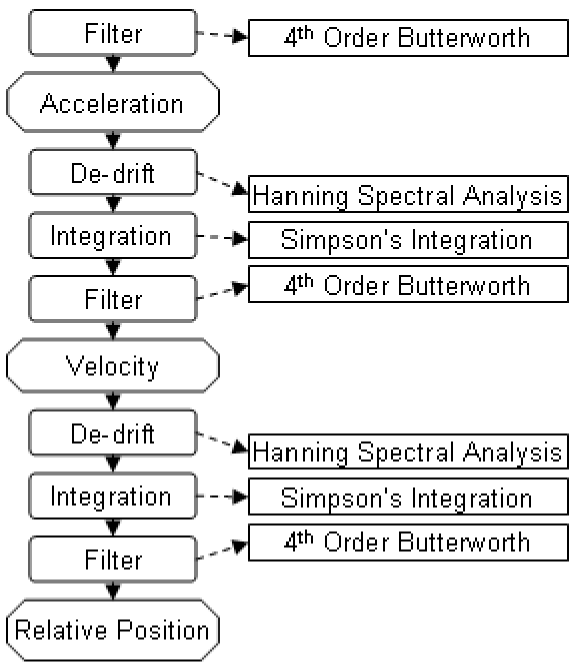

Figure 19 Flow diagram of double integration with parts of the digital signal processing

Throughout this chapter it becomes clear which parts of digital signal processing needed to be done in order to drive the gait models from Chapter 1 with data gathered by IMU devices attached to the projected CoM. As seen above there are many factors that have to be considered to measure vertical displacement of an object in space.

In the following chapters the CoM vertical acceleration is measured after which it is transposed from object to global system by combining the Quaternion output. The Quaternions are chosen as they are free of risk of singularities. After rotation double integration of the signal according to Simpson's rule of integration is performed to minimize the error. Furthermore low frequency drift is subtracted between each integration by means of a Hanning Window. The combinations of these steps are sound; however they need to be validated against the gold standard of OMCS in order to determine their accuracy.

Chapter 3: IMU Validation with OMCS

3.1 Relevant Publications to chapter

Esser P, Dawes H, Collett J, Howells K. IMU: Inertial Sensing of Vertical CoM Movement. *Journal of Biomechanics* 2009;42:1578-81.

Esser P, Dawes H, Collett J, Howells K, Maynard K. United Kingdom patent UK0823374.4 (*Applied for*)

3.2 Summary

The aim of this Chapter was to examine the accuracy of a method utilizing a quaternion rotation matrix in combination with an integration approach to transform translatory accelerations from the object to the global frame. Measurements were taken from the centre of mass (CoM) using an inertial measurement unit (IMU) during walking. Secondly this chapter utilised double integration to determine the relative change in position of the CoM from the vertical acceleration data. The results showed that quaternions, in combination with Simpsons rule of integration, can be used in transforming translatory acceleration from the object frame to the global frame and therefore obtain relative change in position, thus offering a solution for using accelerometers in accurate global frame kinematic gait analyses.

3.3 Introduction

Optical motion capture systems (OMCS) are often used for kinematic analyses of an object in a 3 dimensional calibrated volume and are seen as the gold standard[155]. The downside of these systems is that they are relatively expensive, and time consuming and not easily applicable outside laboratory conditions[156]. Accelerometers may offer an alternative way to obtain kinematic data and offer opportunities to utilize motion analyses in a wide range of objects[3 157]. However, when using accelerometers, certain methodological problems need to be addressed[23]. When using accelerometers on cyclic movements, such as in human gait, the 3D axes rotate while moving. Thus vectors in the object system are not equal to the global system, and do not allow speed and displacement to be derived in relation to the environment.

Commercially available systems combining accelerometers, gyroscopes and magnetometers into an algorithm, known as Inertial Measurement Units (IMUs), create the possibility to transpose translatory acceleration from the object system to the global system using a rotation matrix[2 31].

Conventional rotation matrices use Euler Angle matrices to perform their rotations[2 31 33]. Euler Angle rotation matrices show singularities when using a certain sequence of rotations. Quaternions (as discussed in section 2.2.2, page 30) are geometrical operators that represent rotations by using complex numbers forming an algebra existing of 4 scalar variables[121 158]. Quaternions require less time than other representations and are not affected by singularities[123 124]. In addition the existence of an algebra (i.e. quaternion algebra) means that simple expressions may be developed for complex rotations and rotating reference frames[123].

This study investigated a lower spine point estimate of Centre of Mass (CoM), as it offers a simple reference to indicate global gait quality[98]. Quaternions were chosen as rotation matrix operators, as fixation of an IMU over the lower spine has an increased risk of showing singularities using conventional methods, due to anatomy and movement of the lower back during walking.

3.4 Materials and Methods

3.4.1 Subjects and experimental design

Four men and one woman (age: 23.4 ± 3.8 years, weight: 80.5 ± 14.3kg and height: 181 ± 5.4 cm) volunteered for the study. The IMU (MTx, Xsens, Enschede, Netherlands) was fixed with adhesive tape, at an angle of $\pm 90^0$ (due to sensor design), over the 4^{th} lumbar vertebra. A reflective marker was placed on the middle of the IMU to measure the displacement with the OMCS (Proflex, Qualisys, Stockholm, Sweden). Both systems were synchronized and measured at a sample frequency of 100Hz.

Before the subject walked through the three dimensional calibrated measurement volume, they were asked to stand rigid for three seconds for baseline gravitational measurements. Subjects walked three times through the calibrated measurement volume at their self selected walking speed (SSWS).

Global axes are defined as, *x* being forward movement in the transverse plane perpendicular to the frontal plane, *y* pointing to the left in the transverse plane perpendicular on the sagittal plane and *z* upwards vertical movement in the frontal plane perpendicular to the transverse plane[68].

3.4.2 Data analyses

Position data of the OMCS was smoothed by using a Savitzky-Golay smoothing filter[159] with a window of 5 points. Acceleration was symmetrically derived from position[160] by using $\vec{a}_z = (\Delta^2 \vec{r}_z) / \Delta t^2)$ where $\vec{a}$ represents the translatory acceleration in the object frame, and $\vec{r}$ represents the position of the reflective marker in the calibrated global frame.

IMU data was analysed using LabVIEW 8.5.1 to transpose the accelerations from the object system onto the orthogonal system using a matrix multiplication. (3.1)

$$a_{(gs)} \begin{bmatrix} x \\ y \\ z \end{bmatrix} = a_{(os)} \begin{bmatrix} x \\ y \\ z \end{bmatrix} \cdot R_{(q)} \begin{bmatrix} q_0 \\ q_1 \\ q_2 \\ q_3 \end{bmatrix} \tag{3.1}$$

Where $a_{(gs)}$ is the translatory acceleration in the global system, $a_{(os)}$ is the translatory acceleration in the object system displayed as a 3x1 matrix and $R_{(q)}$ is the quaternion rotation matrix with q_0 as real value and q_1,q_2 and q_3 as complex numbers combined in a 4x4 matrix. Rotation matrix $R_{(q)}$ is displayed in equation(3.2).

$$R_{(q)} = \begin{bmatrix} (q_0^2+q_1^2\text{-}q_2^2\text{-}q_3^2) & (2q_1q_2\text{-}2q_0q_3) & (2q_1q_3+2q_0q_2) & 0 \\ (2q_1q_2+2q_0q_3) & (q_0^2\text{-}q_1^2+q_2^2\text{-}q_3^2) & (2q_2q_3\text{-}2q_0q_1) & 0 \\ (2q_1q_3\text{-}2q_0q_2) & (2q_2q_3+2q_0q_1) & (q_0^2\text{-}q_1^2\text{-}q_2^2+q_3^2) & 0 \\ 0 & 0 & 0 & (q_0^2+q_1^2+q_2^2+q_3^2) \end{bmatrix} \tag{3.2}$$

A 4th order Butterworth low-pass filter with a cut-off frequency of 25Hz was applied to the transposed acceleration. An average of the gravitational forces during rest was set to -1G (-9.82 ± 0.02 ms^{-2}) and subtracted from z-axis translatory acceleration in order to make a comparison with the z-axis data from the optical motion capture system.

The gravity corrected acceleration in the global frame was de-drifted by subtracting the estimate of the DC component determined by using a Hanning window of 3 points, as previously described by Karié et al[161]. Afterwards the signal was integrated to velocity [ms^{-1}] according to Simpsons rule[128] as described in equation(3.3), with the initial and final condition being zero as a state of rest assumed at the start and end of measurement. By repeating this step, relative position [*cm*] could be achieved. Dedrift value was calculated by 3rd order polynomial and applied to the relative position. Differences between peak and trough were taken to calculate relative change in velocity and position. Error in velocity and relative position was calculated as being the difference between the OMCS and IMU at t_n. Random error of acceleration, velocity and position was calculated as twice the standard deviation. Step time was calculated as being the difference in time between the troughs in position.

$$y_i = \frac{1}{6}\sum_{j=o}^{i}(x_{j-1} + 4x_j + x_{j+1})\Delta t \qquad (3.3)$$

3.4.3 Statistical analyses

Peak amplitudes of acceleration, velocity and position for each gait cycle in vertical direction were extracted from both data sets and imported into SPSS 14 for Windows. Data sets were compared using a paired sample *t*-test and a Two–Way Mixed effect with consistency Intra Class Correlation test (ICC) according to McGraw[162] et al. BIAS, defined as the mean of differences between tests and standard deviation was calculated. Also a partial linear correlation test between the speed in the x-axes and the BIAS was performed. Adequate test-retest reliability was defined as an ICC $\geq$ 0.75 for continuous variables[163].

Relative peak and trough difference of velocity and position of the CoM in the vertical axes were calculated for both systems and compared using a paired sample *t*-test. A Two-Way ICC was performed as previously described. Error described as the relative difference in speed and position of the OMCS subtracted from the IMU error was calculated for as many peaks and troughs as were visible in both data sets.

3.5 Results

The data is displayed in Table 2 and Figure 20. Table 2 shows the average difference and standard deviation over 3 walks for 5 healthy subjects in the *z*-axis. Error between both systems of a representative participant is plotted in Figure 20.
The data between the IMU and OMCS acceleration shows good agreement between the OMCS and IMU.

Table 2 Mean data collected from IMU and OMCS over 3 walks for each subject including the standard deviation calculated over the three walks.

Subject	$\Delta\, \boldsymbol{a}_{IMU}$ (ms^{-2})	$\Delta\, \boldsymbol{a}_{OMCS}$ (ms^{-2})	$\Delta\, \mathbf{v}_{MU}$ (ms^{-1})	$\Delta\, \boldsymbol{v}_{OMCS}$ (ms^{-1})	$\Delta\, \boldsymbol{p}_{IMU}$ (cm)	$\Delta\, \boldsymbol{p}_{OMCS}$ (cm)
1	2.16 ± 0.30	2.36 ± 0.26	0.40 ± 0.06	0.44 ± 0.06	4.11 ± 0.40	4.22 ± 0.44
2	2.65 ± 0.26	2.70 ± 0.20	0.57 ± 0.05	0.57 ± 0.04	5.08 ± 0.29	4.99 ± 0.40
3	1.75 ± 0.17	1.92 ± 0.18	0.36 ± 0.01	0.36 ± 0.01	3.34 ± 0.27	3.34 ± 0.07
4	1.58 ± 0.09	1.83 ± 0.10	0.31 ± 0.05	0.35 ± 0.04	3.24 ± 0.38	3.33 ± 0.36
5	2.38 ± 0.08	2.64 ± 0.09	0.45 ± 0.01	0.47 ± 0.05	4.42 ± 0.13	4.43 ± 0.48

Z-axis amplitudes from the IMU (2.1 ± 1.2 ms^{-2}) and the optical motion capture system (2.3 ± 1.2 ms^{-2}) were not significantly different ($p \geq 0.05$) indicating agreement between systems. In addition ICC = 0.952 and random error 0.176ms^{-2} also demonstrates strong agreement between systems. The partial linear correlation among subjects, between speed in the x-axis in the orthogonal system and the BIAS (Figure 21) were not correlated (r^2 =0.065).

A paired sample t-test between the relative change in speed (peak to trough) in the OMCS and IMU shows a significant difference (p<0.05). A Two-Way Mixed ICC was performed as previously described and showed a significant relationship between the IMU and OMCS (ICC=0.888 and p<0.01) with a random error of 0.121ms-1. Error between the OMCS and IMU is visible in Table 4.

A paired sample *t*-test between the relative position (peak to trough) in the OMCS and IMU shows no significant difference ($p \geq 0.05$). A Two-Way Mixed ICC shows a highly significant correlation (ICC =0.782 and $p<0.01$) and a random error of 1.35cm.

Step time (shown in Table 3) showed no significant difference ($p \geq 0.05$). A two-way mixed ICC showed a significant correlation (ICC=0.757 and p<0.05) with a random error of 8.62ms.

Table 3 Step time calculated as the difference in time between troughs of position measured by the IMU and OMCS

Subject	**Step time$_{IMU}$** [s]	**Step time$_{OMCS}$** [s]
1	0.598 ± 0.01	0.591 ± 0.02
2	0.572 ± 0.01	0.571 ± 0.01
3	0.632 ± 0.01	0.633 ± 0.01
4	0.615 ± 0.01	0.616 ± 0.01
5	0.579 ± 0.02	0.567 ± 0.03

Table 4 Error between Inertial Measurement Unit and Optical Motion Capture System displayed as the mean value over 3 walks between subjects.

Error in *z*-axe IMU-OMCS over three walks				
Subject	***a*** **[ms^{-2})**	***v*** **[ms^{-1}]**	***p*** **[cm]**	**Step time [s]**
1	-0.197	-0.037	-0.026	-0.064
2	-0.050	-0.004	-0.128	0.108
3	-0.260	0.006	0.002	0.100
4	-0.268	-0.039	-0.091	0.015
5	-0.174	0.014	0.008	0.377
avg	-0.190	-0.012	-0.047	0.107
std	0.088	0.025	0.060	0.166

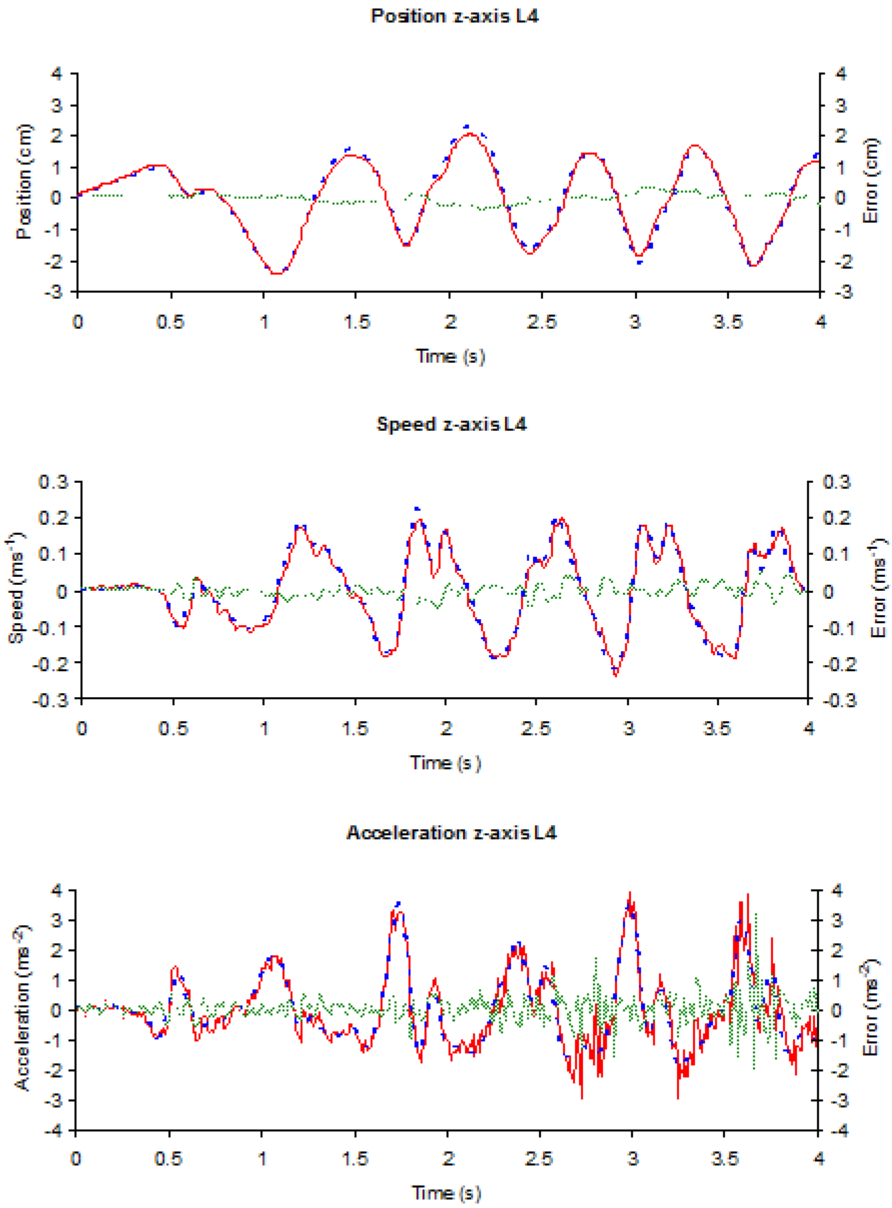

Figure 20 Representative data collected from a subject 3 who initiated their gait at t_0 and walked out of the pre-calibrated frame of the optical motion capture system at t=*4*s (capture volume of 2.8m for this subject). Graphs are showing relative position, speed and translatory vertical acceleration from subject 3. The blue dotted line represents the IMU, and the solid red line represents the OMCS. The acceleration, speed and position are de-drifted using the DC estimate acquired by using the Hanning window. The dotted line represents the *overall* error which is calculated as the data at the difference between OMCS and IMU at t_n

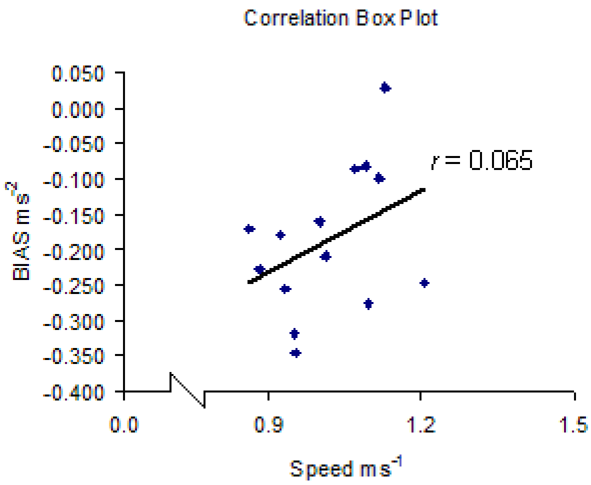

Figure 21 Correlation Box Plot representing the speed in the orthogonal x axes compared with the BIAS between the peaks of the IMU and OMCS

3.6 Discussion

This study found that the mathematical transformation using quaternions in combination with double integration according to Simpsons rule applied to IMU data resulted in accurate speed and relative position in the global z-axis during self selected walking.

Translatory acceleration in the global axes showed a high correlation between the IMU and OMCS data. There was no significant difference in IMU and OMCS peak acceleration. However, an error is visible when comparing both signals in the *z*-axis. The OMCS is the gold standard for measuring position with an accuracy of ±0.1% of motion capture volume[164 165]. When deriving position to speed and finally acceleration the error increases with each step[166]. This error can result in higher peak accelerations due to artefacts which have been multiplied by the differentiation process. These errors are unavoidable due to the limitations in primary output of both systems.

Farrell[147] has shown that the standard deviation of the measured position due to acceleration noise, in the absence of drift and initialization errors, increases as $\varepsilon = t^{1.5}$ where t is the integration time and ε the error[167]. Therefore a de-drifting technique using the Hanning window[161] was applied after every integration in order to resolve this.

There was a significant difference in z-axis CoM speed between the IMU and OMCS, However peak and trough difference was highly correlated demonstrating good agreement between systems. Due to the typical double peaks in the speed data, Δv becomes less accurate to calculate as the peaks vary during locomotion. There was a strong correlation, as the difference in peak and trough followed each other in IMU as well in OMCS data, but a significance difference between peak speeds were not equal between both systems as the average peak is taken. Error in speed compared between the average error and OMCS was less than -2.5%.
Deriving position from the IMU requires two steps of integration. The error increases during this process. After subtracting the drift from the signal it becomes apparent that both signals were not significantly different. Position compared between the IMU and OMCS shows a highly significant correlation.
Errors in translatory acceleration, speed and relative position can be introduced due to the use of a low-pass filter. The dampening effect of the low-pass filter has been addressed by Kartić et al[161] and shows a reduction in the peak and trough amplitudes within commonly used averaging filters. Error in relative position compared between the average error and OMCS was shown to be -1.2%

Limitations of the present study need to be considered. Participants walked at SSWS and therefore the results may not apply to extreme walking speeds. However, the results show no correlation between the BIAS and the SSWS, suggesting that the error was not related to the speed of participants. The correlation between walking speed and accuracy of the presented method needs to be addressed in future research in a wider range of speeds.
Skin movement has been observed to influence data accuracy[168]. Different techniques have been used to reduce the skin artefacts on signal such as firm fitting belts[23], Velcro straps[169] and direct skin fixation (e.g. taping). In the presented method, however, at the location of the projected CoM skin movement is minimal as shown by Fuller et al[170]. The marker was fixed on the IMU and therefore skin movement artefact between IMU and OMCS data collection should be equal. The only difference would occur with angular displacement of the IMU resulting in increased acceleration with radius. The IMU needs to be placed over the projected CoM (lower spine) at an angle of ±90 degrees due to curvature of the back which increases the risk of losing data as a result of mathematical gimbal lock[171]. In this present research,

this will not be noticeable as only one dimensional movement is required, but in planned future research this might be of interest.

Issues regarding IMU sensor accuracy are critical for this method. A combination between gyroscopes, magnetometers and accelerometers fused into a Kalman algorithm resulted in an almost driftless orientation signal[2,31]. However, it has been shown by several researchers that in static as well as in dynamic circumstances the RMS error is >15^0 and >30^0 respectively[172,173]. We utilised an IMU from the same supplier as used in this research. Cutti[174] compared the manufacturer specifications with collected data and found that instead of the 3^0 RMS error there was a 12^0 error.
Pfau et al[17] showed that, with tracking position in horses with an IMU placed horizontally on the horses back, errors in z-axis in walk, trot and canter are respectively within -0.6; +0.6mm, -4.3; +4.9mm and -4.5; +5.1mm in comparison with OMCS. These values were obtained using Euler angles and using a step-by-step analysis method described in previous publications[17,33]. Our results however show good correlation between measurement systems with the IMU placed in the vertical plane. For this method, the IMU used in this research was sufficiently accurate for short periods of measurements (~10 seconds) as only a few strides were required. There is a need however to look into long term effects of drift

Our results show good agreement between IMU and OMCS over short time measurements. However, error over time is affected by drift[2]. Therefore it has to be noticed that this method is valid for short term measurements but for long term measurements further research is required. Furthermore in order for this method to have clinical value, validation in patient groups is needed.

Chapter 4: Parkinson's disease

4.1 Summary

Parkinson's disease is one of many long term neurological conditions which affect people around the world. With the cause unknown and the increasing number of people suffering from Parkinsonism symptoms this condition threatens to overtake cancer as the second most common cause of death by 2040. This chapter sets out to explore the underlying symptoms of Parkinson's disease focussing on motor symptoms, their effect on gait and the most used measurements when describing gait in Parkinson's disease.

4.2 Parkinson's Disease

Parkinson's disease (PD) is a neurodegenerative disorder of unknown cause, which is mainly related to progressive loss of dopaminergic-cells in the substantia nigra, a brainstem structure belonging to the basal ganglia[175]. It has been estimated that there are 400,000 dopaminergic neurons in the substantia[176]. Interestingly about 80% of the dopamine needs to disappear before the first symptoms of PD become visible[176 177]. First symptoms were discovered by James Parkinson in 1817 followed by another hundred years until the cause was found in the substantia nigra and another 40 years to find the deficit in dopamine[178]. The World Health Organisation (WHO) reported[179] that PD is expected to overtake cancer as the second most common cause of death by the year 2040. A study by Elbaz et al[180] revealed that there is a 1% chance of developing PD before the fourth decade. Another study by Marras et al[181] showed that over a 13 year period 37% (out of 800 participants) participants, suffering from PD, died. The medical costs for people with PD in the United States were estimated to be £7 billion in 2009, of which 58% was related to direct medical costs[182]. This worked out to be £6,545 to £8,434 more than people requiring medical care who did not suffer from PD that year.

PD is considered to be an age related neurodegenerative disorder with symptoms usually starting after the fifth decade of life[183]. About 7% of the general population will develop parkinsonism symptoms after their fifth decade[184]. Recent studies however have shown that in 2.7% of people with PD the disease is drug induced[185]. The prevalence within the United Kingdom is estimated between 6 – 11 per 6000 people with a rising prevalence and incidence in males[186]. It has also been assumed that the biology of the disease might start earlier in life and be dependent on several environmental[178 187-189] and inherited factors[190] (see Figure 22). PD can be divided in three main groups based on age. PD with an onset after the age of twenty is classified as *juvenile*-onset PD, before the age of fifty is also known as *early*-onset of PD, the onset above the age of fifty are considered to have *late*-onset PD[191]. Clinical pathological studies have suggested that the pre-symptomatic phase of PD starts about 4 to 6 years prior to the onset of the symptoms[190]. Barlow et al[189] suggest that the amount of environmental '*hits*' can determine damage to the dopaminergic-cells during perinatal and prenatal periods and therefore speed-up symptoms of PD. A recent study by Tanner et al[192] found that there was an increased risk of developing Parksonism symptoms when working with pesticides. However there was no relation found between any specific occupation and the early onset of Parkinson's disease (<50years)[192]. As such the presence and prediction of PD is variable.

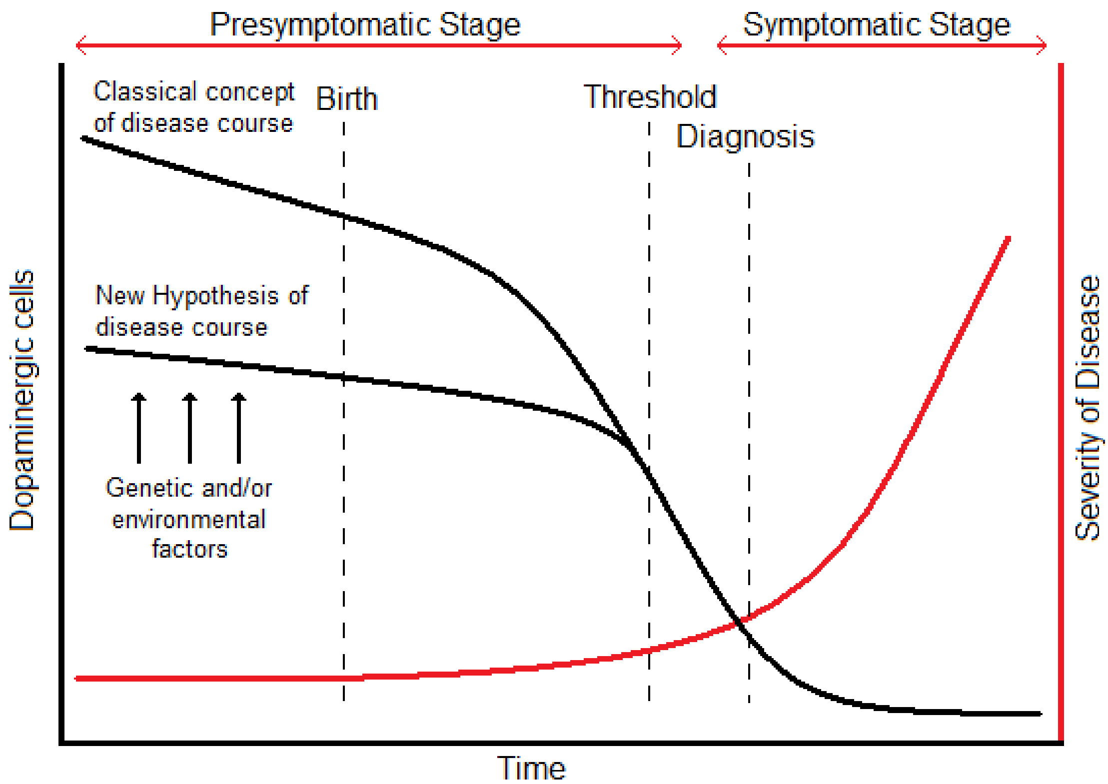

Figure 22 Common concept of Parkinson's Disease course and the new disease course suggested by Le et al[183] and Barlow et al[187] which shows that the disease starts at a very early age, perhaps even during pre or perinatal periods. (Source Le et al[183], Etiopathogenesis of Parkinson Disease: A new beginning?)

It has also been shown that PD can have a negative effect on the quality of life[193]. Hristova and colleagues[193] have shown that under a sample of 866 participants with PD, there was a significant lesser score on *'mobility'*, *'activities of daily living'* and *'emotional well-being'* on the Parkinson's Disease Questionnaire (PDQ-39) quality of life questionnaire. This and other research shows that there is an increasing need to understand how to diagnose and treat PD at an early stage[194 195].

4.2.1 Pathophysiology of Parkinson's Diseases

There are several differences between voluntary movements and reflexes. Voluntary movements are organized around the optimal performance of a task and can be divided into three stages. First of all a plan of the movement to reach the objective or goal is made, followed by the program in which the necessary movements are described in kinetic and dynamic variables for which the body has to adapt[177]. The final stage is the execution of the movement with a feedback loop to adjust the program to adapt for variables. Reflexes on the other hand are involuntary motor responses initiated by a stimulus applied to the peripheral receptors[196].
The following paragraph will explain the role of the basal ganglia, which is involved in movement coordination, in typical developed adults. Later in this chapter these control mechanisms will be discussed in relation to Parkinson's disease.

The basal ganglia consist of three main nuclei, the caudate, putamen and the globus pallidus[197]. The global pallidus (GP) is the most primitive structure present and is divided by the *medial medullary lamina* into the internal (GPi) and external part (GPe) which is bigger than the GPi. The two remaining and smaller nuclei are the substantia nigra (SN) and the subthalamic nucleus (STN)[197]. The major outputs of the basal ganglia can be found in the GPi and the ventral region of the SN, also called the '*substantia nigra pars reticulata*' (SNr) which are connected to the thalamus[177 197]. Wide areas of the cerebral cortex create the input for the basal ganglia, after which the processed signals are returned through the thalamus back to the cerebral cortex, creating a cortex-basal ganglia-cortex loop[197 198]. This cycle can be divided into the direct and indirect pathway. Information from the direct pathway flows from the caudate and putamen to the GPi and SNr whereas the information from the indirect pathway flows via the GPe and STN which have no direct output to the thalamus[197].
The thalamus is part of the diencephalon together with the hypothalamus. The thalamus integrates motor information coming from the basal ganglia and redirects it to the motor control areas on the cortex. It is also the essential link between the sensory information returning towards the cortex[199].

Dopaminergic cells can be found in the substantia nigra which deliver dopamine to the caudate and putamen, which inhibits the neuronal motor pathway. To be more specific, dopamine inhibits the neurons of the indirect pathway, and excites the neurons of the direct pathway[200]. Dopamine receptors can be found throughout the central nervous system (CNS) There are two main groups of receptors, the D_1 and D_2 family receptors which are excitatory and inhibitory respectively[201]. Knowing that the indirect pathway is inhibited by dopamine, there must be D_2 receptors present and vice versa. Research by Severson et al[202] in 1982 showed a decrease in dopaminergic binding sites in the caudate nucleus and SN due to age by a factor of three. They found however that there was no reduction in binding sites in the putamen.

The output of the basal ganglia to the cerebellum can be responsible for voluntary movements such as mastication[203] or locomotion[204] as mentioned above. The outputs of the cerebellum are excitatory, while the outputs of the basal ganglia are inhibitory.

Dopamine is produced by dopaminergic-cells in the substantia nigra (SN) from where it is being transported to the caudate and putamen. Studies using positron emission tomography scanning within people suffering from PD showed that after administering fluorodopa, radioactivity was highest in the corpus striatum, indicating a high metabolism of fluorodopa within the corpus stratium[205]. This indicates that the dopaminergic cells within the SN are degenerating, since Levodopa is replacing the need for dopamine within the corpus striatum.

The presence of Lewy-bodies in neurons is a well known histology marker of idiopathic PD[206 207]. Until recent it was not possible to detect the presence of Lewy-bodies in PD without straining of post-mortem brain tissue. Koh et al[208] developed a way to detect Lewy-bodies in midbrain tissue by using phase contrast radiography but only post-mortem.

4.2.2 Motor characteristics of Parkinson's Disease

Typical motor symptoms such as bradykinesia, resting tremor, rigidity, freezing, also known as cardinal symptoms, are typical for Parkinson's disease[178]
Bradykinesia refers to the slowness of movement and is the most characteristic clinical feature of PD. The initial expression of bradykinesia is often slowness in performing activities of daily living and slow movement and reaction times[209]. Weakness, tremor and rigidity may contribute to, but can not fully explain bradykinesia[209].

Resting tremor is the most common and easily recognised symptom of PD. Tremors are unilateral and occur at a frequency ranging between 4 and 6Hz[191 210] and are often found at the end of the upper limbs (hand and fingers) but can also spread to the lower limbs[209].It has however been shown by Hughes and colleagues that tremors do not occur in all cases and can disappear during the progressions of the disease[211].

Rigidity is cause by an increased resistance during movement. This can also be accompanied by a circular jerking rigidity combined with a slight tremor, which is known as the *cogwheel phenomenon*[211]. Rigidity often limits the range of limb movement which on its turn can decrease the distance in the swing phase during walking[212].

Freezing of gait is a characteristic feature of PD, however does not occur in all cases[213]. AResearch by the German Parkinson Association reported that 47% out of 12,000 members experienced freezing during gait initiation and it occurred less in people who experienced tremors[214]. There are several sub-types of freezing[215], however tricks such as walking to music or shifting body weight can overcome these freezing moments[216 217].

As shown above, the Basal Ganglia plays a role in the planning, initiation and execution of movement. With a decrease in dopamine production these functions become decreased[204]. It is therefore not unsurprising that the cardinal symptoms of Parkinson’s disease correlate with the degree of dopamine deficiency[218].

Other symptoms include postural instability and deformity as well as disturbed blinking rate, speech disorders or respiratory disturbances[178].

4.2.2.1 Functional effects of motor symptoms

The cardinal motor symptoms affect function and activities of daily living. Buckley et al[219] let patients with PD make the transition from sit to stance to walk (SSW) and found that some participants had trouble in making this transition. A study from Franzén et al[220] concluded that patients with PD in the ‘*off*’-state (person not under the influence of any medication for Parkinsonism symptoms) had a reduced SSW performance including higher muscle tones which affected posture and therefore balance. Studies looking at the impact of gait disorders within the PD community showed that gait disorders have a substantial impact upon the ‘*quality of life*’ with extra attention to the ‘*fear of falling*’[221]. Research directed at fall detection confirm that cadence[222 223] or walking speed[224] can predict a history of falls within healthy age matched controls.

Other research looking into sit-to-stance (STS) and gait initiation (GI) phases by means of a '*Timed get-up and go*' test showed that there are clear differences between healthy and neurological groups[225]. When looking in more detail into the STS and GI phases there was a clear overlap of both within healthy young adults, however with age these phases seemed to become more separated[225 226]. This separation of phases found was also found within the Parkinson's population[227]. This could partially be explained by impaired balance[227], fear of falling[228] or affected posture stability[229]. Therefore Buckley et al[225] suggest that healthy elderly as well as people with PD prioritise stability versus speed.

4.2.3 Non-motor characteristics of Parkinson's Disease

Besides motor symptoms there are also less noticeable symptoms in people who suffer from Parkinson's Disease. Symptoms such as anxiety, fatigue and sleep disorders have been described[230]. Moreover, psychosis, depression and cognitive problems have been mentioned with a strong correlation with disability in PD[231 232]. A study by Raudino[233] studying 47 PD participants revealed that 60% recognized non-motor symptoms. These were classified in autonomic, cognitive and sensory symptoms and were not related to age, severity or length of the disease[233]. Rinne et al[234] showed a relation between dementia and Parkinsonism when looking at neural loss in the medial SN. The most common form of dementia in PD is dementia with Lewy Bodies. Cognitive problems within PD affect 80% of the PD population[235]. Another 30% will suffer from mild to profound dementia at a later stage which makes this condition a very frequently disabling non-motor complication[236 237].

4.2.4 Current diagnosis and treatment of Parkinson's Disease

According to the '*United Kingdom Parkinson's Disease Society Brain Bank Clinical Diagnostic Criteria*' PD can be determined in three steps[211 238], the first of which is the typical Parkinsonism symptoms such as bradykinesia, tremor and muscle rigidity. The second and third steps are related to specific inclusion and exclusion criteria as shown in the table first printed by Hughes et al[211] (see Appendix 10.1)

Currently there is no cure for PD, however some drug companies like ProSavin (Oxford BioMedica, UK) have recently launched phase III trails to investigate if the production of dopamine could be stimulated[239]. Furthermore developments such as stem cell treatment could be the solution to the degeneration of dopaminergic cells in the substantia nigra[240]. However since these treatments are still in the experimental stages future research needs to point out if they are actually effective.

Medical treatment for people with PD is considered as being on a ‘honeymoon’ within the first few months since they enjoy symptomatic relief with minimal side effects[241-243]. Levodopa is the most successful and most often used treatment to reduce motor and non-motor symptoms specific to PD[238]. Research showed that while under treatment of Levodopa, the effects on motor as well as non-motor functions could start wearing off after two years of treatment[244 245]. Therefore Levodopa is not often used in mild symptoms of PD. In these stages the use of monoamine oxidase type B (MOA-B) inhibitor or a dopamine agonist is preferred[246]. A typical and often used MOA-B is l-Deprenyl. One of the most famous branded drugs containing l-Deprenyl is Seleginine. Research looking into the effects of Seleginine goes more than two decades back. Golbe et al[247 248] looked into the use of l-Deprenyl within 96 people with PD. They found that l-Deprenyl was found to increase gait scores in 56% of cases. Side effects such as nausea and hallucinations were reported and confirmed by other research in the years following[247-249]. A study by Riederer[250] showed that the start of treatment with Levadopa could be delayed by 12-18 months. Exposure to l-Deprenyl was not associated with mortality, but the severity and rate of worsening of parkinsonism remained associated with mortality[181]. A Cochrane review from 2008 on 29 trials with 5247 patients with PD found that treatment of a dopamine agonist compared to Levodopa resulted in less chance of developing dyskinesia, dystonia or motor fluctuations[251]. The disadvantage however was that non-motor symptoms such as oedema, constipation, dizziness and hallucinations were more likely to occur[251].

Levodopa/Carbidopa (Sinemet) can be seen as the gold standard for symptomatic treatment of PD, however, long-term treatment can cause adverse effects and therefore affect the quality of life[252]. There is some evidence that people with PD who are being treated by Levodopa/Carbidopa can develop compulsive gambling or hyper sexuality (18.7%)[253]. A study by Bowes et al[254] looked into the effects of Levodopa/Carbidopa compared to a placebo treatment. They found that stride length increased for the Levodopa/Carbidopa as well as the placebo treatment (7% and 0.5% respectively) compared to the ‘*OFF*’ phase[254]. L-Deprenyl can be given in combination with Levodopa/Carbidopa. This will reduce the doses of Levodopa/Carbidopa with the same effects as a higher doses of Levodopa/Carbidopa alone[255].

A study looking into the effects of Levodopa/Benserazide found that there was a significant increase in walking speed, stride length and range of motion of hip, knee and ankle[256]. They furthermore found that these effects were not found in patients who substituted Levodopa/Benserazide for Tolcapone[256]. Tolcapone is known as the first inhibitor available for use as adjunctive therapy for PD. Ondo et al[257] found that after administering Tolcapone in daily treatment only 22% noticed an improvement in gait, however these results did not reach statistical significance. Even so, finger tapping increased in 7% of cases but did also not reach statistical significance[257]

Švehlík et al[258] looked at the effects of participants with PD taking short-acting dopaminergic medications in the '*OFF*' stage. They found that people with PD in the '*OFF*' stage walked more slowly, however cadence did not significantly differ from the control subjects. The PD group did however have a prolonged double stance phase compared to the control group both in '*ON*' and are '*OFF*' phase[258]. Double stance can be defined as the point during the gait cycle where both feet are in contact with the ground[42].

A common phenomenon within PD is restless leg syndrome. This is often treated by Requip and Pramipexole which are dopamine agonists[259]. Research has shown that the use of these drugs could be related to pathological gambling addictions[260]. A comparison between people with PD and Amyotrophic Lateral Sclerosis showed that people with PD under treatment with either Requip or Pramipexole showed a higher gambling rate than people with ALS (13% and 3% respectively). This compared to healthy population (.25-1.7%) shows an increase in gambling activity within people with PD[260]. These results are also confirmed by Bostwick et al[253] who found that gambling rates were higher in people taking dopamine agonists.

Chastan et al[261] looked at the effects of subthalamic nucleus (STN) stimulation on gait initiation, posture and gait. They found that under treatment with Levodopa compared to 'OFF' stage, step length and walking speed increased by 32% and 33% respectively. Under stimulation conditions step length and walking speed increased by another 41% and 40% respectively compared to Levodopa treatment[261]. These results were confirmed by Kelly et al[262] who found an increase directly after STN stimulation on an individual bases. However results directly after the operation compared to pre-surgical function did not show a significant increase[262]. Deepbrain stimulation over a five year period was found to increase the Unified Parkinson's Disease Rating Scale score by 54%, however functional measures did not show improvement in daily activities[263]. Furthermore it was found that Levodopa doses was decreased by 69% compared to pre-implant after which stimulus energy were progressively increased over time[263].

Gait initiation can be measured by the centre of pressure (CoP), which can be defined as the point where all the mass of a body is concentrated[264], that is shifted backwards causing a prolongation of the stepping phase[265]. Due to less effective anticipatory postural adjustments and less dynamic stepping characteristics there is an increased chance to create an imbalance in dynamic conditions[266] (i.e walking). It has been found that patients with PD moved with slower velocities (0.85±0.23 ms^{-1}) leading to shorter, slower steps and decreased separation of the CoM and CoP[219]. In comparison a study by Ferrarin et al[267] found that patients with PD did not significantly differ from controls in steady state walking, and changes emerged on gait initiation and turning strategies. Yang et al[268] found that those with PD demonstrated a significantly slower gait speed (0.89±.27ms^{-1}) and shorter stride length (1.036±.242m) compared to age matched controls (1.12±.21ms^{-1} and 1.25±.178m). This effect is often compensated by an increase in cadence[269 270].

4.2.5 Outcome measures in Parkinson's disease research

Following the recommendations from the International Classification of Functioning, Disability and Health (ICF) to structure patient outcome measurements a classification in outcome measures can be made[271]. The framework shown in Figure 23 describes aspects of a person's health and health-related well-being in terms of restrictions, limitations in functional activities as well as impairment in body structure and function[271]. The mostly used outcome measures in PD research have been divided in two groups following this framework namely '*activity and participation'* and *'body function and structure'*.

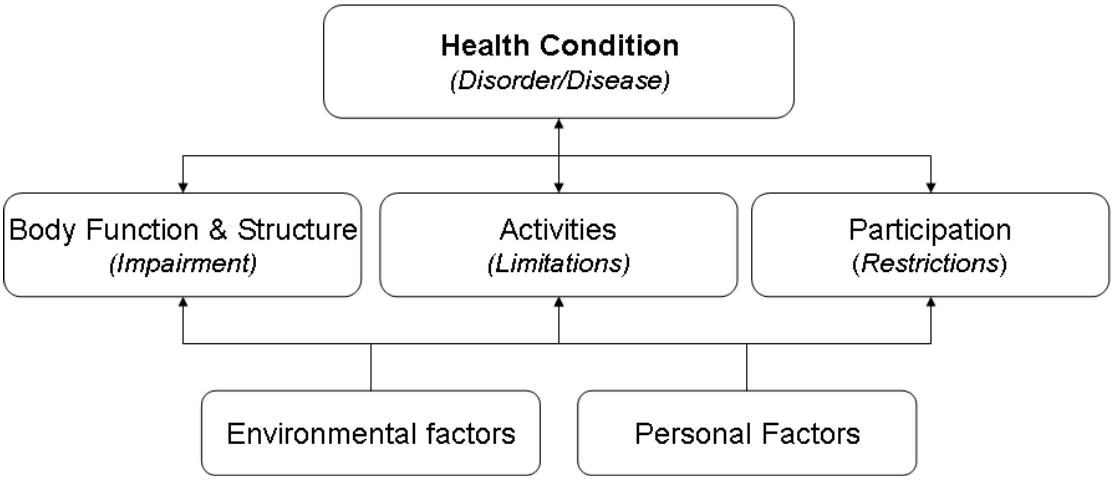

Figure 23 Framework set by the World-Health-Organisation for the international classification of function, disability and health to structure outcome measures in physiotherapy evaluations

4.2.5.1 Activity and Participation outcome measurements

This section allows description of the tasks (activities) and/ or life situations (participation) the person wishes to be involved in, and the impact the impaired body function/ structure is having on these aspects[271]. This section focuses on motor symptoms and the effect on activities of daily life.

The '*Parkinson's Disease Questionnaire 39*' (PDQ-39) which was developed by Jenkinson et al[272] in the late 1990's is often used as an outcome measurement within research. This questionnaire can be divided in eight parts, mobility, activities of daily living, emotional well-being, stigma, social support, cognitions, communication and bodily discomfort. Scores of the PDQ-39 will range from not affected by PD (score of zero) with a higher number indicating more severely affected in daily life. Research looking into the validity of the PDQ-39 however shows that it is not more specific than a generic questionnaire[194 273]. It has recently been concluded once more that the interpretation of the PDQ-39 needs to be done carefully since it could suggest multi-dimensionality and therefore result in misinterpretation[274]. The PDQ-39 is currently still being used in gait research[221 275 276].

PD is hard to classify on a severity rating. However several attempts have been made throughout the decennia. The most commonly accepted rating scale is known as the Hoehn & Yahr (H&Y) scale[134 220 226 268-270 275-298]. This scale is divided in six sections where zero describes no symptoms of PD whereas five describes severe symptoms with possible wheelchair bound circumstances. However with the introduction of the use of Levodopa this scale was modified by Jankovic in 1990 adding increments of .5 to the scale[299]. Quinn et al[300] mention that the H&Y scale can either show a scaling of 4-5 in the '*off*' phase, however under the influence of Levodopa it can go down to 2-3. A brief review by the '*Movement Disorder Society Task Force*' recommended that the modified H&Y scale should be used in its original form since the addition of the .5 rating scale would over-complicate the analysis as well as the actual scoring of the modified H&Y scale[301]. They also mentioned that the H&Y scale is losing its use to the Unified Parkinson's Disease Rating Scale (UPDRS)[301].

The UPDRS is an outcome measure to follow the longitudinal course of PD. It exists in three main sections assessing mental capacity (part I), daily activities (part II) and motor skills (part III)[302]. Part I contains another two subsections assessing behaviour and mood[303]. Starkstein & Merello[304] looked into the validity of Part I of the UPDRS to screen for dementia, psychosis, depression and apathy. They found that part I is an adequate screening test to detect depression and apathy in people with PD. However it could not be used solely to detect dementia or psychosis unless used in combination with the mini-mental state examination[304]. Mostly used within PD research (as shown in Table 5) is the motor section (part III) of the UPDRS. The motor examination section of the UPDRS provides a useful measure of PD function[305]. An inter-rater reliability study by Richards et al[306] showed that there was good-to-excellent agreement for the motor section of the UPDRS but found poor agreement for speech disorder and facial immobility. These results show that there is satisfactory inter-rater reliability with the UPDRS motor scoring[306]. However the motor section of the UPDRS was found to be time consuming and not sensitive enough when compared to a brief timed motor test[307].

After the UPDRS received critiques by the Movement Disorder Society (MDS)[308] a follow-up was presented and named the MDS-UPDRS[309 310]. The MDS-UPDRS puts more emphasis on the mild and non-motor symptoms related to PD. A set of detailed instructions are also provided which supply international standardisation across multiple centres[310].

With gait being a marker for mortality in the elderly[311] and a sensitive indicator for progression of Parkinson's disease (PD)[296], the focus of this work explores the possibility of gait being a descriptive of body function and participation. In the next section the main outcome measurements for gait are explored in a short review.

4.2.6 Gait outcome measurements in Parkinson's Disease

As described above, many measurement tools are available for the description of motor and non-motor symptoms of PD. In order to determine what the main outcome measurements are within clinical research, a short review was performed to determine the most common outcome measurements in PD research. Furthermore this review set out to determine what equipment was used to obtain gait measurements.

A search on PubMed was performed on the terms '*Parkinson's disease Gait*', *'Parkinson's Gait', 'Parkinson's Locomotion'* and *'Parkinson's walking'* resulted in 83 papers related to gait specific research. After initial screening for primary walking outcome (spatio-temporal outcome measurements), measures 47 papers remained. Collected data is shown in a table that can be found in Table 5.

A recent study by Ellis et al[281] measured the effects of physical therapy in two clinics in Boston (United States) and Amsterdam (Netherlands). They used the H&Y scale as a descriptive of PD, MMS as cognitive measure and the UPDRS as a motor function descriptive. A study by Rochester et al[296] compared the relationship between gait activity and fatigue using the UPDRS and the MMS. They found this relationship remained unclear due to the complex relationship between these factors[296]. These two previous studies however show the three main outcome scales and questionnaires used within PD gait related research. The H&Y scale was used in 68% to describe the state of PD, 49% used the UPDRS of which 15% used the full UPDRS and the remaining 85% the UPDRS motor subscale[308]. Current exploring the affects of PD on gait, use the motor subscale as a descriptive of PD severity[134 220 275-278 281-284 286-292 296-298 312-314].

Temporal measures of gait are measured in several ways such as by electronic walkways[268 278 291], accelerometry[226 288], treadmill[275 315], force platforms[220], optical motion capture systems[269 283] or newly invented devices[292]. Also standard measures such as stopwatch based measurements are used within research[316 317]. Ebersbach et al[316] conducted a study looking into walking differences within different social cultural environments within PD. They found that people with PD in Berlin (Germany) walk faster than their counterparts in Innsbruck (Austria)[316]. Roiz et al[276] looked into the relation between clinical and spatio-temporal and kinematic measurements within people with PD. They found that clinical measurements did not present psychometric measures compared to advanced 3-dimensional analysis. These studies represent the general outcome measurements in PD gait studies. The top three outcome measures found in this short review were walking speed [ms^{-1}], stride length [m] and cadence [steps/min] in 60%, 55% and 44% respectively. Furthermore it was noticeable how these gait parameters were matched. In half the cases where walking speed was measured, stride length and cadence were naturally measured as well. These parameters were mainly acquired during the 10-metre walking test and the Timed up & go (TUG) for 38% and 28% of all cases as shown in Table 5.

Table 5 Research outcome measures found during the short PD review with percentages as shown taken from the total amount of reviewed papers.

Outcome measure	Percentage use	*'n'* participants	References found
Freezing of gait questionnaire	10.64%	415	280 282 287 289 314
Timed up&go	27.66%	527	220 226 275 276 278 282-284 289 290 292 297 317
10 metre walking test	38.30%	425	268-270 275-278 280 288 290 294 316 318-320
2 minute walking test	4.26%	79	281 320
6 minute walking test	12.77%	194	275 277 282 288 313 314
Walking speed	59.57%	1067	134 256 261 268-270 276-279 281 283 285 288 290 291 294 295 313 314 316-319 321 322
Stride length	55.32%	879	134 256 261 268-270 276-278 283 285 288 291 293-295 314 318 319 321 323
Cadence	44.68%	479	134 268-270 276-278 288 293-295 312 314 316 318 320 321
Step frequency	10.64%	86	290 291 293 320 322
Step time	23.40%	270	268 276 280 283 288 293 297 312 314 318 320
Step symmetry	2.13%	22	322
Single stance	14.89%	180	134 268 276 278 283 285 318
Double stance	17.02%	195	134 268 276 278 283 285 318 319
Energy (oxygen measure)	8.51%	123	275 279 298 313

Based on 29 papers which were accessible and provided information about their gait analysis it was found that in most cases a timing device such as a stopwatch was used (38%)[282 287 316 319]. This was often combined with the use of a camera system (7%)[296 312] or the GAITRite pressure mat (14%)[256 276]. Secondly an OMCS was used when using gait as an outcome measurement (34%)[261 268 289]. Force-plates were used 24% of the time, but often combined with OMCS or stopwatch measurements[269 294 298].

Gait outcome measurements in clinical PD research are therefore often reliant on measurements taken over the 10-metre walk[269] and the times up and go[317]. As mentioned by Toro et al[36] access to advanced systems that measure gait are inaccessible to clinicians around the world as there is a lack of technical knowledge. Therefore a stopwatch is often used as an alternative to gain more insight into for example the 10 metre walk or the timed up and go. A review on gait analysis published by Baker in 2006, mentioned that gait can be accurately measured over 10 metres with the right equipment[324]. He hereby referred to sophisticated systems such as optical motion capture systems and force platforms. Therefore it can be assumed that an IMU system (as proposed throughout this thesis) can potentially add value to current gait measurements as it can be easy to use for clinicians as it doesn't require technical knowledge when measuring gait analysis over 10-metres. These results are in agreement with data found in Cochrane reviews by Deane[302 303] and Mehrholtz[315].

Therefore in order to use inertial measurement units in combination with the method proposed in Chapter 3, validity and reliability measurements in PD are required and will be explored in the next chapters.

Chapter 5: IMU Gait Validation & Reliability within PD

5.1 Summary

Walking models driven by data obtained from Inertial Measurement Units (IMU) can be used to objectively measure gait. However current models have only been validated within typically developed adults (TDA). The purpose of this study was to validate an inverted pendulum model to obtain gait measures within Idiopathic Parkinson's disease (PD) and to explore its inter-rater reliability. Ten people with PD showed no difference (p>0.05) for vertical, translatory acceleration, speed and relative position between IMU and optical motion capture system data. Furthermore no difference (p>0.05) was found for step time, stride length and walking speed for people with PD. Inter-rater reliability was found not to be different for step time (p=.299), stride length (p=.883) and walking speed (p=.751) with an adequate %-variability (-7.7±9.5%, 2.7±7.7% and 2.9±6.1% respectively). Results show that gait measurements taken from an IMU are valid and reliable within people with PD and shows good inter-rater reliability.

5.2 Introduction

National Institute for Health and Clinical Excellence (NICE) guidelines in the UK direct the need for clinicians to obtain objective outcome measurements in order to provide quality assurance[109]. Walking has been indicated as a marker for mortality in the elderly[311] and a sensitive indicator for progression of Parkinson's disease (PD)[296]. Gait analysis systems such as optical motion capture (OMCS) provide an objective means of measuring walking, but are expensive, time-consuming and inaccessible to most clinicians[36]. Inertial Measurement Units (IMU) can be used to obtain objective measurements of gait parameters inexpensively, quickly and easily in a clinical environment[5]. However their validity, reliability and utility has not been established in pathological populations[5-8].

People with PD have an altered gait pattern including: a significantly slower gait speed (0.89±.27ms^{-1}), shorter stride length (1.036±.242m) and increased cadence[269-270] compared to age matched controls (1.12±.21ms^{-1} and 1.25±.178m)[268]. Gait has also been shown to be a sensitive marker of degeneration in PD[293]. As such careful observation of gait is clinically desirable in PD.

IMU gait analysis requires accurate double integration of translatory acceleration towards relative position, which has been shown to be valid in typically developed adults (TDA) as shown in Chapter 3, but in older adults increased peak acceleration of the CoM may affect the double integration[325]. Considering the altered gait pattern in PD, exploration of IMU gait analysis in this group was needed. This study compared IMU to OMCS data to explore 1) the validity of vertical translatory acceleration, velocity and relative position of CoM and 2) temporal spatial aspects of walking calculated from models driven by change in relative position of the CoM. Furthermore clinical utility was explored by 3) investigating the accuracy of temporal spatial parameters measured by a clinician using the IMU in a clinical setting.

5.3 Materials and Method

5.3.1 Participants

Ten people with PD as diagnosed by a consultant neurologist were recruited under National Health Service ethical approval 10/H0308/12 at Oxford Brookes University. The experiment was conducted in accordance with the Declaration of Helsinki.

Participants were excluded when they 1) scored eight or lower on the Rivermead Mobility Index (RMI)[9] indicating safe mobility, 2) they were not able to complete a two minute walk or 3) had insufficient mental capacity to consent. Furthermore the physical activity readiness-questionnaire[326] (PAR-Q) was administered to assess readiness to partake in this procedure.

5.3.2 Protocol

Participants were asked to choose a time for their assessment which suited their daily routine. Prior to the gait assessment the Barthel Index of independence in daily activities[327] was administered (a range from zero to twenty, with a higher score suggesting lesser impairment). Participants were asked to partake in a 2 minute walking test[328] (2minWT) where the total covered distance is recorded after 2 minutes walking.

Validity and inter-rater reliability measurements were taken on 10 metre walking tests[329] (10MWT) where the recorded time over 10 metres was taken from a standing start. These tests were conducted at the participants self selected walking speed in a quiet and obstruction free 16 metre corridor. Measurements from the 10MWT were conducted by a clinician without previous knowledge of the IMU gait system and an expert (defined as a person with at least 1 year's of experience with the IMU system) in random order. For this study two clinicians (physiotherapist and medical doctor) and two experts performed the measurements independently of each other with an IMU (Pi-Node AGWorldium-11-07, Philips, Eindhoven, Netherlands) comprising a tri-axial accelerometer, gyroscope and magnetometer. Additionally, participants were measured with an OMCS (Qualisys, Stockholm, Sweden), which was synchronized on gait initiation. Both systems measured at a sample frequency of 100Hz. A standard operating procedure was followed for all measurements.

IMU data analysis was performed according to previously described methods (Chapter 3.4) using a customised program written in LabVIEW 8.5 (National Instruments, Austin, USA). Step time, stride length and average walking speed were calculated according to methods previously described using the inverted pendulum model including a personal correction factor[71 78].

5.3.3 Statistical Analysis

OMCS data was exported to Excel 2003 (Microsoft Windows, Redmond, USA) where peaks and troughs were extracted for vertical translatory acceleration, velocity and relative position, according to the method described in Chapter 3. Temporal spatial measures were derived by using a model reliant on vertical CoM excursion[76]. Step time, stride length and average walking speed were calculated from peak interval times and average forward change in position over time.

For concurrent validity, peak and trough values from z-axis translatory acceleration, velocity and relative position were extracted and compared between IMU and OMCS using a paired sample *t*-test and intra class correlation test 3.1 (ICC3.1), according to McGraw and Wong[162]. Root mean square (RMS) error was calculated for vertical acceleration, velocity and excursion. Identical analyses were performed on step time and stride length analyses between the OMCS and IMU as well on average walking speed derived from an inverted pendulum model as proposed by Zijlstra & Hof[330].

Inter-rater reliability between expert and clinician measurement was tested by a paired sample *t*-test, ICC3.1 with consistency as well as %-variability on step time, stride length and average walking speed. Adequate test-retest reliability is defined[163] as an ICC≥0.75. 95% confident intervals (95%CI) were calculated for reliability ICCs.

5.4 Results

Participants (age 59.7±11.7years) covered 125±34m during the 2MWT. The time recorded for the 10MWT was 10.05±1.8s for PD. The Barthel Index score for the participants with PD was found to have a median 19, range 15-20, whereas the RMI score was found to be median 14.5, range 13-15. Individual descriptive measures are displayed in Table 6.

Table 6 Individual, average and standard deviations of descriptive measurements taken of age, height, weight, Barthel Index, RMI and two minute walking test (2MWT).

Patient ID	**Sex** M/F	**Age** [years]	**Height** [m]	**Weight** [kg]	**2MWT** [m]	**Barthel** [au]	**RMI** [au]
1	M	56.47	1.82	91.3	80	18	13
2	F	61.49	1.68	77.2	136	20	15
3	M	55.65	1.79	82.1	132	20	15
4	F	58.81	1.72	64.7	160	15	15
5	F	32.15	1.56	67.6	70	18	13
6	M	70.64	1.83	95.8	123	20	14
7	M	70.8	1.76	83.2	120	20	15
8	M	71.2	1.74	85.9	100	19	15
9	M	53.73	1.82	89.3	168	19	14
10	M	66.10	1.87	96.7	164	20	15
Average		59.7	1.76	83.4	125.3		
Stdev		11.7	0.09	10.9	34.1		

5.4.1 Validity

Figure 24 shows data from a representative trial of the IMU vs. OMCS data. For concurrent validity vertical translatory acceleration measured by the IMU and OMCS did not show any significant difference in either peaks (IMU 4.31±2.21ms^{-2}; OMCS 3.58±1.87ms^{-2}) or troughs (IMU -2.70±1.29ms^{-2}; OMCS -2.68±1.11ms^{-2}) (p=0.13 and p=0.90 respectively) and showed a high significant correlation (ICC=0.953 and .0.894, p<0.001 respectively). The same results were found for vertical velocity (IMU$_{Peak}$ 0.38±0.27ms^{-1}; OMCS$_{peak}$ 0.33±0.12ms^{-1} and IMU$_{through}$ -0.19±0.15ms^{-1}; OMCS$_{trough}$ -0.17±0.12ms^{-1}), which were not significantly different (p=0.33 and p=0.21), with a high significant correlation (ICC=0.924 and 0.77, p<0.001). Finally no significant difference was found between the IMU and OMCS in vertical relative position in either peaks (IMU 1.29±0.32cm; OMCS 1.11±0.52cm) or troughs (IMU -3.55±0.46cm; OMCS -3.64±0.61cm) (p=0.13 and p=0.57) which was found to have a high significant correlation (peak; ICC=0.954 and trough ICC=0.982, p<0.001). RMS error for vertical acceleration, velocity and excursion was found to be 1.21±1.11ms^{-2} (10.2±9.3%), 0.05±0.04ms^{-1} (8.9±6.4%) and 0.6±0.5cm (9.3±7.6%) respectively.

Results of model derived step time, stride length and walking speeds are displayed in Table 7. There was no significant difference for step time between the IMU and OMCS measurements (p=0.357), which also showed a significant correlation (ICC=0.982, p<0.001). Same results were found for stride length (p=0.876) also with a significant correlation (ICC=.705, p=0.042). Furthermore no significant difference was found for the IMU and OMCS within the average walking speed (p=0.177).

Table 7 Concurrent validity measurements showing step time, stride length and walking speed for the IMU and OMCS systems and the differences between the two systems for individual participants and as a group in percent.

	Step Time			**Stride Length**			**Walking Speed**		
Patient ID	**OMCS** [s]	**IMU** [s]	**Diff** [%]	**OMCS** [m]	**IMU** [m]	**Diff** [%]	**OMCS** [ms^{-1}]	**IMU** [ms^{-1}]	**Diff** [%]
1	0.67	0.66	-0.50	1.01	1.13	10.52	0.59	0.68	13.95
2	0.53	0.53	0.00	1.00	1.11	9.51	1.20	1.18	-1.01
3	0.59	0.58	-1.74	1.05	1.10	4.34	1.13	1.13	0.32
4	0.45	0.46	1.46	1.15	1.15	-0.16	1.68	1.68	0.19
5	0.69	0.69	0.61	0.97	1.01	4.26	0.69	0.70	0.16
6	0.72	0.71	-0.96	0.95	1.01	5.30	0.65	0.66	0.48
7	0.70	0.69	-1.45	1.04	1.12	6.84	0.73	0.72	-0.54
8	0.57	0.57	0.00	1.05	0.97	-8.41	0.97	0.95	-1.80
9	0.53	0.53	0.94	1.05	1.01	-3.98	1.52	1.56	2.82
10	0.57	0.57	0.00	1.14	1.14	0.25	1.66	1.66	-0.19
Average	0.60	0.60	-0.16	1.04	1.07	2.85	1.08	1.09	1.44
Stdev	0.09	0.09	1.02	0.06	0.07	5.95	0.42	0.42	4.56

5.4.2 Reliability

To test the inter-rater reliability a paired sample t-tests between measurements taken by the expert and clinician found no significant difference for step time (p=.299 and ICC=.979 p<0.001; 95%CI=0.942-0.993), stride length (p=.883 and ICC=.958 p<0.001; 95%CI=0.884-0.985) and walking speed (p=.751 and ICC=.978 p<0.001; 95%CI=0.963-0.992) with a significant correlation. % variability between expert and clinician 10MWT for step time, stride length and walking speed were found to be -7.7±9.5%, 2.7±7.7% and 2.9±6.1% correspondingly. Data for both users is shown in Table 8.

Table 8 data collected by expert user and clinician

	Steptime [s]	**Stride Length [m]**	**Walking Speed [ms^{-1}]**
Expert	0.51±0.12	1.26±0.31	1.25±0.26
Clinician	0.49±0.10	1.26±0.30	1.27±0.26

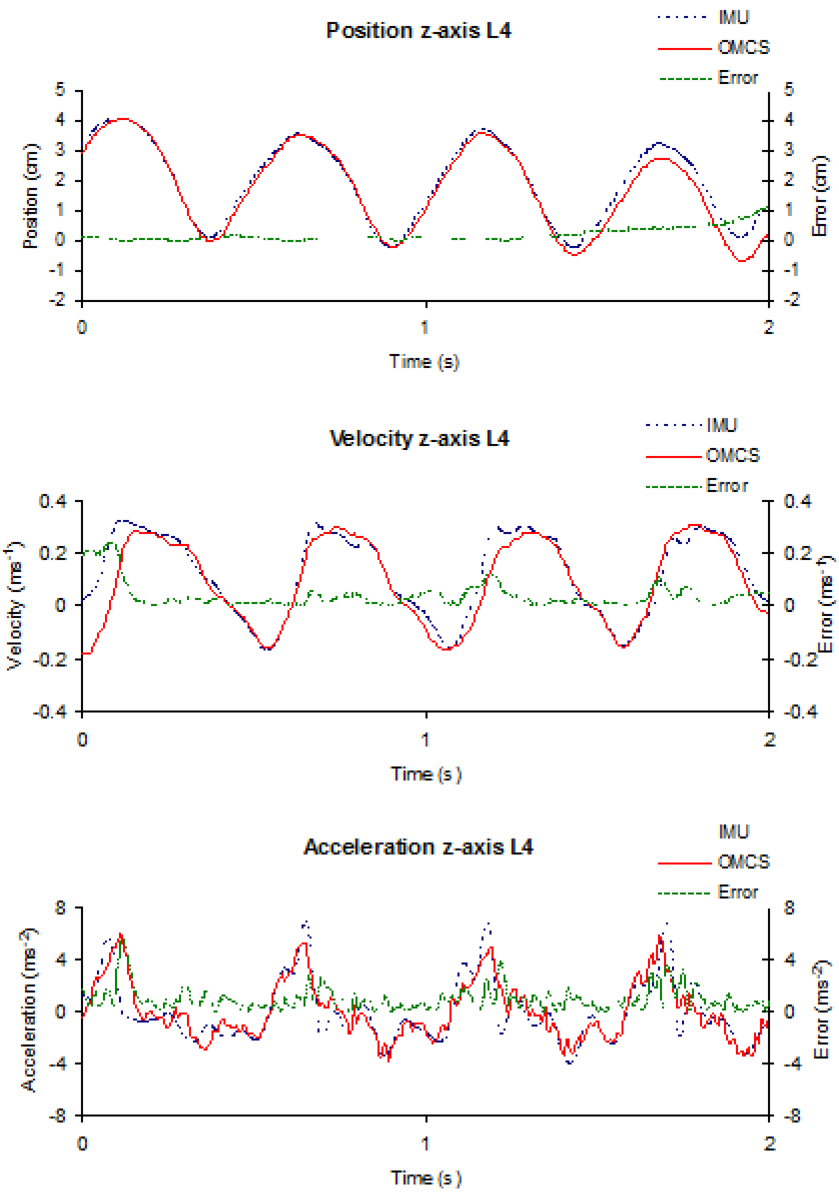

Figure 24 Data from a representative participant, walking during their steady walking phase (i.e. middle 10 metre walk) at 1.13ms^{-1}, showing relative position, speed and translatory vertical acceleration. The blue dotted line represents the IMU, and the solid red line represents the OMCS. The acceleration, speed and position are de-drifted using the DC estimate acquired with a Hanning window[161]. The green dotted line represents the overall error between the two systems which is calculated as the difference between OMCS and IMU at any time.

5.5 Discussion

The results show that IMU data had concurrent validity with the OMCS, which enabled accurate derivation of temporal spatial parameters in people with PD. In addition, temporal spatial gait parameters were accurately measured by clinicians in PD. These results support the accuracy of clinicians measuring gait in PD.

Vertical translatory acceleration, velocity and excursion of the CoM did not show any significant differences when comparing IMU to OMCS measurements. Results have previously been reported in typical developed adults[131], although a slightly higher error for acceleration, velocity and relative position ($0.176ms^{-2}$, $0.05ms^{-1}$ and 0.12cm) in PD participants could be explained by tremors and rapid movements expressed in their day-to-day gait[178]. It was noted by Farrell and Borth[147] that the error by each integration increases as $\varepsilon = t^{1.5}$, where t is the integration time and ε is the error. However, by applying the method for integration and de-drifting[131] a relatively small RMS error was found in the PD group.

Walking speed as derived by IMU was accurate to $0.02ms^{-1}$ (1.4% walking speed difference) in PD. Whilst there is no comparable data using IMU, a study by Webster and colleagues[331] found that gait in patients post-knee replacement measured by GAITRite® instrumented mat compared to OMCS gave an error of $0.02ms^{-1}$. Step time compared between IMU and OMCS showed a maximum difference of 0.01s whereas maximum difference of the GAITRite® was found to be 0.05s at SSWS.

Participants were randomly recruited to include a wider range of PD. The statistics between the IMU and OMCS measurements on average walking speed shows a strong significant agreement indicating that the range of speeds are not affecting the inverted pendulum model. Inter-rater reliability between expert and clinician was found to be similar. Studies looking into inter-rater reliability in brain injured trauma participants found ICCs of 0.95-0.99 indicating excellent agreement. ICCs found within this study were lower, however a greater variability in gait was present due to natural PD gait variability[178]. Inertial measurement units can be used by clinicians to objectively measure gait within routine clinical practice in line with NICE clinical guidance.

A limitation of the present study however is the use of gait models developed for TDA to determine gait spatio-temporal parameters; however the gait parameters are in agreement with previous studies[269 270]. This current study compared the outcome of the gait model driven by both the OMCS and IMU data which did not require any adjustments to the model. Future studies are needed in order explore the use of the inverted pendulum model to determine its accuracy and reliability when driven by IMU collected data.

So far it has been shown that the IMU collected data is in agreement with OMCS derived vertical acceleration, velocity and relative position in TDA (Chapter 3) and PD. The next chapter will therefore investigate the accuracy and reliability of the use of the inverted pendulum model[71 330] when driven by IMU collected data in TDA and PD.

Chapter 6: Assessment of spatiotemporal modelling

6.1 Summary

Laboratory based gait analysis techniques are expensive, time consuming and require technical expertise. Inertial measurement units can directly measure temporal parameters and in combination with gait models may provide a solution to obtain quick spatial gait measurements within daily clinical assessments. However it is not known if a model used to accurately derive step / stride length parameters in typically developed adults (TDA) can be used in pathological gaits.

This research set out to determine the correction factor required to derive step/stride length in TDA and participants with Parkinson's disease (PD) when using the inverted pendulum model during a ten metre walk at self selected walking speed.

Ten TDA of similar age, and twenty-nine people with PD participated. Correction factors determined for step length for TDA (1.25±0.01) agreed with previous data and were the same for PD (1.25±0.03) Walking impairment as measured by speed did not relate to the required correction factor.

Inertial measurement units can be used to obtain step/stride length using a correction factor which needs to be calculated on an individual basis.

6.2 Introduction

Neurological populations such as Parkinson's disease (PD) include a wide variety of people including an ethnical and demographic spread and comprise about 3 million individuals in the UK[179]. Maintaining mobility is one of the most consistently cited key concerns in these and other clinical populations[332]. As such, objective measurements of mobility and gait are a critical marker for clinicians to accurately diagnose medical conditions and monitor their progression[109]. Tests such as the ten metre or six minute walking tests can be used to assess walking performance[327] but do not provide insightful information on underlying gait performance. However spatio-temporal gait parameters such as individual leg step time, step length, step speed, cadence and walking speed can be used to direct rehabilitation[332]. Gait mats measure these parameters but offer a limited capture volume and have limitations in accurately measuring pathological gaits[331]. Inertial measurement units (IMU), which combine gyroscope, accelerometer and magnetometer data, provide an alternative method for obtaining objective measurements of pathological gait in a variety of settings[131]. Accurate vertical acceleration, speed and position measurements of the Centre of Mass (CoM) can be obtained during walking by transposing acceleration from the object to the global system[131]. The resulting data of the CoM can then be used to determine temporal gait parameters. However, spatial parameters (i.e. step length) need to be derived from additional mathematical equations such as equation (6.1)

$$d = \gamma\left(2\sqrt{2lh - h^2}\right) \tag{6.1}$$

where (h) is the CoM vertical excursion, (*l*) is the leg length and (γ) is the correction factor. In typically developed adults (TDA) the model underestimates step length by 25%, which has been shown to be stable across individuals and testing days. Therefore, a correction factor of 1.25 is implemented to accurately determine step length with the IMU[71 76].

However the model may not be accurate or stable in clinical populations[333] who may not walk with a typical gait pattern and have higher levels of day to day variability in motor performance. However, considering the utility of measuring gait using IMUs in these individuals, the accuracy of, and possible adaptations to this model should now be explored. From previous investigations where walking speed was shown to relate to the level of disability and gait impairment[332], this study proposes that, for gait in PD, the correction factor may be different for people with altered gait patterns and that there will be a negative correlation between walking ability and the required correction factor.

In contrast with the previous chapter (Chapter 5) where the validity and reliability of IMU measurements has been established, this study set out to determine the correction factor required to derive spatial parameters using the inverted pendulum model for PD when using IMU acquired data.

6.3 Materials and method

6.3.1 Participants

Data from Individuals with PD and typical developed adults (TDA) was included in the analysis (Ethics #07/H0606/81; #10/H0308/12). Participants data was included if they were able to walk 10 metres unassisted. Barthel Index[327] (BI) was administered for people with PD. The study was conducted in accordance with the Declaration of Helsinki.

6.3.2 Protocol

Participants performed a standard clinical ten metre walk with participants asked to walk twice over a predefined distance at self selected walking speed (SWSS). The time taken to walk ten metres was recorded by a stopwatch.

A commercially available IMU (MTx, Xsens, The Netherlands) was attached over the skin of the 4th lumbar vertebra, reflecting the participant's projected CoM[87] during walking. The IMU signals from the tri-axial accelerometer, gyroscope and magnetometer were processed with quaternion rotation matrices and integrated to obtain vertical excursion of the CoM in the global frame (as shown in Chapter 3).

Step time was taken as the time interval between peak-to-peak CoM excursions during one gait cycle. Step length was calculated [78 330] from equation (6.1) with the initial correction factor set at 1.25 (Zijlstra et al[76]) for all groups, after which walking speed (V_I) was derived by dividing step length by step time. Walking speed was also calculated by dividing the time it took the participant to cover the 10 metres measured by stopwatch (V_S). Furthermore the duration of the ten metre walk was derived from vertical IMU acceleration data. Correction factors for each participant were optimised by comparing V_I *and* V_S. If the two velocities did not equate, V_I was adjusted by an iterative process which manipulated the correction factor in equation (6.1) until V_I matched V_S. A mean group correction factors for each neurological condition was calculated.

6.3.3 Statistical Analysis

Descriptive statistics analyses were performed on the spatiotemporal gait parameters. Group correction factors from each neurological condition were submitted to independent sample *t*-tests. Significance was set at $p \leq 0.05$. In addition correlations between correction factor, walking disability expressed as walking speed and disability level expressed as BI were tested. Intra class correlation between IMU and stopwatch gait timing was tested where adequate test-retest reliability is defined[163] as an ICC≥0.75. All statistical tests were conducted in SPSS17 for Windows.

6.4 Results

Descriptive measurements, group correction factors and derived data from the inverted pendulum model are displayed in Table 9.

No significant difference was found for the group correction factors between TDA and PD (p=0.833).

After optimising the correction factor, the derived spatiotemporal gait parameters (i.e. walking speed, cadence and stride length) in PD were found to be significantly different (p<0.05) from TDA.

Table 9 Characteristics for the typical developed adults and Parkinson's disease. The level of impairment in PD as measured by *Barthel Index* (BI) is displayed with the adjusted individual correction factor (γ) and sex is indicated as the number of males (M) taking part.

Diagnosis	n	Sex	BI scores (median & range)	Age (years)	Diagnosis (years)	Cadence (steps/min)	Adjusted γ	Stride Length (m)	Speed (ms^{-1})
Control	10	M = 6		66.4± 4.4		123.2±5.6	1.25±0.01	1.37±0.08	1.36±0.33
PD	29	M = 25	20 range 16-20	63.4± 7.7	6.1± 4.8	109.5±11.6	1.25±0.03	1.16±0.29	1.08±0.22

Considering the relationship of the level of disability to the calculated correction factor, no correlation was found for PD (R^2<0.01) between BI scores and the individual correction factor. Furthermore no significant correlation (Figure 25) was found between walking ability measured by walking speed and the individual correction factors for the TDA (rho = 0.380; p=0.099) or PD (rho= -0.026; p=0.893). Results are shown in Figure 25.

Time over the ten metre walk as measured by stopwatch (9.5±1.9s) and IMU (9.6±2.0s) did not show any significant difference (p=0.28) and showed a high correlation (ICC=0.996, p<0.01). RMS Error between measurements was 1.4%.

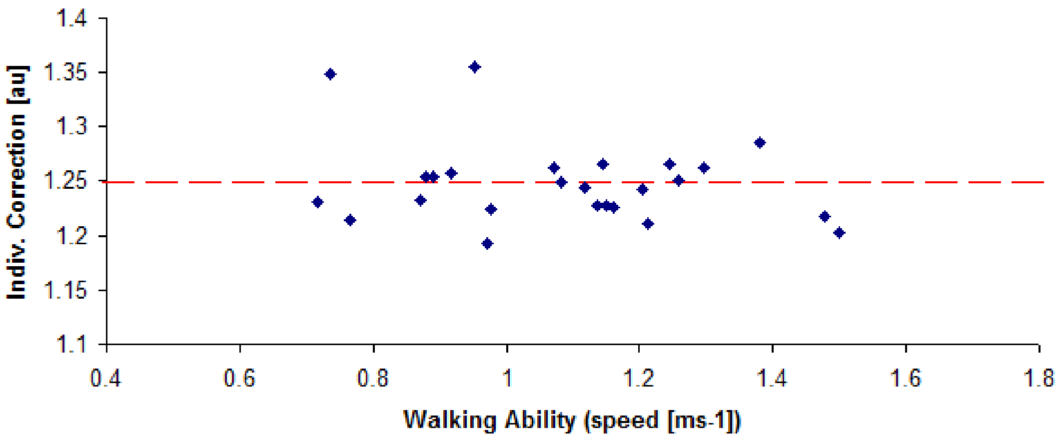

Figure 25 Relationship between the individual correction factor and walking ability measured as walking speed. Showing Parkinson's disease where the horizontal dotted line represents the standard correction factor of 1.25 set by Zijlstra et al.

6.5 Discussion

This study shows that correction factors calculated for people with PD were not significantly different from the correction factor of 1.25 that was confirmed to be representative of TDA[76]. Furthermore a high degree of heterogeneity was observed within the TDA and PD group.

The findings of this study demonstrate that a group correction factor of 1.25 used to model gait in TDA can be generalised to a PD group but that individual correction factors should be used to model gait irrespective of PD or severity of disability. The stability of individual correction factors over time and replication of these findings in a wider population should now be determined.

Indeed the correction factor for TDA of 1.25 is equal to the results found by previous research[71 78] which used less sophisticated analysis. As TDA walk relatively smoothly with 5-10degrees deviation in the sagittal plane[334], this was an expected finding. However the strength in this approach lies in the applicability within a vast range of neurological gait patterns as, for example, stroke survivors have a larger lateral hip movement during walking[335] which could affect the outcome of the inverted pendulum model. Within this particular tested group of people suffering from Parkinson's disease the digital signal processing method (Chapter 2.4), showed that the data of the IMU could be used in combination with the inverted pendulum model in order to derive spatio-temporal parameters accurately.

During this study stopwatch measurements are used for the timing of the ten metre walk. This is standard practice within clinical environments in order to describe walking ability[329]. It has been reported before by Youdas et al[336] that measurements performed by a stopwatch contribute for 1% total variance within gait measurements in persons with gait impairments. The comparison between IMU and stopwatch timing did not show any significant difference over the ten metre walk.

Furthermore it was found that walking ability expressed as walking speed is not related to the individual correction factor within PD. Identical results were found when correlating BI score to the individual correction factors. This indicates that the individual correction factor cannot be estimated based on the gait speed or ability.

Indeed step length has not been validated versus the gold standard (OMCS). Due to limitations in the measurement location these measurements could not be taken.

Appendix 10.3 however describes a single case study of step length validation within a 75 year participant who suffers from PD.

Analysis of IMU technology, using the methods developed through this thesis, has shown that PD spatio-temporal gait characteristics can be derived from the inverted pendulum model in combination with an individual correction factor. Whilst these measures are the most commonly used to investigate walking in PD (Table 5), gait may be better characterised by more sophisticated analysis[276], as common spatio-temporal parameters can not stand alone when describing gait severity[337]. The next chapter will therefore explore a more sophisticated analysis method, which could describe and visualise gait variability Parkinson's disease.

Chapter 7: Non Linear analysis applied to gait

7.1 Summary

Gait variability has been shown to be increased when comparing typical developed adults (TDA) with Parkinson's disease (PD). Variability analysis can, for example, be an indication for risk of falling. Current methods rely on relatively large datasets which can be seen as a demanding for people suffering from a walking impairment. We set out to explore a simple phase plot variability analysis to differentiate TDA from PD based on data collected over a standard ten-metre walk.

Fourteen people with PD and ten TDA aged matched controls were recruited and asked to walk over a ten-meter at self selected walking speed. All participants scored eight or higher on the Rivermead Mobility Index indicating good mobility. An inertial measurement unit (IMU) was placed over the projected CoM with double adhesive tape sampling at 100Hz. Relative vertical CoM position was derived by means of double integration after which the proposed phase plot analysis was applied in order to describe the CoM variability.

Cadence (p=.342) and stride length (p=.615) did not show a significance between TDA and PD however a difference was found for walking speed (p=.041). Furthermore a significant difference was found for β (p=.010) and SD_A (p=.004) other than SD_B (p=.385) or $\forall$ (p=.830).

Two sequential ten-metre walks showed an insignificant difference in PD for cadence (p=.193), stride length (p=.683), walking speed (p=.684) and β (p=.194), SD_A (p=.051), SD_B (p=.145) or $\forall$ (p=.226).

This study indicated that the proposed phase plot analysis, performed on CoM motion could be used to reliably differentiate PD from TDA over a ten-meter walk whereas standard spatio-temporal parameters could not.

7.2 Introduction

Parkinson's Disease (PD), a progressive disorder of the central nervous system, presents with resting tremor, short slow steps, decreased CoM movement[219] and an increase in variability of temporospatial parameters such as stride length and step time[338]. Variability in stride-to-stride time and length can be an indication for risk of falling[297]. Spatio-temporal gait asymmetry is higher in PD[339] which has been found to relate to "*freezing of gait*"[340]. As such, temporal spatial variability is a sensitive marker of gait, however in these studies fractal analysis has been used, which relies on longer walks (i.e. two and six minute walking tests). Similar analysis have been used to explore variability in spatio-temporal analysis such as coefficient of variation analysis[341] or other '*diagnostic*' variability analysis[342]. An issue with these studies is that the data sets required are relatively large. Gathering this amount of data can be seen as time consuming and therefore rather stressful for participant, especially those with gait disabilities.

IMU technology can be used to measure centre of mass (CoM) movement, providing a quick and relatively cheap way of gathering larger amounts of data over relative few steps where a high sample frequency is used. Inspired by the Poincaré analysis, we developed phase plot analysis using IMU technology, in order to describe gait step-to-step variability in vertical CoM movement. This simple approach requires only a small amount of steps utilizing all individual data points of the CoM excursion (measured at 100Hz) which can be employed in this analysis over a short walking distance.

This study will initially explore the fidelity of a simple phase plot analysis based on Poincaré methods in order to detect step-to-step variability using theoretically generated sine waves. Secondly this study explores the use the phase plot method applied to human gait in order to compare gait variability between TDA and PD.

7.3 Materials and Method

Vertical CoM excursion can be derived using IMU translatory acceleration in combination with previously published methods using quaternion rotation matrices in combination with double integration[131]. Vertical CoM excursion can be used to determine temporal aspect of gait such as step time or cadence. Furthermore when using gait models such as the inverted pendulum[330] spatial parameters such as step and stride length can be estimated[343]. Models like these describe the mechanical energetic state during a gait cycle[62 72] in which the CoM excursion behaves like a sine wave.

For this study further analysis is performed on vertical CoM excursion, whereby CoM Excursion (CoM Excursion_i) is plotted against the same data minus one step (CoM Excursion_{i-1}), based on peak and trough analysis.

In order to better understand this analysis the theoretical exploration of these CoM plots by means of generated sine waves was performed in LabVIEW2010 by means of a sine-generator which varied frequency, amplitude and phase shift. In order to mimic changes typically observed over a ten-meter walk the following components were altered:

1) Amplitude ranges from 5 to 7cm, which represent typical vertical CoM movement during human walking[69] (Figure 30A)
2) Frequency values vary between 10-10.4Hz, representing the change in walking frequency during a 10 metre walk based on previous collected data as observed in Chapter 5 (Figure 30B)

Firstly a least square linear fit[129] was applied and superimposed on this cloud, r^2 was recorded and the linear fit was plotted as a function $f = ax + b$. The slope (*a*) was derived to angle (degrees) as shown in equation (7.1).

$$\beta = \tan^{-1}(a) \cdot (180 / \pi) \qquad (7.1)$$

A computer generated sine wave which assumes consistency and therefore no variability, would result as shown in Figure 26 will result in $\beta = 45^{O}$.

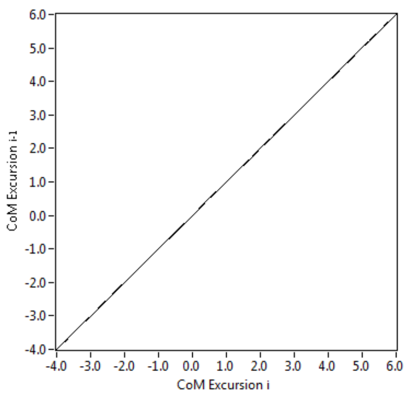

Figure 26 Sine wave mimicking no step-to-step variability with a constant phase shift of 180 degrees, indicating β=45^{o}

A circle was fitted onto the data in order to find the origins of the cloud (x_0, y_0, z_0) with the spread (SD_A) of the given data cloud[128] as shown in equation (7.2)

$$SD_A = \sum_{i=1}^{n}\left(\left(x_i - x_0\right)^2 + \left(y_i - y_0\right)^2 + \left(z_i - z_0\right)^2 - r^2\right)^2 \qquad (7.2)$$

which leads to a linear equation in x_0, y_0, z_0 where (x_i, y_i, z_i) are the given points, (x_0, y_0, z_0) is the origins or midpoint and r is the unknown radius[128]. Using the previously fitted sum of least squares the data was de-trended by subtracting the outcome of $y_i = ax_i + b$ from CoM Excursion$_{i-1}$ after which the standard deviation around the best fit was calculated (SD_B).

An ellipse was fitted around the spread of data based on two standard deviations where SD_A determine the length and SD_A the width. Ratio $\forall$, between SD_A and SD_B was determined to describe the ellipse. Furthermore angle β shows the direction of the data points indicating a level of symmetry as shown in Figure 27.

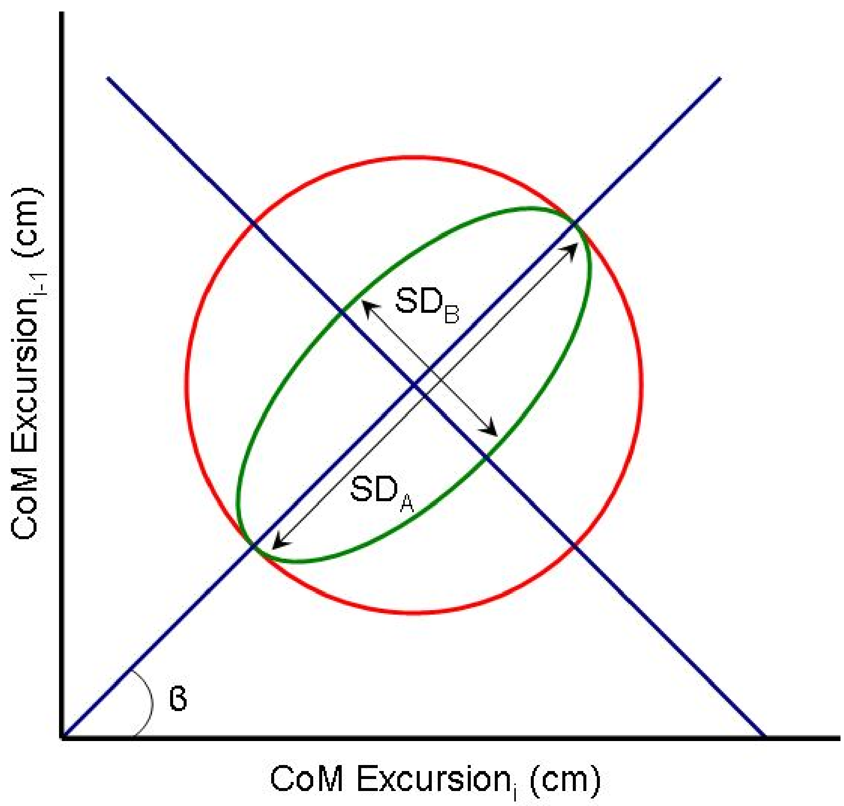

Figure 27 Showing the phase plot analysis and variables SD_A and SD_B indicating the standard deviations of the data cloud with β indicating the angle of the least square fit[129]

7.3.1 Theoretical exploration

A double sine wave (being theoretically non variable) generated within LabVIEW8.5 containing a frequency of 10.1Hz, amplitude of 5cm with an intersect of 1cm, indicating a phase shift, sampled at 100Hz will result in an angle $\beta = 45^O$ with an R^2 value of 1.00, SD_A of 4.98cm and SD_B of 0. When changing the phase shift (in steps of 45 degrees) of CoM_{i-1} the plots will change according to the plots shown in Figure 28.

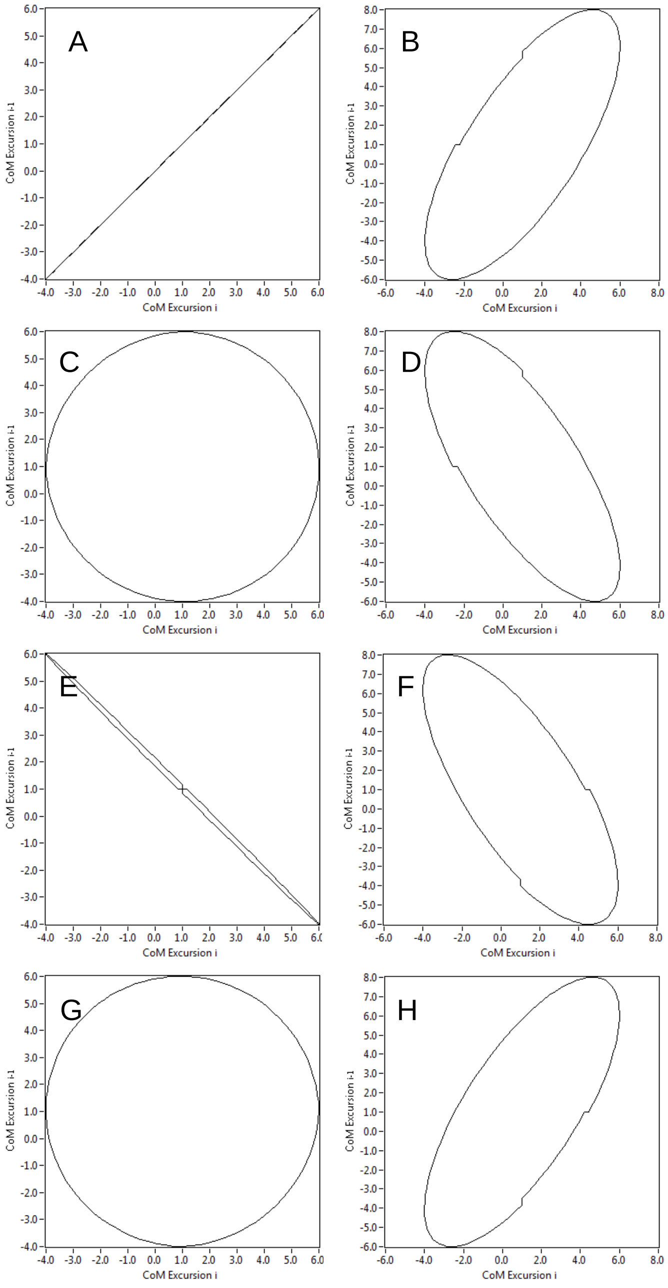

Figure 28 Phase plots based on equal sine waves (frequency 10.1Hz, amplitude 5cm) while being out of phase by 180^0 (A), 225^0 (B) 270^0 (C), 315^0 (D), 360^0 (E), 45^0 (F), 90^o (G) and 135^0 (H). It becomes clear that the sine wave produced data clouds rotate around their own axes (anti-clockwise) with change in phase shift.

CoM vertical excursion can vary with differing limb or stride length. In order to explore the theoretical models two sine waves were generated with an amplitude of 5cm and 7cm respectively which represents typical human walking[69]. The remaining configurations were similar to the previously used sine wave. Figure 29 shows the generated plots where it becomes visible that any variance in the CoM excursion results in a change in β (54.5 degrees) and SD_A (3.04) , however SD_B (0).

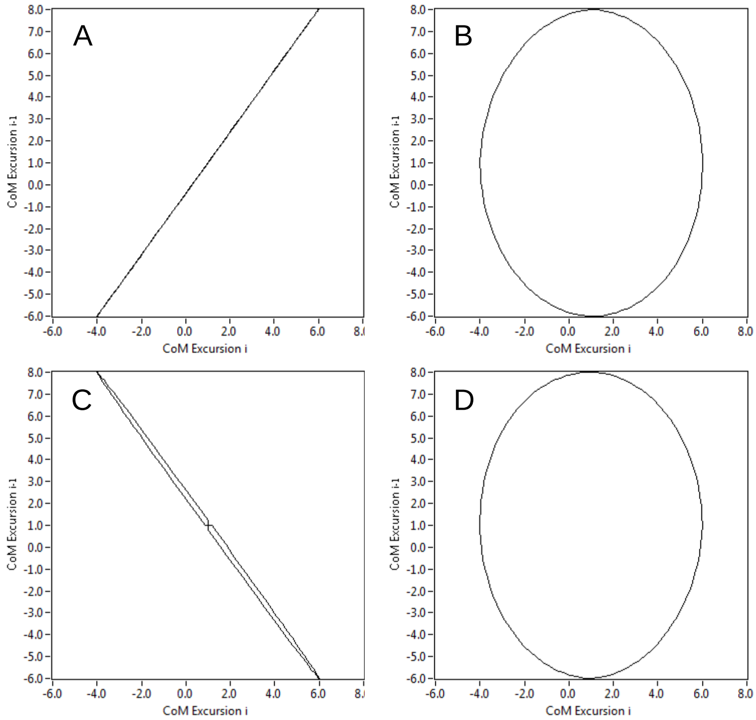

Figure 29 Phase plots based on two sine waves (frequency 10.1Hz, amplitude 5 and 7cm) with different while being out of phase by 180^0 (A), 170^0 (B) 360^0 (C) and 90^0 (D).

Changes such as walking speed can be related to an increase in step length and cadence. Change in step length will be followed by a change in CoM vertical excursion when assuming the inverted pendulum model[330]. The effects of the variability of step length is shown by creating three sine waves with different amplitudes (3, 5 and 7cm respectively) representing typical vertical CoM excursions during human walking[69] which effect is visible in Figure 30A. It becomes visible that β is 47.2 degrees, SD_A is 2.62 and SD_B is 0.23. Analysis with three sine waves with different frequency (10Hz, 10.2Hz and 10.4Hz), in which the change (steps of 0.1Hz) represents human gait step time or cadence variability[344], is shown in Figure 30B. It becomes visible that β = 44.8 degrees, SD_A = 1.41 and SD_B is 0.04.

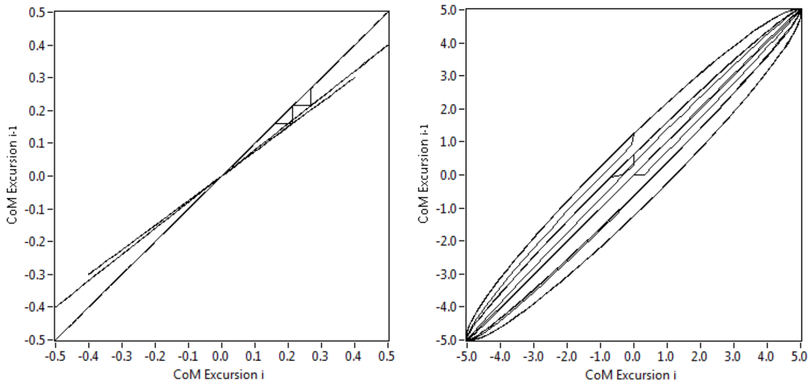

Figure 30 Phase plots based on three sine waves (constant amplitude of 5cm and phase shift of 180^{o}) representing a change in step length (A) and step frequency (B)

7.3.2 Practical application

7.3.2.1 Participants

Data collected from participants suffering from Parkinson's disease was re-analysed (Chapter 6). Data from aged matched typical developed adults who were recruited on a different study, was re-analysed. Both studies were approved by local ethical committees (#07/H0606/81 and #09/H0606/45 respectively) and were performed in agreement with the declaration of Helsinki.

7.3.2.2 Procedure

The Parkinson's Disease Questionnaire (PDQ) was administered for people with PD before partaking in this study. Participants walked over a ten-metre walkway free of obstacles at their self selected walking speed. Participants started at a static position at the zero-point and came to a complete stop at the ten-metre line. The duration of the walk was recorded by a stopwatch. An IMU was placed over the projected CoM located over the fourth lumbar vertebrae, measuring at a sample frequency of 100Hz.

7.3.2.3 Analysis

IMU data was analysed by a program written in LabVIEW 8.5 (National Instruments, Ireland) to obtain vertical position according to a method described in Chapter 3. Temporal and spatial gait parameters were calculated according to Zijlstra's inverted pendulum model[76] resulting in stride length and walking speed (v_l). β , SD_A , SD_B and $\forall$ were derived by applying the phase plot method as explained in section 7.3.

TDA and PD group were compared using an independent *t*-test on stride length and walking speed as well as β, SD_A and SD_B. Furthermore a Pearson's regression test was used to test for a relationship between walking speed and β for both PD and TDA. $\forall$ was tested by an independent *t*-test between PD and TDA.

7.4 Results

From the theoretical exploration of this phase plot analysis it became clear that β is affected by a change in step length, SD_A is affected by a change in step frequency as well as step length, SD_B is affected by a change in step frequency and $\forall$ is the ratio between SD_A and SD_B.

An independent *t*-test showed no difference between TDA and PD participants for cadence (123±5.6steps/min and 109.5±11.6steps/min respectively; p=.342) and stride length (1.37±0.08m and 1.16±0.29m respectively; p=.615). However, a difference was found for walking speed (1.36±0.33ms^{-1} and 1.08±0.22ms^{-1} respectively; p=.041). Moreover an independent *t*-test between the TDA and PD group revealed a significant difference for β (p=.010) and SD_A (p=.004). No difference was found between groups for SD_B (p=.385) or $\forall$ (p=.830). Results for each group can be found in Table 10.

Table 10 Outcomes from phase plot method applied to gait in typical developed adults (TDA) and Parkinson's disease (PD) showing the angle (β) of the least square fit with SD_A and SD_B describing the standard deviations of the phase plot with ratio $\forall$. An asterix indicates a significant difference between both groups.

Diagnosis	β [deg]	SD_A [cm]	SD_B [cm]	$\forall$ [au]
TDA	42.0 ± 1.8 *	2.5 ± 0.5 *	0.3 ± 0.1	7.8 ± 2.0
PD	39.4 ± 3.9 *	1.9 ± 0.5 *	0.4 ± 0.1	4.6 ± 3.9

No correlation was found between β and walking speed for PD (r^2=.001 p=.996) or TDA (r^2=.060 p=.810). Three representative analysis figures for each condition can be found in Figure 31.

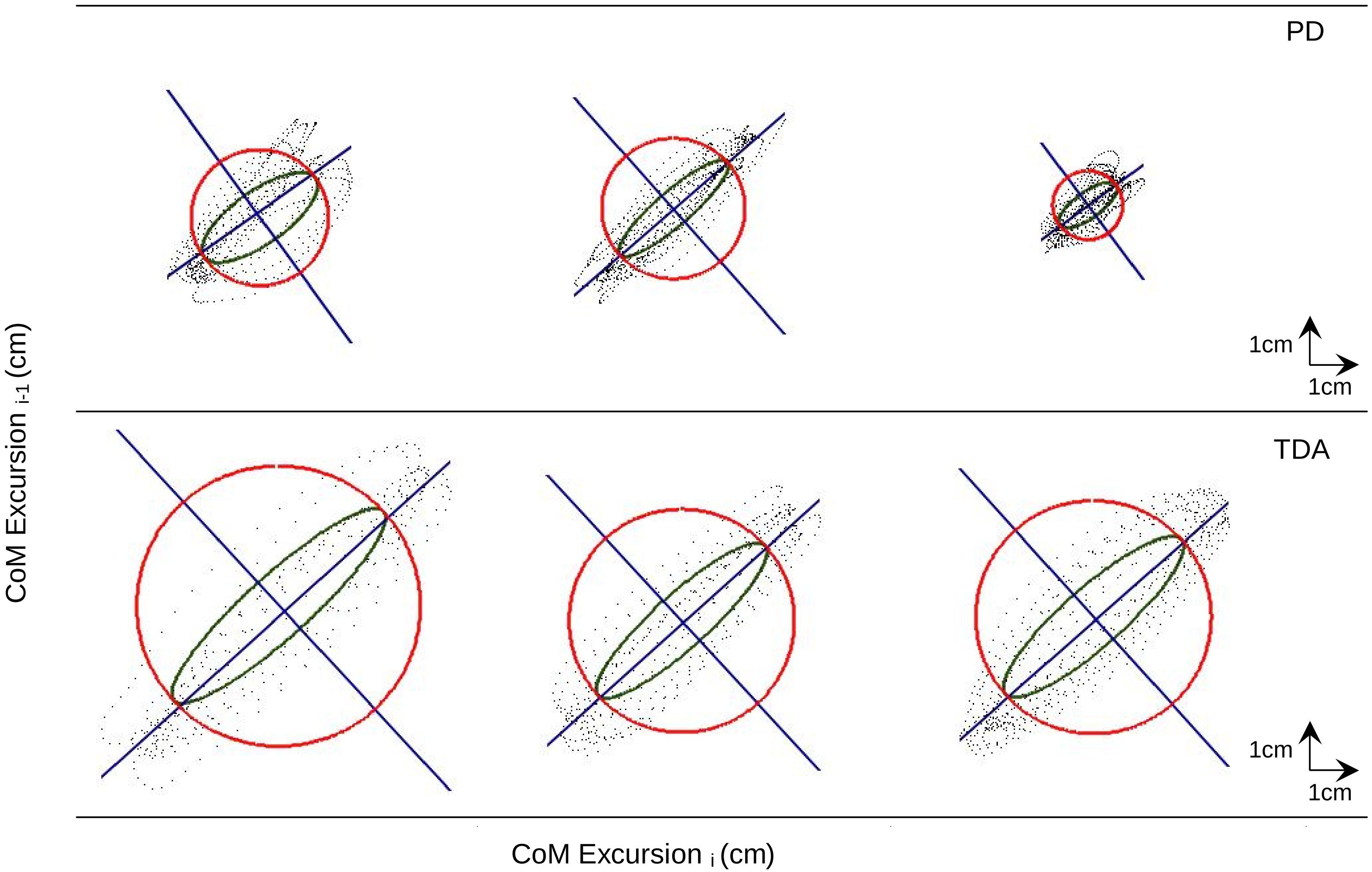

Figure 31 Representative graphs where the top three show typical graphs of participants with Parkinson's disease and the lower three represent typical graphs for typical developed adults.

7.5 Discussion

This study found that a phase plot analysis performed on CoM motion could be used to differentiate PD from TDA collected using IMUs over a 10 metre walk, whereas standard spatiotemporal parameters over the same distance could not. These findings are important as they promote the possibility of utilizing a phase plot variability analysis to objectively quantify gait variability and symmetry over a small sample frame, thus allowing people with PD at all stages of the disease to be monitored.

Previously, reduced step length has been reported as one of the key features of PD gait[268]. Indeed, Hausdorff[345] suggested that variability analysis may be used to closely monitor and describe gait disorders than measurements based on mean values of spatio-temporal walking parameters. The results of the present study support this as, whilst there was no difference in stride length, β and SD_A showed a significant difference between TDA and PD. Thus PD could be differentiated from TDA based on CoM variability (Figure 31). The significant difference in SD_A can be explained due to increased step length variability reflected in CoM excursion[330]. Although it should be noted that walking speed was significantly reduced for PD when compared to TDA which is reported previously[269 270], a significant difference was found for β and SD_A independent of walking speed.

PD has previously shown to be detectable by an increased stride-to-stride variability which is independent of a reduced stride length and is not reflected inconsistent in motor unit recruitment or muscle force output[346]. In more advanced PD where treatment with Levodopa has started this variability has been shown to be decreased[347]; however an increase in severity of PD is accompanied by an increase of stride-to-stride variability[348 349]. Gait timing variability has been related to the risk of falls[350] and freezing of gait within PD[351] during the "*on*" and "*off*" stage. This study demonstrated step to step gait alterations quantified through CoM motion could be explored for variability through the simple phase plot method explained in this studyt.

Considering the novelty of this approach in exploring gait, a range of simulated CoM motions were modelled and run through the phase plot analysis in order to better understand the changes observed in PD. Group stride length variance observed in the data collected during this research, was 17cm for TDA and 21cm for PD during a ten-meter walk without step initiation. Assuming the inverted pendulum methodology[330] and a constant leg length an increase in stride length of 17 and 21cm TDA and PD would increase the vertical CoM excursion by approximately 0.3 and 0.5cm. As shown in Figure 30A the effect of a simulated increase in step length of these values would change the angle of the phase plot plot by 3 and 5 degrees respectively. But it is worth noticing that this diversion in angle will only occur for one gait cycle when the change in step length occurred. Once the CoM excursion is symmetric and in phase between left and right after the asymmetrical cycle, β will return to 45 degrees. Therefore it becomes visible that β is influenced by a change in step length, SD_B is affected by a change in step frequency, SD_A is affected by both a change in step length as well as step frequency and $\forall$ is the ratio between the change in step frequency versus step length. No phase shift has been detected in this particular group of participants. However in case of an inaccuracy in defining the subsequent foot contact this would introduce a constant phase shift. In this particular group of participants it's very unlikely to happen. However in more severely affected participants, who do not walk according to the inverted pendulum model, there is an increased change of introducing a constant phase shift.

As seen in Figure 30B an increase in frequency will enlarge SD_B as measured over the 10 metre walk. An increase of 0.2Hz walking frequency represents an increase of 12 steps per minute. As seen in **Error! Reference source not found.** cadence variance is 5.6 for TDA and 11.6 for PD. A larger change in frequency results in a greater variance of SD_B. Perfect symmetry in lower limb stepping frequency causes the plots to assume a SD_B equal to zero. Indeed, with variability in CoM excursions due to step length variability in combination with step frequency variability a phase shift is expected. As shown in Figure 31 phase shifts will change β, SD_A and SD_B. During this study, however, no phase shift was detected within either TDA or PD measurements.

Novel methods have often been used to look into gait in more depth. For example fractal dynamic analysis has been used in TDA[33, 34] and PD[2, 35] to explore stride-to-stride fluctuations. An increase in stride-to-stride variability both in stride length as step time has been observed in early[27] and late stages[29] of PD. Furthermore a study by Sekine et al[35] used fractal dynamics to describe the motor outputs in PD while walking. Our findings are in agreement with these previous findings by showing an increase in stride length variability (SD_A) as well as an increase in stride-to-stride symmetry (β) within a variety of PD. Despite a visual decrease in SD_A and SD_B in

Figure 4, only SD_A shows a significant difference between PD and TDA. This could be explained by the reduced stride length which has also been reported by other PD research[36]. Furthermore it is noticeable that the ratio $\forall$ does not show a significant difference between PD and TDA. This indicates that the symmetry variability (SD_B) decreases by reducing stride length variability (SD_A).

Fractal and principal component analysis of gait variability require multiple gait cycles. During this study walking measurements were taken during a 10 metre test, which is a standardised clinical measurement[329] and therefore only a limited amount of cycles were required to obtain variability through the phase plot analysis. The IMU records projected CoM excursion at a sample frequency of 100Hz. All individual data points are used within the proposed method. Therefore variabilities can be detected over a short distance in comparison with studies by Hausdorff et al[337 338 347] which required longer walking distances.

Due to the small numbers of participants, which were allowed to partake due to the inclusion and exclusion criteria in this study, there is a limited variety and severity of PD within our data. However when comparing the data to TDA and other studies we find comparable variability and gait temporospatial outcomes[31 43]. Whilst our findings are comparable with those of larger data sets containing around 700steps[38], this method needs to be validated in larger groups and ranges of disability. In addition to standardised clinical tests such as ten-meter and six minute walking tests[39], variability can be objectively measured over ten-meters. This is in contrast with findings published by Hausdorff et al[2, 33] who suggested that variability measurements can only be taken over longer distances.

Results from this study show that IMU-derived data used in combination with a phase plot analysis can provide a quantitative measure for gait variability in spatial and temporal parameters over a 10 metre walk. The major benefit of this proposed method is that it can be employed during standardised clinical assessments. Thus this method may provide a valuable measure for clinical use. Whilst this study has only been conducted within PD alone and more research is required this method may have the potential to indicate the severity of their gait impairment in PD and other populations. This might also be a methodology that can assist in early diagnosis in people with PD and monitor their gait during deep brain stimulation. It may also be possible to use these gait parameters to more accurately monitor efficiency of medication in PD.

Chapter 8: General Conclusion

8.1 Summary

The general conclusions that can be derived from this body of work are discussed in this Chapter. The validity of IMU sensing and modelling is described followed by the reliability of this method and the phase plots are discussed as a novel means of obtaining variability analysis in gait.

8.2 Inertial measurement unit tracking of CoM movement

There is a pressing need for objective outcome measurements within clinics with the introduction of the National Institute for Health and Clinical Excellence (NICE) guidelines[109]. Whereas walking has been indicated as a sensitive marker for mortality[296 354] and neurological function[324], objective measurements can only be accurately collected by relatively expensive and time consuming systems such as optical motion capture systems (OMCS) measurements, which remain inaccessible to most clinicians[36].

OMCS measurements are also time consuming, require specific technical expertise and laboratory space in order to be able to successfully collect data. During this work an inertial measurement unit (IMU) was used to measure vertical CoM movement in order to provide an objective way of describing human gait. With the introductions of micro electro mechanical systems (MEMS) technology, new technological opportunities have arisen to measure human motion. A sensor fusion of tri-axial accelerometers, gyroscopes and magnetometers within an IMU sensor was used to measure accurate orientation and acceleration. This sensor was used to measure centre of mass motion during walking. Using the orientation expressed in complex numbers (quaternions) instead of Euler angles, which are susceptible to singularities, it became possible to rotate the accelerations from the object to global frame and thus capture centre of mass acceleration without loss of data. Digital signal processing was then developed, which consisted of a 4th order Butterworth low-pass filter with subtraction of the estimated direct current (DC) component determined by a Hanning window[161] and double integration by using Simpson's rule of integration[128]. These findings are unique, previous research[17 33] or IMU-based systems (Pegasus, Cambridge, UK) has only found centimetre instead of millimetre accuracy. The process described above provided a possible means to determine outcome measurements such as vertical acceleration, vertical velocity and vertical position of the centre of mass during walking that require validation in not only healthy individuals, both young and old, but also in clinical populations.

The current “gold” standard for measuring CoM displacement remains the kinetic method, by means of utilizing force plates. As discussed in Chapter 1.2.2 this has been used to determine internal CoM motion accurately avoiding errors which are known to be present when using the segmental method[92]. The segmental method refers to the kinematic approach by means of OMCS, such as VICON or Qualisys. The latter was used throughout this work and was found to be prone to errors with an increase in capture volume as discussed by Ehara et al[164 165]. Since a less complicated system was required as indicated by the Gait Survey (Chapter 1.3) a single reference method was chosen. Therefore the CoM referred to in this thesis refers to the “projected centre of mass” which reflects the movement of the internal CoM most accurately[96].

This thesis indicates that the fourth lumbar vertebra method of estimating vertical CoM displacement can be accurately measured over short time measurements by the use of inertial measurement units (IMU) and using the described quaternion and filtering methods with millimetre accuracy. This accuracy is not only held in typical developed adults[131] as shown in Chapter 3, but also in people with altered gait patterns such as Parkinson’s disease as shown in Chapter 5. This was an important finding as clinical populations have altered gait patterns[325] which can affect peak acceleration and therefore the double integration required to estimate the CoM relative displacement. This work supports the utility of this measurement system for use in clinical applications as a similar level of accuracy within OMCS measurements, when capturing data over similar volumes, has been reported by Ehara et al[164 165]. Indeed, other researchers, who validated the use of IMUs in order to measure CoM displacement in previous work, when using Euler angles to rotate the acceleration vectors, have only achieved an accuracy of 0.6 to 4cm error when measuring horses over different gait speeds[17]. There is to date no other study published that describes the accuracy of IMUs of CoM displacement within human subjects. The first two studies show that the method proposed to rotate, integrate and filter the acceleration, velocity and position of the CoM movement, was accurate within typical developed gait as well as in participants suffering from Parkinson’s disease when compared to the OMCS.

The second study (Chapter 5) further explored whether the IMU could be reliably used by experts and clinicians to obtain the same spatiotemporal gait parameters in clinical populations of PD. This group was selected due to well documented specific motor abnormalities, such as tremor and reduced walking speed, in their walking patterns[355] which could affect the analysis difficulty. A standard operating procedure both for data collection and analysis was developed with a non-expert user (defined as no previous experience in using the system) in mind. Whilst it was shown that the acceleration peaks did increase in amplitude, when performing the data analysis according to the standard operating procedures, the level of concurrent validity and intra-rater reliability support the use of this system as an objective gait measure for this clinical group by non experts such as clinicians.

8.3 Gait model validation of human gait

Maintaining mobility is one of the most consistently cited key concerns in clinical populations[332]. As such, objective spatial and temporal measurements of gait are critical markers for clinicians to accurately diagnose medical conditions and monitor their progression[109]. Currently however in daily clinical routine these measurements are taken by tests such as the ten metre or six minute walking test to assess walking performance[327]. These tests however are prone to error introduced by the subjectivity or the assessor, involved in timing the gait events with a stopwatch. Indeed it has been shown that within abnormal gait patterns, stopwatch measurements are valid in persons with gait impairments[336]. Furthermore these tests do not provide information of the underlying gait pathology. A more detailed and objective measure giving accurate and reliable spatial and temporal measurements can be used to give feedback to the clinician who can incorporate the results into in the decision making in rehabilitation programs[109 324].

Preliminary quantitative research carried out with clinicians (Chapter 1.3) revealed that clinicians are mostly interested in measuring gait parameters such as cadence, walking speed, symmetry, but also smoothness and effort. However measurement tools providing these parameters were inaccessible for clinicians because of budget and time constraints. A recent update from the “Gait and Clinical Movement Analysis Society”, revealed that gait analysis is an effective tool in the clinical decision making process for improving patient treatment outcomes for individuals[356]. This research set out to use accurate CoM position data to provide useful clinical measures of gait.

There are several models for determining spatial as well as temporal parameters proposed by other researchers[71 77 330]. Looking at the feedback received from the survey (Chapter 1.3) which was in agreement with previous results published by Toro et al.[36], a simple model was chosen to limit the amount of technical expertise required to provide valid and reliable data. Therefore a single reference point, the CoM, was chosen as this has proven to provide valuable gait information in the past[62 73 105 337 347]. The inverted pendulum model proposed by Zijlstra & Hof[330] was used throughout this work as it requires the CoM position data and leg length only. Utilizing this model, parameters such as step time, cadence, step length and walking speed can be derived, but are prone to a constant error, due to forward movement of the CoM during double stance, in typical developed adults (TDA)[71]. For TDA it has been found that this model reliably underestimates step length by 25% allowing its use to determine speed and step length. Throughout this work, the correction factor has been altered by measuring the timing (as defined by acceleration signals) from gait initiation to termination. By knowing the distance and the fact that step time has been proven to be accurate (Chapter 3) the average stride length can be derived from the estimated walking speed. Gonzalez et al[78] have previously adapted the inverted pendulum model to adjust for the forwards displacement of the CoM during double stance. As reported by Han et al[79] and Schmid et al[357] this horizontal displacement is proportional to the foot length by a varying factor of 0.83 and 0.67 as found by both researchers respectively. Gonzalez et al took this variation in account and calculated the individual factor from a random experiment of each individual by asking them to walk over a timed 25 meters. For these models, to be applied in clinical populations that have altered walking mechanics it is important that they are specifically validated [333]. Outcome parameters, estimated from the inverted pendulum model combined with a correction factor, are in agreement with previous data published by others who had access to more sophisticated systems[268 358].

Validation of this model, as described in Chapter 6, found that there was no significant difference found when comparing the use of the inverted pendulum model and clinical tests to obtain walking speed in people with PD. However it was noted that individual correction factors varied to a degree both within individuals on different walks and between individuals, therefore supporting the use of individual correction factors determined at each walk when measuring neurological conditions such as Parkinson’s disease. It was also found that the correction factor was not correlated to disability level or walking ability, suggesting that prediction of utility of the TDA correction factor based on ability or disability is unlikely.

During numerous analyses, it became visually clear that there was a lot of variability within steps and strides in clinical populations. Indeed as shown by Hausdorff et al. [337 338 347 349 359 360] gait variability could be an important marker of gait, but requires participants to walk for a long duration of time (~15minutes) which could be seen as a unfeasible for many patients.

8.4 Variability Analysis

Variability within measurements is often seen as noise and therefore unwanted. Variability analysis within heart rate beat-to-beat measurements has shown to change with disease and age[361]. Hausdorff et al[337] suggested that variability analysis in gait can convey important information regarding gait dynamics. Alterations in gait dynamics can determine disease severity[348 349], risk of falling[350] and freezing of gait (FoG)[351].

As conventional gait analysis relies on spatial and temporal gait parameters, larger datasets need to be gathered in order to look for variability. A recent study by Bollens et al[362] found that variability analysis could be successfully applied to detect gait variability over a 15 minute walk on a controlled treadmill. People suffering from neurodegenerative conditions such as PD might not be able to walk for 15 minutes. Therefore the final study looked into a novel phase plot method in order to explore the variability within TDA and PD gait over a standard 10 metre walk as described in Chapter 7. It was found that gait measurements at self selected walking speed over a standardised clinical distance of 10 metres could provide variability measurements. Where the study did not point to any significant difference between step length in TDA and PD, step length variability measured by vertical CoM movement was increased in PD. This is in agreement with previous data from Baltadjieva et al[346] who showed that stride-to-stride variability is independent of a reduced stride length. Furthermore this study found an increased step timing variability which can be an indicator for risk of falling and FoG[337].

This study showed that variability in gait measurements, collected during clinical assessments of gait over a short distance[363], can be objectively measured. Thus this approach could provide valuable information regarding disease severity and therefore be an outcome parameter for gait mobility and potential risk assessments for falls in PD.

8.5 Limitations of the proposed studies

The insight gained from the studies of this thesis should be viewed in the light of the limitations of this work. In Chapter 3 the main limitation of the validity study in TDA, is the relatively small capture volume. This study might not have been statistically powered to evaluate differences between new measurement approaches and reference systems. The number of participants in these studies is based on comparable studies looking into new measurement techniques using inertial measurement units[26]. TDA may not have reached their self selected walking speed. Furthermore the participants were asked to walk at their self selected walking speed and therefore the results may not apply to extreme walking speeds. Gait spatio-temporal parameters however, were in agreement with previous studies looking at TDA and PD gait characteristics[269 270] and we did not find a relationship of walking speed to accuracy. The capture volume is also typical of that used when measuring both using OMCS and if attempting to measure in the clinic.

All the studies were statistically powered to detect differences between groups; however the variance of severity of PD was limited and a larger sample size would generate greater confidence in the application of our findings to people with PD per se. All participants were recruited from Oxfordshire via consultants working at the Nuffield Orthopaedic Centre of Enablement and the John Radcliffe Hospital to ensure the widest spread possible within the county. Questionnaires such as the Parkinson's disease questionnaire (PDQ39; Chapter 10.2.2) might be biased due to the higher level of education in the South East Region[364] and not represent a true reflection of the state of PD.

As suggested by Meichtry[98] accelerometers have unresolved methodological considerations, such as issues regarding drift over long term measurements. Indeed as demonstrated by an Alan variance analysis (Chapter 2.3.3) the drift will behave exponentially after an initial 15-20 seconds[140]. To overcome this problem this system is solely meant for short term measurements. Longer measurements (i.e. two or six minute walks) need to be analysed in small sections.

The model proposed to derive spatio-temporal parameters from inertial sensed CoM movement as by Zijlstra & Hof[330] has been proven to be valid in TDA and PD. Since this model is based on the inverted pendulum analogy, it is worth noticing that this validation might not always hold in clinical conditions. For example stroke survivors tend to swing more bilaterally, increasing oxygen consumption costs but reducing the CoM mechanical energetic cost[365].

8.6 Final Remarks

Inertial measurement units can measure the lower spine projected centre of mass displacement in human gait within TDA and PD. This, in combination with gait models, to estimate temporal and spatial measurements, can provide clinicians with information in order to accurately diagnose medical conditions and monitor their progression. With indication from the World Health Organisation that PD will become increasingly predominant over the incoming years, there will be an increasing need for accurate monitoring of this and other neurological conditions.

9 References

1. A genealogy of Biomechanics. in 23rd Annual Conference of the American Society of Biomechanics; 1999.

2. Roetenberg D. Inertial and Magnetic Sensing of Human Motion Twente University, 2006.

3. Schneck DJ. *The Biomedical handbook*. second ed: CRC Press & IEEE Press, 2000.

4. Meijer O. Making things happen: An introduction to the history of movement science. In: Latash M, Zatsiorsky V, editors. *Classics in Movement Science*: Human Kinetics, 2006.

5. Marey EJ. De la mesure des forces dans les differents actes de la locomotion. *CRAS* 1883;97:782 - 86.

6. Godfrey A, Conway R, Meagher D, Olaighin G. Direct measurements of human movement by accelerometry. *Medical Engineering & Physics* 2008;30:1354-86.

7. Gonzalez MC, Hidalgo CA, Barabasi AL. Understanding individual human mobility patterns. *Nature* 2008;453:779-82.

8. Dickens WE, Smith MF. Validation of a visual gait assessment scale for children with hemiplegic cerebral palsy. *Gait & Posture* 2006;23(1):78-82.

9. Lord SE, Halligan PW, Wade DT. Visual gait analysis: the development of a clinical assessment and scale. *Clin Rehabil* 1998;12(2):107-19.

10. Wolfson L, Whipple R, Amerman P, Tobin JN. Gait assessment in the elderly: a gait abnormality rating scale and its relation to falls. *J Gerontol* 1990;45(1):M12-9.

11. Lauder MA, Lake JP. Biomechanical Comparison of Unilateral and Bilateral Power Snatch Lifts. *J Strength Cond Res* 2008.

12. Walsh MS, Ford KR, Bangen KJ, Myer GD, Hewett TE. The validation of a portable force plate for measuring force-time data during jumping and landing tasks. *J Strength Cond Res* 2006;20(4):730-4.

13. Doke J, Donelan JM, Kuo AD. Mechanics and energetics of swinging the human leg. *J Exp Biol* 2005;208(Pt 3):439-45.

14. Lee HK, Cho SP, You JH, Lee KJ. The concurrent validity of the body center of mass in accelerometric measurement. *Conf Proc IEEE Eng Med Biol Soc* 2007;2007:659-61.

15. Lin JH, Chou YL, Ju MS, Sung YT. Application and evaluation of the VICON system in gait analysis. *Gaoxiong Yi Xue Ke Xue Za Zhi* 1990;6(1):6-11.

16. Israel I, Chapuis N, Glasauer S, Charade O, Berthoz A. Estimation of passive horizontal linear whole-body displacement in humans. *J Neurophysiol* 1993;70(3):1270-3.

17. Pfau T, Witte TH, Wilson AM. A method for deriving displacement data during cyclical movement using an inertial sensor. *J Exp Biol* 2005;208(Pt 13):2503-14.

18. Collett J, Dawes H, Howells K, Elsworth C, Izadi H, Sackley C. Anomalous centre of mass energy fluctuations during treadmill walking in healthy individuals. *Gait & Posture* 2007;26(3):400-6.

19. Klimek A, Chwala W. The evaluation of energy cost of effort and changes of centre of mass (COM) during race walking at starting speed after improving the length of lower extremities. *Acta Bioeng Biomech* 2007;9(2):55-60.

20. Newman MA, Dawes H, van den Berg M, Wade DT, Burridge J, Izadi H. Can aerobic treadmill training reduce the effort of walking and fatigue in people with multiple sclerosis: a pilot study. *Mult Scler* 2007;13(1):113-9.

21. Adamczyk PG, Collins SH, Kuo AD. The advantages of a rolling foot in human walking. *J Exp Biol* 2006;209(Pt 20):3953-63.

22. Godfrey A, Hourigan T, Olaighin GM. Pendulum Analysis of an Integrated Accelerometer to assess its suitability to measure Dynamic Acceleration for Gait Applications. *Conf Proc IEEE Eng Med Biol Soc* 2007;1:4891-4.

23. Kavanagh JJ, Menz HB. Accelerometry: A technique for quantifying movement patterns during walking. *Gait & Posture* 2008;28:1-15.

24. Billing DC, Hayes JP, Hayes EC, Baker J. Measurement of Ground Reaction Forces using Unobtrusive, on-athlete instrumentation. *IEEE* 2004(Intelligent Sensing and Information Processing, 2004. Proceedings of International Conference on):218 - 21.

25. Light LH, McLellan GE, Klenerman L. Skeletal transients on heel strike in normal walking with different footwear. *J Biomech* 1980;13(6):477-80.

26. Moe-Nilssen R. Test-retest reliability of trunk accelerometry during standing and walking. *Arch Phys Med Rehabil* 1998;79(11):1377-85.

27. Foster R, Lanningham-Foster L, Levine J. Optimization of accelerometers for measuring walking. *Journal of Sports Engineering and Technology* 2008;222(P1):53-60.

28. Yeon Fuh Jiang YPL. Error analysis of quaternion transformations [inertial navigation]. *IEEE Transactions on Aerospace and Electronic Systems* 1991;27(4):634 - 39.

29. Luinge HJ, Veltink PH. Measuring orientation of human body segments using miniature gyroscopes and accelerometers. *Med Biol Eng Comput* 2005;43(2):273-82.

30. Borenstein LOaJ. Non-GPS Navigation for Emergency Responders. *Sharing Solutions for Emergencies and Hazardous Evironments*. Salt Lake City, Utah, USA: University of Michigan, 1101 Beal Avenue, Ann Arbor MI, 48109, 2006.

31. Luinge HJ. Inertial Sensing of Human Movement. Twente University Press, 2002.

32. Moore GE. Cramming more components onto integrated circuits. *Electronics* 1965;38(8).

33. Pfau T, Witte TH, Wilson AM. Centre of mass movement and mechanical energy fluctuation during gallop locomotion in the Thoroughbred racehorse. *J Exp Biol* 2006;209(Pt 19):3742-57.

34. Kavanagh JJ, Barrett RS, Morrison S. Upper body accelerations during walking in healthy young and elderly men. *Gait & Posture* 2004;20(3):291-8.

35. Yack HJ, Berger RC. Dynamic stability in the elderly: identifying a possible measure. *J Gerontol* 1993;48(5):M225-30.

36. Toro B, Nester C, Farren P. The status of Gait assessment among physiotherapists in the United Kingdom. *Archives of physical medicine and rehabilitation* 2003;84(12):1878-84.

37. Insel P, Roth W, ROllins L, Petersen R. *Core concepts in health*. Mountain View, California: Mayfield Publishing Company, 1996.

38. Guerra N, Huesmann L, Spindler A. Community Violence Exposure, Social Cognition, and Aggression among Urban Elementary School Children. *Child Development* 2003;74(5):1561-76.

39. Moritz DJ, Kasl SV, Berkman LF. Cognitive functioning and the incidence of limitations in activities of daily living in an elderly community sample. *Am J Epidemiol* 1995;141(1):41-9.

40. Spirduso W, Francis K, MaxRae P. *Physical Dimensions of Aging - 2nd Edition*. 2 ed, 2005.

41. Hirose M, Ogawa K. Honda humanoid robots development. *Philos Transact A Math Phys Eng Sci* 2007;365(1850):11-9.

42. Perry J, Burnfield J. *Gait Analysis: Normal and pathological funtion*: Thorofare, NJ: SLACK, c2010, 1992.

43. Thomas S, Supan T. A comparison of current biomechanical terms. *Journal of Prosthetics & Orthotics* 1990;2(2):107-14.

44. Woollacott M, Shumway-Cook A. Attention and the control of posture and gait: a review of an emerging area of research. *Gait & Posture* 2002;16(1):1-14.

45. Woollacott M, Tang P. Balance Control During Walking in the Older Adult: Research and its Implications. *Physical Therapy* 1997;77(6):646-60.

46. Matsusaka N. Control of the medial-lateral balance in walking. *Acta Orthop Scand* 1986;57(6):555-9.

47. Ott E, Munih M, Benko H, Kralj A. Comparison of foot-switch and hand switch triggered FES correction of foot drop. *Proc of 6th Vienna International Workshop on FES* 1998:22-24.

48. Jasiewicz JM, Allum JH, Middleton JW, Barriskill A, Condie P, Purcell B, et al. Gait event detection using linear accelerometers or angular velocity transducers in able-bodied and spinal-cord injured individuals. *Gait & Posture* 2006;24(4):502-9.

49. Verdejo R, Mills NJ. Heel-shoe interactions and the durability of EVA foam running-shoe midsoles. *J Biomech* 2004;37(9):1379-86.

50. Collins JJ, Whittle MW. Influence of gait parameters on the loading of the lower limb. *J Biomed Eng* 1989;11(5):409-12.

51. Forner-Cordero A, Koopman HJ, van der Helm FC. Inverse dynamics calculations during gait with restricted ground reaction force information from pressure insoles. *Gait & Posture* 2006;23(2):189-99.

52. Tong K, Granat H. A practical gait analysis system using gyroscopes. *Med. Eng & Physics* 1999;21:87-94.

53. Winter DA, Yack HJ. EMG profiles during normal human walking: stride-to-stride and inter-subject variability. *Electroencephalogr Clin Neurophysiol* 1987;67(5):402-11.

54. Sutherland DH, Olshen R, Cooper L, Woo SL. The development of mature gait. *J Bone Joint Surg Am* 1980;62(3):336-53.

55. Beck RJ, Andriacchi TP, Kuo KN, Fermier RW, Galante JO. Changes in the gait patterns of growing children. *J Bone Joint Surg Am* 1981;63(9):1452-7.

56. Judge JO, Davis RB, 3rd, Ounpuu S. Step length reductions in advanced age: the role of ankle and hip kinetics. *J Gerontol A Biol Sci Med Sci* 1996;51(6):M303-12.

57. Schulz BW, Ashton-Miller JA, Alexander NB. The effects of age and step length on joint kinematics and kinetics of large out-and-back steps. *Clin Biomech (Bristol, Avon)* 2008;23(5):609-18.

58. Monaco V, Rinaldi LA, Macri G, Micera S. During walking elders increase efforts at proximal joints and keep low kinetics at the ankle. *Clin Biomech (Bristol, Avon)* 2009;24(6):493-8.

59. Monaco V, Ghionzoli A, Dario P, Micera S. Muscle synergies during walking: comparison between young and elderly people. Preliminary results. *Conf Proc IEEE Eng Med Biol Soc* 2008;2008:5370-3.

60. Beauchet O, Allali G, Annweiler C, Bridenbaugh S, Assal F, Kressig R, et al. Gait Variability among Healthy Adults: Low and High Stride-to-Stride Variability Are Both a Reflection of Gait Stability. *Gerontology* 2009;55:702-06.

61. Saunders JBM, Inman VT, Eberhart HD. The major determinants in normal and pathological gait. *The Journal of Bone & Joint Surgery* 1953;35:543-58.

62. Cavagna GA, Saibene FP, Margaria R. External work in walking. *J Appl Physiol* 1963;18:1-9.

63. Della Croce U, Riley PO, Lelas JL, Kerrigan DC. A refined view of the determinants of gait. *Gait & Posture* 2001;14(2):79-84.

64. Godges JJ, MacRae PG, Engelke KA. Effects of exercise on hip range of motion, trunk muscle performance, and gait economy. *Phys Ther* 1993;73(7):468-77.

65. Bauby CE, Kuo AD. Active control of lateral balance in human walking. *J Biomech* 2000;33:1433-40.

66. Donelan JM, Kram R, Kuo AD. Mechanical and metabolic determinants of the preferred step width in human walking. *Proc Biol Sci* 2001;268(1480):1985-92.

67. Greenwood DT. *Principles of Dynamics*. New Jersey: Prentice-Hall, Inc, 1988.

68. Cavagna GA, Willems PA, Heglund NC. The role of gravity in human walking: pendular energy exchange, external work and optimal speed. *J Physiol* 2000;528(Pt 3):657-68.

69. Lee CR, Farley CT. Determinants of the center of mass trajectory in human walking and running. *J Exp Biol* 1998;201(Pt 21):2935-44.

70. Peyrot N, Thivel D, Isacco L, Morin JB, Duche P, Belli A. Do mechanical gait parameters explain the higher metabolic cost of walking in obese adolescents? *J Appl Physiol* 2009;106(6):1763-70.

71. Zijlstra W. Assessment of spatio-temporal parameters during unconstrained walking. *Eur J Appl Physiol* 2004;92(1-2):39-44.

72. Cavagna GA, Heglund NC, Taylor CR. Mechanical work in terrestrial locomotion; two basic mechanisms for minimizing energy expenditure. *Am. J. Physiol* 1977;233:243-61.

73. Cavagna GA, Thys H, Zamboni A. The sources of external work in level walking and running. *J Physiol* 1976;262(3):639-57.

74. Usherwood JR, Szymanek KL, Daley MA. Compass gait mechanics account for top walking speeds in ducks and humans. *J Exp Biol* 2008;211(Pt 23):3744-9.

75. Winiarski S. Mechanical energy fluctuations during walking of healthy and ACL-reconstructed subjects. *Acta Bioeng Biomech* 2008;10(2):57-63.

76. Zijlstra W, Hof AL. Assessment of spatio-temporal gait parameters from trunk accelerations during human walking. *Gait & Posture* 2003;18:1-10.

77. Kuo AD. The six determinants of gait and the inverted pendulum analogy: A dynamic walking perspective. *Human Movement Science* 2007;26(4):617-56.

78. Gonzalez RC, Alvarez D, Lopez AM, Alvarez JC. Modified pendulum model for mean step length estimation. *Conf Proc IEEE Eng Med Biol Soc* 2007:1371-4.

79. Han TR, Paik NJ, Im MS. Quantification of the path of center of pressure (COP) using an F-scan in-shoe transducer. *Gait Posture* 1999;10(3):248-54.

80. Schmid M, Beltrami G, Zambarbieri D, Verni G. Centre of pressure displacements in trans-femoral amputees during gait. *Gait Posture* 2005;21(3):255-62.

81. Alvarez JC, Gonzalez RC, Alvarez D, Lopez AM, Rodriguez-Uria J. Multisensor approach to walking distance estimation with foot inertial sensing. *Conf Proc IEEE Eng Med Biol Soc* 2007;1:5719-22.

82. Dempster WT. Space requirements of the seated operator : geometrical, kinematic, and mechanical aspects of the body, with special reference to the limbs. *Engineering, College of - Technical Reports*. Ohio: Wright-Patterson Air Force Base, 1955.

83. Gard SA, Miff SC, Kuo AD. Comparison of kinematic and kinetic methods for computing the vertical motion of the body center of mass during walking. *Human Movement Science* 2004;22:597-610.

84. Marey E-J. Apparatus for registering animal movements. *Nature (London)* 1876;XIV:214-15.

85. Takeda R, Tadano S, Todoh M, Morikawa M, Nakayasu M, Yoshinari S. Gait analysis using gravitational acceleration measured by wearable sensors. *J Biomech* 2009;Epub(Epub):Epub.

86. Smet KD, Segers V, Lenoir M, Clercq DD. Spatiotemporal characteristics of spontaneous overground walk-to-run transition. *Gait & Posture* 2009;29:54-58.

87. Kerrigan DC, Viramontes BE, Corcoran PJ, LaRaia PJ. Measured versus predicted vertical displacement of the sacrum during gait as a tool to measure biomechanical gait performance. *Am J Phys Med Rehabil* 1995;74(1):3-8.

88. Harless E. The static moments of human limbs (German). *Treatises of the Math.-Phys. Class of the Royal Acad. of Sc. of Bavaria* 1860;8(69):257-94.

89. Braune W, Fischer O. The Human Gait. *Springer - Verslag* 1987.

90. Elftman H. A cinematic study of the distribution of pressure in the human foor. *Anat. Rec.* 1934;59:481-87.

91. Elftman H. The measurement of the external force in walking. *Science* 1938;88:152-53.

92. Kirtley C. *Clinical Gait Analysis: Theory and practice*. London: Elsevier, Churchill Livingston, 2006.

93. Saini M, Kerrigan DC, Thirunarayan MA, Duff-Raffaele M. The vertical displacement of the center of mass during walking: a comparison of four measurement methods. *J Biomech* 1998;120(1):133-9.

94. Saini M, Kerrigan DC, Thirunarayan MA, Duff-Raffaele M. The vertical displacement of the center of mass during walking: a comparison of four measurement methods. *J Biomech Eng* 1998;120(1):133-9.

95. Cavagna GA, Franzetti P. Mechanics of competition walking. *J. Physiol* 1981;315:243-51.

96. Auvinet B, Berrut G, Touzard C, Moutel L, Collet N, Chaleil D, et al. Reference data for normal subjects obtained with an accelerometric device. *Gait & Posture* 2002;16(2):124-34.

97. Lundberg A. On the use of bone and skin markers in kinematics research. *Human Movement Science* 1996;15:411-22.

98. Meichtry A, Romkes J, Gobelet C, Brunner R, Muller R. Criterion validity of 3D trunk accelerations to assess external work and power in able-bodied gait. *Gait & Posture* 2007;25(1):25-32.

99. Gard SA, Childress DS. The effect of pelvic list on the vertical displacement of the trunk during normal walking. *Gait & Posture* 1997;5(3):233-38.

100. Cavagna GA. Force platforms as ergometers. *J Appl Physiol* 1975;39(1):174-9.

101. Tesio L, Lanzi D, Detrembleur C. The 3-D motion of the centre of gravity of the human body during level walking I. Normal subjects at low and intermediate walking speeds. *Clin Biomech* 1998;13(2):77-82.

102. Tesio L, Lanzi D, Detrembleur C. The 3-D motion of the centre of gravity of the human body during level walking. II. Lower limb amputees. *Clin Biomech* 1998;13(2):83-90.

103. Sadaghi H, Allard P, Duhaime M. Functional gait assymmetry in able-bodied subjects. *Human Movement Science* 1997;16:243-58.

104. Gard SA, Knox EH, Childress DS. Two-dimensional representation of three-dimensional pelvic motion during human walking: An example of how projects can be misleading. *Journal of Biomechanics* 1996;29(10):1387-91.

105. Cavagna GA, Franzetti P, Fuchimoto T. The mechanics of walking in Children. *J. Physiol* 1983;343:323-39.

106. White SC, Yack HJ, Tucker CA, Lin HY. Comparison of vertical ground reaction forces during overground and treadmill walking. *Med Sci Sports Exerc* 1998;30(10):1537-42.

107. Alton F, Baldey L, Caplan S, Morrissey MC. A kinematic comparison of overground and treadmill walking. *Clin Biomech (Bristol, Avon)* 1998;13(6):434-40.

108. Murray MP, Spurr GB, Sepic SB, Gardner GM, Mollinger LA. Treadmill vs. floor walking: kinematics, electromyogram, and heart rate. *J Appl Physiol* 1985;59(1):87-91.

109. Marks DF. Perspectives on evidence-based practice. London: City University, 2002:53.

110. Shams QA, Moniuszko M, Ingham JC. Applying MEMS technology to field, flight & space deployable systems. *IEEE* 2001;1:246 - 56.

111. Hooke R. De Potentia Restitutiva. London, 1678:23 - 28.

112. Newton. Mutationem motus propertionalem esse vi motrici impressae, et fieri secundum lineam rectam qua vis illa imprimitur. *Motte's* 1729.

113. Lemkin M, Boser B. A Three-Axis Micromachine Accelerometer with a CMOS Position-Sense Interface and Digital Offset-Trim Electronics. *IEEE Journal of Solid-State Circuits* 1999;34(4):456 - 68.

114. Foucault L. Les vitesse relatives de la lumiere dans l'air et dans l'eau. A La Faculte des Sciences de Paris, 1853.

115. Gray J. *Electrical Influence machines*. London: Whittaker & co., 1890.

116. Gelfrand IM. *Calculus of Variations*. Dover, 1963.

117. Gauss CF. Intensitas vis magnetcae terrestris ad mensuram absolutam revocata (translated: The intensity of the earth's magnetic force reduced to absolute measurement). *Royal Scientific Society* 1832;8:3-44.

118. Sheynin OB. C.F. Gauss and the theory of errors. *Archive for History of Exact Sciences* 1979;20(1):21-79.

119. Tomayko JE. *Computers take flight: A history of NASA's Pioneering Digital Fly-By-Wire Project*. Washington D.C., 2000.

120. Henriksen K, Sporring J, Hornbaek K. Virtual trackballs revisited. *IEEE Trans Vis Comput Graph* 2004;10(2):206-16.

121. Wilkins DR, editor. On a new species of imaginary quantities connected with a theory of quaternions; 1844 1999; Royal Irish Academy.

122. Wilkins DR, editor. On quaternions and the rotation of a solid body; 1848 1999; Royal Irish Academy.

123. Spring KW. Euler Parameter and the use of Quaternion Algebra in the manipulation of finite rotations: A review. *Mechanism and Machine Theory* 1986;21(5):365-73.

124. Hanson AJ. *Visualizing Quaternions*. San Francisco: Morgan Kaufmann Publishers, Elsevier, San Francisco, 2006.

125. Altman SL. *Rotations, Quaternions and Double Groups*. Oxford: Claredon Press, 1986.

126. Liesenfeld R. Digital Signal Processing.

127. Tan L. *Digital Signal Processing: fundamentals and applications*. San Diego, California: Elsevier, 2008.

128. Bishop RH. *LabVIEW 8 student edition*: Upper Saddle River, NJ: Pearson Prentice Hall, 2007.

129. Travis J, Kring J. *LabVIEW for Everyone*. Third ed. Upper Saddle River: Pearson Education, Inc. , 2007.

130. Bruijn S, Dieen Jv, Meijer O, Beek P. Is slow walking more stable? *Journal of Biomechanics* 2009;42(10):1506-12.

131. Esser P, Dawes H, Collett J, Howells K. IMU: Inertial Sensing of Vertical CoM Movement. *Journal of Biomechanics* 2009;42:1578-81.

132. Brandes M, Zijlstra W, Heikens S, van Lummel R, Rosenbaum D. Accelerometry based assessment of gait parameters in children. *Gait & Posture* 2006;24(4):482-6.

133. Bourke AK, O'Donovan KJ, OLaighin G. The identification of vertical velocity profiles using an inertial sensor to investigate pre-impact detectionof falls. *Medical Engineering & Physics* 2008;30:937 - 46.

134. Carpinella I, Crenna P, Calabrese E, Rabuffetti M, Mazzoleni P, Nemni R, et al. Locomotor Function in the Early Stage of Parkinson's Disease. *IEEE Transactions on Neural Systems and Rehabilitation Engineering* 2007;15(4):543 - 51.

135. Smith JO. Introduction to Digital Filters with Aurio Applications. In: Smith JO, editor. Stanford, California, 2007.

136. OKU T. 1999. US Patent.

137. Collett JC. Evaluation of gait economy using centre of mass displacement in healthy individuals and individuals with stroke. Oxford Brookes University, 2007.

138. Dawes H, Enzinger C, Johansen-Berg H, Bogdanovic M, Guy C, Collett J, et al. Walking performance and its recovery in chronic stroke in relation to extent of lesion overlap with the descending motor tract. *Exp Brain Res* 2008;186(2):325-33.

139. Allan DW. Statistics of atomic frequency standards. *Proceedings of the IEEE* 1966;54(2):221-30.

140. 647™. *IEEE Standard Specification Format Guide and Test Procedure for Single-Axis Laser Gyros - Annex C*. New York, NY: IEEE - 3 Park Avenue, 2006.

141. Woodman OJ. An Introduction to inertial navigation. Cambridge: University of Cambridge, 2007.

142. Thong Y, Woolfson M, Crowe J, Hayes-Gill B, Challis R. Dependence of intertial measurements of distance on accelerometer noise. *Meas. Sci. Technol.* 2002;13:1163-72.

143. Schroder D, Babcock J. Negative bias temperature instability: Road to cross in deep submicron silicon semiconductor manufacturing. *Journal of Applied Physics* 2003;94(1):1-18.

144. Stockwell W. Angle Random Work. Milpitas, CA, USA: Crossbow Technology, Inc, 1997:4.

145. De La Republique Francaise - Assemblee Nationale. Compte Rendu Integral; 1958.

146. The International System of Units (SI). In: Taylor N, editor. Gaithersburg: National Institute of Standards and Technology, 2001.

147. Farrell JA, Borth M. *The Global Positioning System and Intertial Navigation*. New York: McGraw-Hill, 1999.

148. Haid M, Marquardt G, Breitenbach J. 2004.06.17 2004. Bundesrepublik Deutschland patent DE10312154A1.

149. Handhelddesign.com. Dynamometers Based on Acceleration Sensors -- Theory and Practice, 1999.

150. Rehbinder H, Hu X. Drift-free attitude estimation for accelerated rigid bodies. *Automatica* 2004;40:653 - 59.

151. Horan R, Lavelle M. Introductory Differentiation. *Basic Mathematics*. Plymouth: University of Plymouth, 2004.

152. Kranzer H. An Error Formula for Numerical Differentiation. *Numerische Mathematik* 1963;5:439-42.

153. Tachev G. Approximation, numerical differentiation and integration based on taylor polynomial. *Journal of inequalities in pure and applied mathematics* 2009;10(1):1-7.

154. Floater M. Error formulas for divided difference expansions and numerical differentiation. *Journal of Approximation Theory* 2003;122:1-9.

155. Wong W, Wong M, Lo K. Clinical applications of sensors for human posture and movement analysis: a review. *Prosthet Orthot Int* 2007;31(1):62-75.

156. Mayagoitia RE, Nene AV, Veltink PH. Accelerometer and rate gyroscope measurement of kinematics: an inexpensive alternative to optical motion analysis systems. *J Biomech* 2002;35(4):537-42.

157. Refshauge KM, Chan R, Taylor JL, McCloskey DI. Detection of movements imposed on human hip, knee, ankle and toe joints. *J Physiol* 1995;488 (Pt 1):231-41.

158. Gravelle M. Quaternions and their Applications to Rotation in 3D Space, 2006.

159. Savitzky A GMJE. Smoothing and differentiation of Data by Simplified Least Squares Procedures. *Anal. Chem.* 1964;36(8):1627-39.

160. Malmivuo J, Plonsey R. *Bioelectromagnetism*. New York, Oxford: Oxford University Press, 1995.

161. Karié VA, Knežević JM, Graovac D. Application-Oriented Comparison of the Methods for AC/DC Converter Harmonics Analysis. *IEEE Trans on industrial electronics* 2003;50(6):1100-08.

162. McGraw KO, Wong SP. Forming Inferences About Some Intraclass Correlation Coefficients. *Psychological Methods* 1996;1(1):30-46.

163. Sim J, Wright C. *Research in Health Care: Concepts, Designs and Methods*. Cheltenham: Thornes, 2000.

164. Ehara Y, Fujimoto H, Miyazaki S, Mochimaru M, Tanaka S, Yamamoto S. Technical Note: Comparison of the performance of 3D camera systems II. *Gait & Posture* 1997;5(3):251-55.

165. Ehara Y, Fujimoto H, Miyazaki S, Tanaka S, Yamamoto S. Technical Note: Comparison of the performance of 3D camera systems. *Gait & Posture* 1995;3(3):166-68.

166. Y K Thong, Woolfson MS, Crowe JA, Hayes-Gill BR, Challis RE. Dependence of intertial measurements of distance on accelerometer noise. *Meas. Sci. Technol.* 2002;13:1163-72.

167. Y.K. Thong, Woolfson MS, Crowe JA, Hayes-Gill BR, Challis RE. Dependence of intertial measurements of distance on accelerometer noise. *Meas. Sci. Technol.* 2002;13:1163-72.

168. Cutti AG, Paolini G, Troncossi M, Cappello A, Davalli A. Soft tissue artefact assessment in humeral axial rotation. *Gait & Posture* 2005;21(3):341-9.

169. Sabatini AM. Quaternion-based extended Kalman filter for determining orientation by inertial and magnetic sensing. *IEEE Trans Biomed Eng* 2006;53(7):1346-56.

170. Fuller J, Liu LJ, Murphy MC, Mann RW. A comparison of lower-extremity skeletal kinematics measured using kin- and pin-mounted markers. *Human Movement Science* 1997;16(2-3):219-42.

171. Kavanagh JJ, Morrison S, James DA, Barrett R. Reliability of segmental accelerations measured using a new wireless gait analysis system. *J Biomech* 2006;39(15):2863-72.

172. Brodie MA, Walmsley A, Page W. The static accuracy and calibration of intertial measurement unit for 3D orientation. *Computer Methods in Biomechanics and Biomedical Engineering* 2008;iFirst arcticle:1-8.

173. Brodie MA, Walmsley A, W.Page. Dynamic accuracy of inertial measurement units during simple pendulum motion. *Computer Methods in Biomechanics and Biomedical Engineering* 2008;11(3):235-42.

174. Cutti AG, Giovanardi A, Rocchi L, Davalli A. A simple test to assess the static and dynamic accuracy of an inertial sensors system for human movement analysis. *Conf Proc IEEE Eng Med Biol Soc* 2006;1:5912-5.

175. Lang A, Lozano A. Parkinson's Disease: Second of Two Parts. *The New England Journal of Medicine* 1998;339(16):1130 - 43.

176. Leenders K, Salmon E, Tyrrell P, Perani D, Brooks D, Sager H, et al. The nigrostantial dopaminergic system assessed in vivo by positron emission tomography in healthy volunteer subjects and patients with Parkinson's disease. *Arch Neurol* 1990;47:1290 - 98.

177. Lemon R. Cortical control of skilled movements. In: Cody F, editor. *Neural control of skilled human movement*. Dorchester: Portland Press, 1995:1 - 12.

178. Jankovic J. Parkinson's disease: clinical features and diagnosis. *J. Neurol. Neurosurg. Psychiatry* 2007;79:368-76.

179. World-Health-Organization. *Atlas Country Resources for neurological disorders*, 2004.

180. Elbaz A, Bower JH, Maraganore DM, McDonnell SK, Peterson BJ, Ahlskog JE, et al. Risk tables for parkinsonism and Parkinson's disease. *J Clin Epidemiol* 2002;55(1):25-31.

181. Marras C, McDermott M, Rochon P, Tanner C, Naglie G, Rudolph A, et al. Survival in Parkinson Disease: thirteen-year follow-up of the DATATOP cohort. *Neurology* 2005;64(1):87-93.

182. Chen JJ. Parkinson's disease: health-related quality of life, economic cost, and implications of early treatment. *Am J Manag Care* 2010;16 Suppl Implications:S87-93.

183. Le W, Chen S, Jankovic J. Etiopathogenesis of Parkinson Disease. *The Neuroscientist* 2009;15(1):28 - 35.

184. Jackson N, Doherty J, Coulter S. Neuropsychiatric complications of commonly used palliative care drugs. *Postgrad Med J* 2008;84(989):121-26.

185. Barbosa MT, Caramelli P, Maia DP, Cunningham MC, Guerra HL, Lima-Costa MF, et al. Parkinsonism and Parkinson's disease in the elderly: a community-based survey in Brazil (the Bambui study). *Mov Disord* 2006;21(6):800-8.

186. Parkinson's disease; diagnosis and management in primary and secondary care. In: Conditions NCCfC, editor. *NICE Clinical Guideline 35*. London: NHS, 2006:45.

187. Barlow B, Cory-Slechta D, Richfield E, Thiruchelvam M. The gestational environment and Parkinson's disease: evidence for neurodevelopmental origins of a neurodegenerative disorder. *Reprod Toxicol* 2007;23:456-70.

188. Dick FD. Parkinson's disease and pesticide exposures. *Br Med Bull* 2006;79-80:219-31.

189. Dick FD, De Palma G, Ahmadi A, Scott NW, Prescott GJ, Bennett J, et al. Environmental risk factors for Parkinson's disease and parkinsonism: the Geoparkinson study. *Occup Environ Med* 2007;64(10):666-72.

190. Wijemanne S, Jankovic J. Hemiparkinsonism-hemiatrophy syndrome. *Neurol.* 2007;69:1585 - 94.

191. Pankratz N, Wojcieszek J, Foroud T. Parkinson Disease Overview. In: Pagon R, Bird T, Dolan C, Stephens K, editors. *GeneReviews*. Seattle (WA): University of Washington, 2009.

192. Tanner CM, Ross GW, Jewell SA, Hauser RA, Jankovic J, Factor SA, et al. Occupation and risk of parkinsonism: a multicenter case-control study. *Arch Neurol* 2009;66(9):1106-13.

193. Hristova DR, Hristov JI, Mateva NG, Papathanasiou JV. Quality of life in patients with Parkinson's disease. *Folia Med (Plovdiv)* 2009;51(4):58-64.

194. Hagell P, Whalley D, McKenna SP, Lindvall O. Health status measurement in Parkinson's disease: validity of the PDQ-39 and Nottingham Health Profile. *Mov Disord* 2003;18(7):773-83.

195. Mutch WJ, Strudwick A, Roy SK, Downie AW. Parkinson's disease: disability, review, and management. *Br Med J (Clin Res Ed)* 1986;293(6548):675-7.

196. Pearson K, Gordon J. Spinal Reflexes. In: Kandel E, Schwartz J, Jessell T, editors. *Principles of Neural Science*. New York: McGraw-Hill, 2000:713 - 35.

197. Rothwell J. The Basal Ganglia. In: Cody F, editor. *Neural control of skilled human movement*. Dorchester: Portland Press, 1995:13 - 30.

198. Alexander G, Crutcher M. Funtional architecture of basal ganglia circuits: neural substrates of parallel processing. *Trends Neuroscience* 1990;13(7):226 -71.

199. Amaral D. The anatomical Organization of the Central Nervous System. In: Kandel E, Schwartz J, Jessell T, editors. *Principles of Neural Science*. New York: McGraw-Hill, 2000.

200. DeLong M, Wichmann T. Circuits and Circuit disorders of the Basal Ganglia. *Neurological Review* 2007;64:20 - 24.

201. Girault J, Greengard P. The Neurobiology of dompamine signaling. *Archives of Neurology* 2004;61(5):641 - 44.

202. Severson J, Marcusson J, Winblad B, Finch C. Age-Correlated Loss of Dopaminergic Binding Sites in Human Basal Ganglia. *Journal of Neurochemistry* 1982;39(6):1623 - 31.

203. Scott G, Westberg KG, Vrentzos N, Kolta A, Lund JP. Effect of lidocaine and NMDA injections into the medial pontobulbar reticular formation on mastication evoked by cortical stimulation in anaesthetized rabbits. *Eur J Neurosci* 2003;17(10):2156-62.

204. Grillner S. The motor infrastructure: from ion channels to neuronal networks. *Nat Rev Neurosci* 2003;4(7):573-86.

205. Leenders KL, Palmer AJ, Quinn N, Clark JC, Firnau G, Garnett ES, et al. Brain dopamine metabolism in patients with Parkinson's disease measured with positron emission tomography. *J Neurol Neurosurg Psychiatry* 1986;49(8):853-60.

206. Kovari E, Horvath J, Bouras C. Neuropathology of Lewy body disorders. *Brain Res Bull* 2009;80(4-5):203-10.

207. Lewy F. Paralysis agitans: I Pathologische Anatomie. In: Lewandowsky M, editor. *Handbuch der Neurologie*. Berlin: Springer, 1912:920-33.

208. Koh SB, Suh SI, Lee DH, Kim AR, Oh CH, Yoon JS, et al. Phase contrast radiography of Lewy bodies in Parkinson disease. *Neuroimage* 2006;32(2):566-9.

209. Berardelli A, Rothwell JC, Thompson PD, Hallett M. Pathophysiology of bradykinesia in Parkinson's disease. *Brain* 2001;124(Pt 11):2131-46.

210. Poewe W. Clinical measures of progression in Parkinson's disease. *Mov Disord* 2009;24 Suppl 2:S671-6.

211. Hughes AJ, Daniel SE, Kilford L, Lees AJ. Accuracy of clinical diagnosis of idiopathic Parkinson's disease: a clinico-pathological study of 100 cases. *J Neurol Neurosurg Psychiatry* 1992;55(3):181-4.

212. de Lau LM, Koudstaal PJ, Hofman A, Breteler MM. Subjective complaints precede Parkinson disease: the rotterdam study. *Arch Neurol* 2006;63(3):362-5.

213. Bloem BR, Hausdorff JM, Visser JE, Giladi N. Falls and freezing of gait in Parkinson's disease: a review of two interconnected, episodic phenomena. *Mov Disord* 2004;19(8):871-84.

214. Macht M, Kaussner Y, Moller JC, Stiasny-Kolster K, Eggert KM, Kruger HP, et al. Predictors of freezing in Parkinson's disease: a survey of 6,620 patients. *Mov Disord* 2007;22(7):953-6.

215. Schaafsma JD, Balash Y, Gurevich T, Bartels AL, Hausdorff JM, Giladi N. Characterization of freezing of gait subtypes and the response of each to levodopa in Parkinson's disease. *Eur J Neurol* 2003;10(4):391-8.

216. Dietz MA, Goetz CG, Stebbins GT. Evaluation of a modified inverted walking stick as a treatment for parkinsonian freezing episodes. *Mov Disord* 1990;5(3):243-7.

217. Marchese R, Diverio M, Zucchi F, Lentino C, Abbruzzese G. The role of sensory cues in the rehabilitation of parkinsonian patients: a comparison of two physical therapy protocols. *Mov Disord* 2000;15(5):879-83.

218. Vingerhoets FJ, Schulzer M, Calne DB, Snow BJ. Which clinical sign of Parkinson's disease best reflects the nigrostriatal lesion? *Ann Neurol* 1997;41(1):58-64.

219. Buckley T, Pitsokoulis C, Hass C. Dynamic postural stability during sit-to-walk transitions in Parkinson disease patients. *Movement Disorders* 2008;23(9):1274-80.

220. Franzen E, Paquette C, Gurfinkel VS, Cordo PJ, Nutt JG, Horak FB. Reduced performance in balance, walking and turning tasks is associated with increased neck tone in Parkinson's disease. *Exp Neurol* 2009;219(2):430-8.

221. Brozova H, Stochl J, Roth J, Ruzicka E. Fear of falling has greater influence than other aspects of gait disorders on quality of life in patients with Parkinson's disease. *Neuro Endocrinol Lett* 2009;30(4):453-7.

222. Kang HG, Dingwell JB. Dynamics and stability of muscle activations during walking in healthy young and older adults. *J Biomech* 2009;42(14):2231-7.

223. Kang HG, Dingwell JB. Dynamic stability of superior vs. inferior segments during walking in young and older adults. *Gait & Posture* 2009;30(2):260-3.

224. Granata KP, Lockhart TE. Dynamic stability differences in fall-prone and healthy adults. *J Electromyogr Kinesiol* 2008;18(2):172-8.

225. Buckley T, Pitsikoulis C, Barthelemy E, Hass CJ. Age impairs sit-to-walk motor performance. *J Biomech* 2009;42(14):2318-22.

226. Weiss A, Herman T, Plotnik M, Brozgol M, Maidan I, Giladi N, et al. Can an accelerometer enhance the utility of the Timed Up & Go Test when evaluating patients with Parkinson's disease? *Med Eng Phys* 2010;32(2):119-25.

227. Buckley TA, Pitsikoulis C, Hass CJ. Dynamic postural stability during sit-to-walk transitions in Parkinson disease patients. *Mov Disord* 2008;23(9):1274-80.

228. Kerr A, Rafferty D, Kerr KM, Durward B. Timing phases of the sit-to-walk movement: validity of a clinical test. *Gait & Posture* 2007;26(1):11-6.

229. Dion L, Malouin F, McFadyen B, Richards CL. Assessing mobility and locomotor coordination after stroke with the rise-to-walk task. *Neurorehabil Neural Repair* 2003;17(2):83-92.

230. Shulman LM, Taback RL, Rabinstein AA, Weiner WJ. Non-recognition of depression and other non-motor symptoms in Parkinson's disease. *Parkinsonism Relat Disord* 2002;8(3):193-7.

231. Weintraub D, Moberg PJ, Duda JE, Katz IR, Stern MB. Effect of psychiatric and other nonmotor symptoms on disability in Parkinson's disease. *J Am Geriatr Soc* 2004;52(5):784-8.

232. Gunal DI, Nurichalichi K, Tuncer N, Bekiroglu N, Aktan S. The clinical profile of nonmotor fluctuations in Parkinson's disease patients. *Can J Neurol Sci* 2002;29(1):61-4.

233. Raudino F. Non motor off in Parkinson's disease. *Acta Neurol Scand* 2001;104(5):312-5.

234. Rinne J, Mlic J, Paljarvi L, Rinne U. Dementia in Parkinson's disease is related to neuronal loss in the medial substantia nigra. *Annals of Neurology* 1988;26(1):47-50.

235. Adler CH. Nonmotor complications in Parkinson's disease. *Mov Disord* 2005;20 Suppl 11:S23-9.

236. Aarsland D, Beyer MK, Kurz MW. Dementia in Parkinson's disease. *Curr Opin Neurol* 2008;21(6):676-82.

237. Cheon SM, Ha MS, Park MJ, Kim JW. Nonmotor symptoms of Parkinson's disease: prevalence and awareness of patients and families. *Parkinsonism Relat Disord* 2008;14(4):286-90.

238. Pahwa R, Lyons KE. Early diagnosis of Parkinson's disease: recommendations from diagnostic clinical guidelines. *Am J Manag Care* 2010;16 Suppl Implications:S94-9.

239. Grosset D. Parkinson's disease and related disorders--XVIII WFN World Congress. *IDrugs* 2010;13(2):82-4.

240. Parekkadan B, Milwid JM. Mesenchymal Stem Cells as Therapeutics. *Annu Rev Biomed Eng* 2010.

241. Weiner WJ. An algorithm (decision tree) for the management of Parkinson's disease (2001): treatment guidelines. *Neurology* 2002;58(1):156; author reply 56-7.

242. Frucht S, Greene PE. An algorithm (decision tree) for the management of Parkinson's disease (2001): treatment guidelines. *Neurology* 2002;58(1):156; author reply 56-7.

243. Olanow CW, Watts RL, Koller WC. An algorithm (decision tree) for the management of Parkinson's disease (2001): treatment guidelines. *Neurology* 2001;56(11 Suppl 5):S1-S88.

244. Stocchi F, Jenner P, Obeso J. When Do Levodopa Motor Fluctuations First Appear in Parkinson's Disease? *European Neurology* 2010;63:257-66.

245. Pramipexole vs levodopa as initial treatment for Parkinson disease: A randomized controlled trial. Parkinson Study Group. *JAMA* 2000;284(15):1931-8.

246. Olanow CW, Stern MB, Sethi K. The scientific and clinical basis for the treatment of Parkinson disease (2009). *Neurology* 2009;72(21 Suppl 4):S1-136.

247. Golbe LI. Long-term efficacy and safety of deprenyl (selegiline) in advanced Parkinson's disease. *Neurology* 1989;39(8):1109-11.

248. Golbe LI, Lieberman AN, Muenter MD, Ahlskog JE, Gopinathan G, Neophytides AN, et al. Deprenyl in the treatment of symptom fluctuations in advanced Parkinson's disease. *Clin Neuropharmacol* 1988;11(1):45-55.

249. Mizuno Y, Kondo T, Takubo H, Yokochi F. [A long-term clinical effect of selegiline hydrochloride on Parkinson's disease]. *No To Shinkei* 1996;48(5):467-72.

250. Riederer P, Lachenmayer L. Selegiline's neuroprotective capacity revisited. *J Neural Transm* 2003;110(11):1273-8.

251. Stowe RL, Ives NJ, Clarke C, van Hilten J, Ferreira J, Hawker RJ, et al. Dopamine agonist therapy in early Parkinson's disease. *Cochrane Database Syst Rev* 2008(2):CD006564.

252. Sethi KD. The impact of levodopa on quality of life in patients with Parkinson disease. *Neurologist* 2010;16(2):76-83.

253. Bostwick JM, Hecksel KA, Stevens SR, Bower JH, Ahlskog JE. Frequency of new-onset pathologic compulsive gambling or hypersexuality after drug treatment of idiopathic Parkinson disease. *Mayo Clin Proc* 2009;84(4):310-6.

254. Bowes SG, Clark PK, Leeman AL, O'Neill CJ, Weller C, Nicholson PW, et al. Determinants of gait in the elderly parkinsonian on maintenance levodopa/carbidopa therapy. *Br J Clin Pharmacol* 1990;30(1):13-24.

255. Brannan T, Yahr MD. Comparative study of selegiline plus L-dopa-carbidopa versus L-dopa-carbidopa alone in the treatment of Parkinson's disease. *Ann Neurol* 1995;37(1):95-8.

256. Shan DE, Lee SJ, Chao LY, Yeh SI. Gait analysis in advanced Parkinson's disease--effect of levodopa and tolcapone. *Can J Neurol Sci* 2001;28(1):70-5.

257. Ondo WG, Hunter C, Vuong KD, Jankovic J. The pharmacokinetic and clinical effects of tolcapone on a single dose of sublingual apomorphine in Parkinson's disease. *Parkinsonism Relat Disord* 2000;6(4):237-40.

258. Svehlik M, Zwick EB, Steinwender G, Linhart WE, Schwingenschuh P, Katschnig P, et al. Gait analysis in patients with Parkinson's disease off dopaminergic therapy. *Arch Phys Med Rehabil* 2009;90(11):1880-6.

259. Erichsen D, Ferri R, Gozal D. Ropinirole in restless legs syndrome and periodic limb movement disorder. *Ther Clin Risk Manag* 2010;6:173-82.

260. Wicks P, MacPhee GJ. Pathological gambling amongst Parkinson's disease and ALS patients in an online community (PatientsLikeMe.com). *Mov Disord* 2009;24(7):1085-8.

261. Chastan N, Westby GW, Yelnik J, Bardinet E, Do MC, Agid Y, et al. Effects of nigral stimulation on locomotion and postural stability in patients with Parkinson's disease. *Brain* 2009;132(Pt 1):172-84.

262. Kelly VE, Israel SM, Samii A, Slimp JC, Goodkin R, Shumway-Cook A. Assessing the effects of subthalamic nucleus stimulation on gait and mobility in people with Parkinson disease. *Disabil Rehabil* 2010;32(11):929-36.

263. Romito LM, Contarino MF, Vanacore N, Bentivoglio AR, Scerrati M, Albanese A. Replacement of dopaminergic medication with subthalamic nucleus stimulation in Parkinson's disease: long-term observation. *Mov Disord* 2009;24(4):557-63.

264. Hamilton N, Luttgens K. Kinesiology, Scientific Basis of Human Motion. Boston: McGraw-Hill, 2002:399-411.

265. Carpinella I, Crenna P, Calabrese E, Rabuffetti M, Mazzoleni P, Nemni R, et al. Locomotor function in the early stage of Parkinson's disease. *IEEE Trans Neural Syst Rehabil Eng* 2007;15(4):543 - 51.

266. Dalton E, Bishop M, Tillman MD, Hass CJ. Simple Change in Initial Standing Position Enhances the Initiation of Gait. *Med Sci Sports Exerc*.

267. Ferrarin M, Carpinella I, Rabuffetti M, Calabrese E, Mazzoleni P, Nemni R. Locomotor Disorders in patients at early stages of Parkinson's disease: a quantitive analysis. *Conf Proc IEEE Eng Med Biol Soc* 2006;1:1224 - 27.

268. Yang Y, Lee Y, Cheng S, Lin P, Wang R. Relationships between gait and dynamic balance in early Parkinson's disease. *Gait & Posture* 2007;27:611-15.

269. Morris ME, Iansek R, Matyas TA, Summers JJ. Stride length regulation in Parkinson's disease. Normalization strategies and underlying mechanisms. *Brain* 1996;119 (Pt 2):551-68.

270. Morris ME, Iansek R, Matyas TA, Summers JJ. The pathogenesis of gait hypokinesia in Parkinson's disease. *Brain* 1994;117 (Pt 5):1169-81.

271. World-Health-Organization. *International Classification of Functioning, Disability and Health*, 2001.

272. Jenkinson C, Fitzpatrick R, Peto V, Greenhall R, Hyman N. The Parkinson's Disease Questionnaire (PDQ-39): development and validation of a Parkinson's disease summary index score. *Age Ageing* 1997;26(5):353-7.

273. Hagell P, Reimer J, Nyberg P. Whose quality of life? Ethical implications in patient-reported health outcome measurement. *Value Health* 2009;12(4):613-7.

274. Hagell P, Nilsson M. The 39-item Parkinson's Disease Questionnaire (PDQ-39): is it a unidimensional construct? *Therapeuric Advances in Neurological Disorders* 2009;2(4):205-14.

275. Pelosin E, Faelli E, Lofrano F, Avanzino L, Marinelli L, Bove M, et al. Effects of treadmill training on walking economy in Parkinson's disease: a pilot study. *Neurol Sci* 2009.

276. Roiz R, Chacho E, Pazinatto M, Reis J, Cliquet A, Barasnevicius-Quagliato E. Gait analysis comparing Parkinson's disease with healthy elderly subjects. *Arq Neuropsiquiatr* 2010;68(1):81-86.

277. Canning CG, Ada L, Johnson JJ, McWhirter S. Walking capacity in mild to moderate Parkinson's disease. *Arch Phys Med Rehabil* 2006;87(3):371-5.

278. Chien SL, Lin SZ, Liang CC, Soong YS, Lin SH, Hsin YL, et al. The efficacy of quantitative gait analysis by the GAITRite system in evaluation of parkinsonian bradykinesia. *Parkinsonism Relat Disord* 2006;12(7):438-42.

279. Christiansen CL, Schenkman ML, McFann K, Wolfe P, Kohrt WM. Walking economy in people with Parkinson's disease. *Mov Disord* 2009;24(10):1481-7.

280. Dijkstra B, Zijlstra W, Scherder E, Kamsma Y. Detection of walking periods and number of steps in older adults and patients with Parkinson's disease: accuracy of a pedometer and an accelerometry-based method. *Age Ageing* 2008;37(4):436-41.

281. Ellis T, de Goede CJ, Feldman RG, Wolters EC, Kwakkel G, Wagenaar RC. Efficacy of a physical therapy program in patients with Parkinson's disease: a randomized controlled trial. *Arch Phys Med Rehabil* 2005;86(4):626-32.

282. Falvo MJ, Earhart GM. Six-minute walk distance in persons with Parkinson disease: a hierarchical regression model. *Arch Phys Med Rehabil* 2009;90(6):1004-8.

283. Frenkel-Toledo S, Giladi N, Peretz C, Herman T, Gruendlinger L, Hausdorff JM. Effect of gait speed on gait rhythmicity in Parkinson's disease: variability of stride time and swing time respond differently. *J Neuroeng Rehabil* 2005;2:23.

284. Gobbi LT, Oliveira-Ferreira MD, Caetano MJ, Lirani-Silva E, Barbieri FA, Stella F, et al. Exercise programs improve mobility and balance in people with Parkinson's disease. *Parkinsonism Relat Disord* 2009;15 Suppl 3:S49-52.

285. Hackney ME, Earhart GM. Backward walking in Parkinson's disease. *Mov Disord* 2009;24(2):218-23.

286. Hong M, Perlmutter JS, Earhart GM. A kinematic and electromyographic analysis of turning in people with Parkinson disease. *Neurorehabil Neural Repair* 2009;23(2):166-76.

287. Jones D, Rochester L, Birleson A, Hetherington V, Nieuwboer A, Willems AM, et al. Everyday walking with Parkinson's disease: understanding personal challenges and strategies. *Disabil Rehabil* 2008;30(16):1213-21.

288. Latt MD, Menz HB, Fung VS, Lord SR. Acceleration patterns of the head and pelvis during gait in older people with Parkinson's disease: a comparison of fallers and nonfallers. *J Gerontol A Biol Sci Med Sci* 2009;64(6):700-6.

289. Lim I, van Wegen E, Jones D, Rochester L, Nieuwboer A, Willems AM, et al. Identifying fallers with Parkinson's disease using home-based tests: who is at risk? *Mov Disord* 2008;23(16):2411-5.

290. Lim LI, van Wegen EE, de Goede CJ, Jones D, Rochester L, Hetherington V, et al. Measuring gait and gait-related activities in Parkinson's patients own home environment: a reliability, responsiveness and feasibility study. *Parkinsonism Relat Disord* 2005;11(1):19-24.

291. Lord S, Rochester L, Baker K, Nieuwboer A. Concurrent validity of accelerometry to measure gait in Parkinsons Disease. *Gait & Posture* 2008;27(2):357-9.

292. Martinez-Martin P, Garcia Urra D, del Ser Quijano T, Balseiro Gomez J, Gomez Utrero E, Pineiro R, et al. A new clinical tool for gait evaluation in Parkinson's disease. *Clin Neuropharmacol* 1997;20(3):183-94.

293. Moore ST, MacDougall HG, Gracies JM, Cohen HS, Ondo WG. Long-term monitoring of gait in Parkinson's disease. *Gait & Posture* 2007;26(2):200-7.

294. Morris M, Iansek R, Matyas T, Summers J. Abnormalities in the stride length-cadence relation in parkinsonian gait. *Mov Disord* 1998;13(1):61-9.

295. Protas EJ, Mitchell K, Williams A, Qureshy H, Caroline K, Lai EC. Gait and step training to reduce falls in Parkinson's disease. *NeuroRehabilitation* 2005;20(3):183-90.

296. Rochester L, Jones D, Hetherington V, Nieuwboer A, Willems AM, Kwakkel G, et al. Gait and gait-related activities and fatigue in Parkinson's disease: what is the relationship? *Disabil Rehabil* 2006;28(22):1365-71.

297. Schaafsma JD, Giladi N, Balash Y, Bartels AL, Gurevich T, Hausdorff JM. Gait dynamics in Parkinson's disease: relationship to Parkinsonian features, falls and response to levodopa. *J Neurol Sci* 2003;212(1-2):47-53.

298. Schenkman M, Hall D, Kumar R, Kohrt WM. Endurance exercise training to improve economy of movement of people with Parkinson disease: three case reports. *Phys Ther* 2008;88(1):63-76.

299. Jankovic J, McDermott M, Carter J, Gauthier S, Goetz C, Golbe L. Variable expression of Parkinson's disease: a base-line analysis of the DATATOP cohort. *Neurology* 1990;50:1529-34.

300. Quinn N, Bhatia K, Brown P, Cordivari C, Hariz M, Lees A, et al. Movement Disorders. In: Clarke C, Howard R, Rossor M, Shorvon S, editors. *Neurology*: Wiley-Blackwell, 2009.

301. Goetz CG, Poewe W, Rascol O, Sampaio C, Stebbins GT, Counsell C, et al. Movement Disorder Society Task Force report on the Hoehn and Yahr staging scale: status and recommendations. *Mov Disord* 2004;19(9):1020-8.

302. Deane KH, Jones D, Ellis-Hill C, Clarke CE, Playford ED, Ben-Shlomo Y. A comparison of physiotherapy techniques for patients with Parkinson's disease. *Cochrane Database Syst Rev* 2001(1):CD002815.

303. Deane KH, Jones D, Playford ED, Ben-Shlomo Y, Clarke CE. Physiotherapy for patients with Parkinson's Disease: a comparison of techniques. *Cochrane Database Syst Rev* 2001(3):CD002817.

304. Starkstein SE, Merello M. The Unified Parkinson's Disease Rating Scale: validation study of the mentation, behavior, and mood section. *Mov Disord* 2007;22(15):2156-61.

305. Stebbins GT, Goetz CG. Factor structure of the Unified Parkinson's Disease Rating Scale: Motor Examination section. *Mov Disord* 1998;13(4):633-6.

306. Richards M, Marder K, Cote L, Mayeux R. Interrater reliability of the Unified Parkinson's Disease Rating Scale motor examination. *Mov Disord* 1994;9(1):89-91.

307. Haaxma CA, Bloem BR, Borm GF, Horstink MW. Comparison of a timed motor test battery to the Unified Parkinson's Disease Rating Scale-III in Parkinson's disease. *Mov Disord* 2008;23(12):1707-17.

308. The Unified Parkinson's Disease Rating Scale (UPDRS): status and recommendations. *Mov Disord* 2003;18(7):738-50.

309. Goetz CG, Fahn S, Martinez-Martin P, Poewe W, Sampaio C, Stebbins GT, et al. Movement Disorder Society-sponsored revision of the Unified Parkinson's Disease Rating Scale (MDS-UPDRS): Process, format, and clinimetric testing plan. *Mov Disord* 2007;22(1):41-7.

310. Goetz CG, Tilley BC, Shaftman SR, Stebbins GT, Fahn S, Martinez-Martin P, et al. Movement Disorder Society-sponsored revision of the Unified Parkinson's Disease Rating Scale (MDS-UPDRS): scale presentation and clinimetric testing results. *Mov Disord* 2008;23(15):2129-70.

311. Cooper R, Kuh D, Hardy R. Objectively measured physical capability levels and mortality: systematic review and meta-analysis. *Bmj* 2010;341:c4467.

312. Ebersbach G, Sojer M, Valldeoriola F, Wissel J, Muller J, Tolosa E, et al. Comparative analysis of gait in Parkinson's disease, cerebellar ataxia and subcortical arteriosclerotic encephalopathy. *Brain* 1999;122 (Pt 7):1349-55.

313. Frazzitta G, Maestri R, Bertotti G, Uccellini D, Bazzini G, Abelli P, et al. Rehabilitation in Parkinson's disease: Assessing the outcome using objective metabolic measurements. *Mov Disord* 2007.

314. Frazzitta G, Maestri R, Uccellini D, Bertotti G, Abelli P. Rehabilitation treatment of gait in patients with Parkinson's disease with freezing: a comparison between two physical therapy protocols using visual and auditory cues with or without treadmill training. *Mov Disord* 2009;24(8):1139-43.

315. Mehrholz J, Friis R, Kugler J, Twork S, Storch A, Pohl M. Treadmill training for patients with Parkinson's disease. *Cochrane Database Syst Rev* 2010(1):CD007830.

316. Ebersbach G, Sojer M, Muller J, Heijmenberg M, Poewe W. Sociocultural differences in gait. *Mov Disord* 2000;15(6):1145-7.

317. Podsiadlo D, Richardson S. The timed "Up & Go": a test of basic functional mobility for frail elderly persons. *J Am Geriatr Soc* 1991;39(2):142-8.

318. Azulay JP, Mesure S, Amblard B, Blin O, Sangla I, Pouget J. Visual control of locomotion in Parkinson's disease. *Brain* 1999;122 (Pt 1):111-20.

319. O'Shea S, Morris ME, Iansek R. Dual task interference during gait in people with Parkinson disease: effects of motor versus cognitive secondary tasks. *Phys Ther* 2002;82(9):888-97.

320. Sekine M, Akay M, Tamura T, Higashi Y, Fujimoto T. Fractal dynamics of body motion in patients with Parkinson's disease. *J. Neural Eng.* 2004;1:8-15.

321. Cantiniaux S, Vaugoyeau M, Robert D, Horrelou-Pitek C, Mancini J, Witjas T, et al. Comparative analysis of gait and speech in Parkinson's disease: hypokinetic or dysrhythmic disorders? *J Neurol Neurosurg Psychiatry* 2009;81(2):177-84.

322. Paquet JM, Auvinet B, Chaleil D, Barrey E. [Analysis of gait disorders in Parkinson's disease assessed with an accelerometer]. *Rev Neurol (Paris)* 2003;159(8-9):786-9.

323. Chastan N, Do MC, Bonneville F, Torny F, Bloch F, Westby GW, et al. Gait and balance disorders in Parkinson's disease: impaired active braking of the fall of centre of gravity. *Mov Disord* 2009;24(2):188-95.

324. Baker R. Gait analysis methods in rehabilitation. *Journal of NeuroEngineering and Rehabilitation* 2006;3(4).

325. Hernandez A, Silder A, Heiderscheit BC, Thelen DG. Effect of age on center of mass motion during human walking. *Gait & Posture* 2009;30(2):217-22.

326. Thomas S, Reading J, Shephard RJ. Revision of the Physical Activity Readiness Questionnaire (PAR-Q). *Can J Sport Sci* 1992;17(4):338-45.

327. Rossier P, Wade D. Validity and reliability comparison of 4 mobility measures in patients presenting with neurologic impairment. *Arch Phys Med Rehabil* 2001;82:9-13.

328. Elsworth C, Dawes H, Winward C, Howells K, Collett J, Dennis A, et al. Pedometer step counts in individuals with neurological conditions. *Clin Rehabil* 2009;23(2):171-5.

329. Dean CM, Richards CL, Malouin F. Walking speed over 10 metres overestimates locomotor capacity after stroke. *Clin Rehabil* 2001;15(4):415-21.

330. Zijlstra W, Hof AL. Displacement of the pelvis during human walking: experimental data and model predictions *Gait & Posture* 1997;6(3):249-62.

331. Webster KE, Wittwer JE, Feller JA. Validity of the GAITRite walkway system for the measurement of averaged and individual step parameters of gait. *Gait & Posture* 2005;22(4):317-21.

332. Dickstein R. Rehabilitation of Gait Speed After Stroke: A Critical Review of Intervention Approaches. *Neurorehabilitation and Neural Repair* 2008;22(6):649 - 60.

333. Buczek FL, Cooney KM, Walker MR, Rainbow MJ, Concha MC, Sanders JO. Performance of an inverted pendulum model directly applied to normal human gait. *Clin Biomech* 2006;21:288-96.

334. Loslever P, Laassel EM, Angue JC. Combined statistical study of joint angles and ground reaction forces using component and multiple correspondence analysis. *IEEE Trans Biomed Eng* 1994;41(12):1160-7.

335. Hyngstrom A, Onushko T, Chua M, Schmit BD. Abnormal volitional hip torque phasing and hip impairments in gait post stroke. *J Neurophysiol*;103(3):1557-68.

336. Youdas JW, Atwood AL, Stiller TL, Egan KS, Therneau TM, Harris-Love M. Measurements of Temporal Aspects of Gait Obtained With a Multimemory Stopwatch in Persons With Gait Impairments *Journal of Orthopaedic & Sports Physical Therapy* 2000;30(5):279-86.

337. Hausdorff JM. Gait dynamics, fractals and falls: finding meaning in the stride-to-stride fluctuations of human walking. *Hum Mov Sci* 2007;26(4):555-89.

338. Hausdorff JM. Gait dynamics in Parkinson's disease: common and distinct behavior among stride length, gait variability, and fractal-like scaling. *Chaos* 2009;19(2):026113.

339. Yogev G, Plotnik M, Peretz C, Giladi N, Hausdorff JM. Gait asymmetry in patients with Parkinson's disease and elderly fallers: when does the bilateral coordination of gait require attention? *Exp Brain Res* 2007;177(3):336-46.

340. Plotnik M, Giladi N, Balash Y, Peretz C, Hausdorff JM. Is freezing of gait in Parkinson's disease related to asymmetric motor function? *Ann Neurol* 2005;57(5):656-63.

341. Bello O, Marquez G, Camblor M, Fernandez-Del-Olmo M. Mechanisms involved in treadmill walking improvements in Parkinson's disease. *Gait Posture*;32(1):118-23.

342. Lakany H. Extracting a diagnostic gait signature. *Pattern Recognition* 2008;41:1627-37.

343. Esser P, Dawes H, Collett J, Feltham MG, Howells K. Assessment of spatio-temporal gait parameters using inertial measurement units in neurological populations. *Gait Posture* 2011.

344. Danion F, Varraine E, Bonnard M, Pailhous J. Stride variability in human gait: the effect of stride frequency and stride length. *Gait & Posture* 2003;18(1):69-77.

345. Hausdorff JM. Gait variability: methods, modeling and meaning. *J Neuroeng Rehabil* 2005;2:19.

346. Baltadjieva R, Giladi N, Gruendlinger L, Peretz C, Hausdorff JM. Marked alterations in the gait timing and rhythmicity of patients with de novo Parkinson's disease. *Eur J Neurosci* 2006;24(6):1815-20.

347. Hausdorff JM, Cudkowicz ME, Firtion R, Wei JY, Goldberger AL. Gait variability and basal ganglia disorders: stride-to-stride variations of gait cycle timing in Parkinson's disease and Huntington's disease. *Mov Disord* 1998;13(3):428-37.

348. Blin O, Ferrandez AM, Serratrice G. Quantitative analysis of gait in Parkinson patients: increased variability of stride length. *J Neurol Sci* 1990;98(1):91-7.

349. Hausdorff JM, Edelberg HK, Cudkowicz ME, Singh MA, Wei JY. The relationship between gait changes and falls. *J Am Geriatr Soc* 1997;45(11):1406.

350. Blin O, Ferrandez AM, Pailhous J, Serratrice G. Dopa-sensitive and dopa-resistant gait parameters in Parkinson's disease. *J Neurol Sci* 1991;103(1):51-4.

351. Nieuwboer A, Dom R, De Weerdt W, Desloovere K, Fieuws S, Broens-Kaucsik E. Abnormalities of the spatiotemporal characteristics of gait at the onset of freezing in Parkinson's disease. *Mov Disord* 2001;16(6):1066-75.

352. Herman T, Giladi N, Gurevich T, Hausdorff JM. Gait instability and fractal dynamics of older adults with a "cautious" gait: why do certain older adults walk fearfully? *Gait & Posture* 2005;21(2):178-85.

353. Sadeghi H, Allard P, Prince F, Labelle H. Symmetry and limb dominance in able-bodied gait: a review. *Gait & Posture* 2000;12(1):34-45.

354. Cooper RA, Quatrano LA, Stanhope SJ, Cavanagh PR, Miller F, Kerrigan DC, et al. Gait analysis in rehabilitation medicine: a brief report. *Am J Phys Med Rehabil* 1999;78(3):278-80.

355. Davie CA. A review of Parkinson's disease. *Br Med Bull* 2008;86:109-27.

356. Engsberg JR, Tucker C, Ounpuu S, Wren TA, Sisto SA, Kaufman KR. Gait and clinical movement analysis research priorities: 2007 update from the research committee of the Gait and Clinical Movement Analysis Society. *Gait & Posture* 2009;29(2):169-71.

357. Schmid M, Beltrami G, Zambarbieri D, Verni G. Centre of pressure displacements in trans-femoral amputees during gait. *Gait & Posture* 2005;21:255-62.

358. Morris ME, Huxham F, McGinley J, Dodd K, Iansek R. The biomechanics and motor control of gait in Parkinson disease. *Clin Biomech (Bristol, Avon)* 2001;16(6):459-70.

359. Hausdorff JM, Edelberg HK, Mitchell SL, Goldberger AL, Wei JY. Increased gait unsteadiness in community-dwelling elderly fallers. *Arch Phys Med Rehabil* 1997;78(3):278-83.

360. Hausdorff JM, Forman DE, Ladin Z, Goldberger AL, Rigney DR, Wei JY. Increased walking variability in elderly persons with congestive heart failure. *J Am Geriatr Soc* 1994;42(10):1056-61.

361. Goldberger AL, Amaral LA, Hausdorff JM, Ivanov P, Peng CK, Stanley HE. Fractal dynamics in physiology: alterations with disease and aging. *Proc Natl Acad Sci U S A* 2002;99 Suppl 1:2466-72.

362. Bollens B, Crevecoeur F, Nguyen V, Detrembleur C, Lejeune T. Does human gait exhibit comparable and reproducible long-range autocorrelations on level ground and on treadmill? *Gait Posture*;32(3):369-73.

363. Vartiainen M, Savolainen S, Alaranta H. Reliability and agreement in gait measurements among patients with brain injury. *Advances in Physiotherapy* 2009;11(1):22-29.

364. Department for Business IS. Number of English domiciled entrants to the UK Higher Education Institutions (excluding the Open University). London, 2008.

365. Brouwer B, Parvataneni K, Olney SJ. A comparison of gait biomechanics and metabolic requirements of overground and treadmill walking in people with stroke. *Clin Biomech (Bristol, Avon)* 2009;24(9):729-34.

10 Appendices

10.1 UK Parkinson's Disease Society Brain Bank Clinical diagnostic

Step 1 Diagnosis of Parkinsonian syndrome

- Bradykinesia (slowness of initiation of voluntary movement with progressive reduction in speed and amplitude of repetitive actions)
- And at least one of the following:
    - Muscular rigidity
    - 4-6 Hz rest tremor
    - Postural instability not caused by primary visual, vestibular, cerebellar, or proprioceptive dysfunction

Step 2 Exclusion criteria for Parkinson's disease

- History of repeated strokes with stepwise progression of parkinsonian features
- History of repeated head injury
- History of definite encephalitis
- Oculogyric crises
- Neuroleptic treatment at onset of symptoms
- More than one affected relative
- Sustained remission
- Strictly unilateral features after 3 years
- Supranuclear gaze palsy
- Cerebellar signs
- Early severe autonomic involvement
- Early severe dementia with disturbances of memory, language, and praxis
- Babinski sign
- Presence of cerebral tumour or communicating hydrocephalus on CT scan
- Negative response to large doses of Levodopa (if malabsorption excluded)
- MPTP exposure

Step 3 Supportive prospective positive criteria for Parkinson's disease
(Three of more required for diagnosis of definite Parkinson's disease)

- Unilateral onset
- Rest tremor present
- Progressive disorder
- Persistent asymmetry affecting side of onset most
- Excellent response (70-100%) to Levodopa
- Severe Levodopa-induced chorea
- Levodopa response for 5 years or more
- Clinical course of 10 years or more

10.2 Questionnaires

10.2.1 Barthel Index

<u>Bowels</u>
0 = incontinent (or needs enema)
1 = occasional accident
2 = continent

<u>Bladder</u>
0 = incontinent, or catheterised and unable to manage alone
1 = occasional accident (maximum once per 24 hours)
2 = continent

<u>Grooming</u>
0 = needs help with personal care
1 = independent face/hair/teeth/shaving (implements provided)

<u>Toilet use</u>
0 = dependent
1 = needs some help, but can do something alone
2 = independent (on and off, dressing, wiping)

<u>Feeding</u>
0 = unable
1 = needs help cutting, spreading butter, etc.
2 = independent

<u>Transfer (bed to chair and back)</u>
0 = unable, no sitting balance
1 = major help (one or two people, physical), can sit
2 = minor help (verbal or physical)
3 = independent

<u>Mobility</u>
0 = immobile
1 = wheelchair independent, including corners
2 = walks with help of one person (verbal or physical)
3 = independent (but may use any aid; for example, stick)

<u>Dressing</u>
0 = dependent
1 = needs help but can do about half unaided
2 = independent (including buttons, zips, laces, etc.)

<u>Stairs</u>
0 = unable
1 = needs help (verbal, physical, carrying aid)
2 = independent

<u>Bathing</u>
0 = dependent
1 = independent (or in shower)

10.2.2 Parkinson's disease questionnaire 39 (PDQ39)

Due to having Parkinson's disease how often <u>during the last month</u> have you.....

		Never	Occasionally	Sometimes	Often	Always
1	Had difficulty doing the leisure activities which you would like to do?	☐	☐	☐	☐	☐
2	Had difficulty looking after your home, e.g. DIY, housework, cooking?	☐	☐	☐	☐	☐
3	Had difficulty carrying bags of shopping?	☐	☐	☐	☐	☐
4	Had problems walking half a mile?	☐	☐	☐	☐	☐
5	Had problems walking 100 yards?	☐	☐	☐	☐	☐
6	Had problems getting around the house as easily as you would like?	☐	☐	☐	☐	☐
7	Had difficulty getting around in public?	☐	☐	☐	☐	☐
8	Needed someone else to accompany you when you went out?	☐	☐	☐	☐	☐
9	Felt frightened or worried about falling over in public?	☐	☐	☐	☐	☐
10	Been confined to the house more than you would like?	☐	☐	☐	☐	☐
11	Had difficulty washing yourself?	☐	☐	☐	☐	☐
12	Had difficulties dressing yourself?	☐	☐	☐	☐	☐

13	Had problems doing up your shoe laces?	☐	☐	☐	☐	☐
14	Had problems writing clearly?	☐	☐	☐	☐	☐
15	Had difficulty holding cutting up your food?	☐	☐	☐	☐	☐
16	Had difficulty holding ad rink without spilling it?	☐	☐	☐	☐	☐
17	Felt depressed?	☐	☐	☐	☐	☐
18	Felt isolated and lonely?	☐	☐	☐	☐	☐
19	Felt weepy or tearful?	☐	☐	☐	☐	☐
20	Felt angry of bitter?	☐	☐	☐	☐	☐
21	Felt anxious?	☐	☐	☐	☐	☐
22	Felt worries about your future?	☐	☐	☐	☐	☐
23	Felt you had to conceal your Parkinson’s from people?	☐	☐	☐	☐	☐
24	Avoided situations which involve eating or drinking in public?	☐	☐	☐	☐	☐
25	Felt embarrassed in public due to having Parkinson’s disease?	☐	☐	☐	☐	☐
26	Felt worried by other people’s reaction to you?	☐	☐	☐	☐	☐
27	Had problems with your close personal relationships?	☐	☐	☐	☐	☐

28	Lacked support in the way you need from your spouse or partner?	☐	☐	☐	☐	☐
29	Lacked support in the ways you need from your family or close friends?	☐	☐	☐	☐	☐
30	Unexpectedly fallen asleep during the day?	☐	☐	☐	☐	☐
31	Had problems with your concentration, e.g. when reading or watching TV?	☐	☐	☐	☐	☐
32	Felt your memory was bad?	☐	☐	☐	☐	☐
33	Had distressing dreams or hallucinations?	☐	☐	☐	☐	☐
34	Had difficulty with your speech?	☐	☐	☐	☐	☐
35	Felt unable to communicate with people properly?	☐	☐	☐	☐	☐
36	Felt ignored by people?	☐	☐	☐	☐	☐
37	Had painful muscle cramps or spasms?	☐	☐	☐	☐	☐
38	Had aches and pains in your joints or body?	☐	☐	☐	☐	☐
39	Felt unpleasantly hot or cold?	☐	☐	☐	☐	☐

Please check that you have ticked **one box for each question** before going on to the next page

10.2.3 Rivermead Mobility Index

Overview: The Rivermead Mobility Index is a measure of disability related to bodily mobility. It demonstrates the patient's ability to move her or his own body. It does not measure the effective use of a wheelchair or the mobility when aided by someone else. It was developed for patients who had suffered a head injury or stroke at the Rivermead Rehabilitation Centre in Oxford England.

Rivermead Motor Index **No**	**Parameter**	**Question**	Yes = 1 No = 0
1	Turning over in bed	Do you turn over from your back to side without help?	
2	Lying to sitting	From lying in bed do you get up to sit on the edge of the bed on your own?	
3	Sitting balance	Do you sit on the edge of the bed without holding on for 10 seconds?	
4	Sitting to standing	Do you stand up (from any chair) in less than 15 seconds and stand there for 15 seconds (using hands and with an aid if necessary)?	
5	Standing unsupported	Observe standing for 10 seconds without any aid or support.	
6	Transfer	Do you manage to move from bed to chair and back without any help?	
7	Walking inside with an aid if needed	Do you walk 10 meters with an aid or furniture if necessary but with no standby help?	
8	Stairs	Do you manage a flight of stairs without help?	
9	Walking outside (even ground)	Do you walk around outside on pavements without help?	
10	Walking inside with no aid	Do you walk 10 meters inside with no calliper splint aid or use of furniture and no standby help?	
11	Picking off floor	If you drop something on the floor do you manage to walk 5 meters pick it up and then walk back?	
12	Walking outside (uneven ground)	Do you walk over uneven ground (grass gravel dirt snow ice etc.) without help?	
13	Bathing	Do you get in and out of bath or shower unsupervised and wash self?	
14	Up and down 4 steps	Do you manage to go up and down 4 steps with no rail and without help but using an aid if necessary?	
15	Running	Do you run 10 meters without limping in 4 seconds (a fast walk is acceptable)?	

10.3 Single case study: step length validation in PD

One participant (75 years old, suffering from PD for 5 years) was recruited under ethics number 10/H0308/12. An inertial measurement unit (IMU) was placed over the projected CoM as reported previously within this thesis. Sample frequency was 100Hz for both the IMU and optical motion capture system (OMCS) which were synchronized on gait initiation.

The participant was asked to walk over ten metres at self selected walking speed along a corridor free of obstacles. Walking measurements recorded included walking time (as measured by stopwatch) and leg length. By utilizing these extra measurements a individual correction factor was derived for all walks.

Four walks were recorded with both systems resulting in 12 steps. By processing the data through Excel for Windows and a custom written program in LabVIEW8.5 step length for both limbs and stride length were derived.

Step and stride length were compared using a paired sample *t*-test and intra class correlation coefficient (ICC3.1) on consistency. Adequate test-retest reliability was set at ICC≥0.75.

Descriptive measurements can be found in table A

Table A Descriptive walking measurements as taken by optical motion capture system

Walk	Steps [#]	walking speed [ms^{-1}]	Step length L [m]	Step length R [m]	Stride length [m]
1	3	0.72	0.63±0.02	0.64±0.02	1.28±0.04
2	3	0.95	0.62±0.01	0.63±0.01	1.24±0.01
3	4	0.90	0.63±0.01	0.64±0.01	1.28±0.01
4	2	0.97	0.70±0.02	0.70±0.03	1.40±0.04

No significant different was found between the OMCS and IMU measurements for left (p=.231) and right (p=.165) step length. Nor was there a significant difference in stride length determined by OMCS and IMU measurements (p=.152). Root mean square error between OMCS and IMU measurements for left and right step length was found to be -1.5±2.1% and -2.4±3.7% respectively. Stride length was found to show an RMS error of -2.1±2.7% when comparing OMCS and IMU measurements. ICC showed an significant correlation between OMCS and IMU measurements for left (ICC=0.959 p<0.01) and right step length (ICC=0.802, p=0.04) but also stride length (ICC=0.916, p=0.02).

10.4 Flow diagram LabVIEW8.5

10.4.1 Program Background

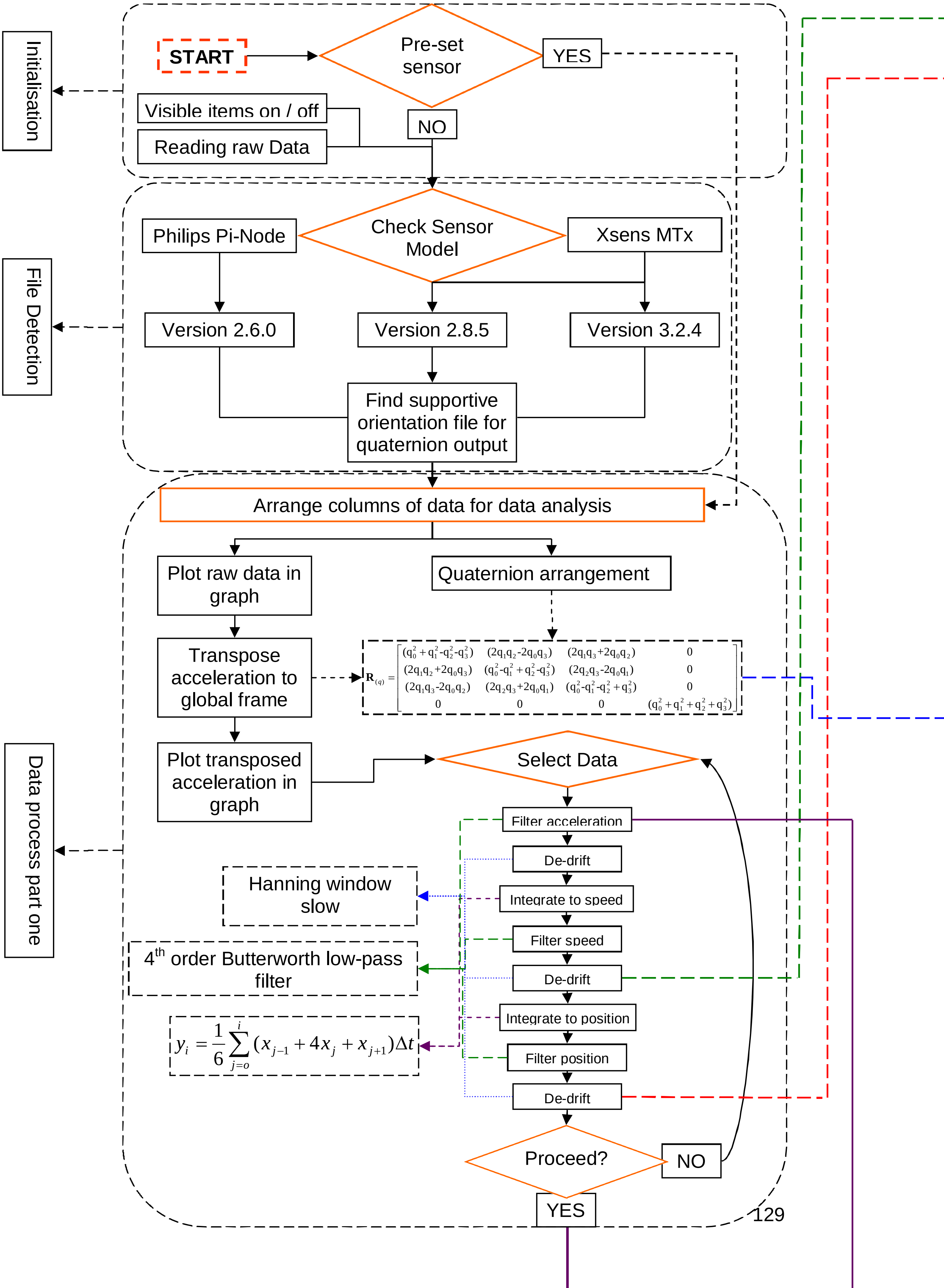

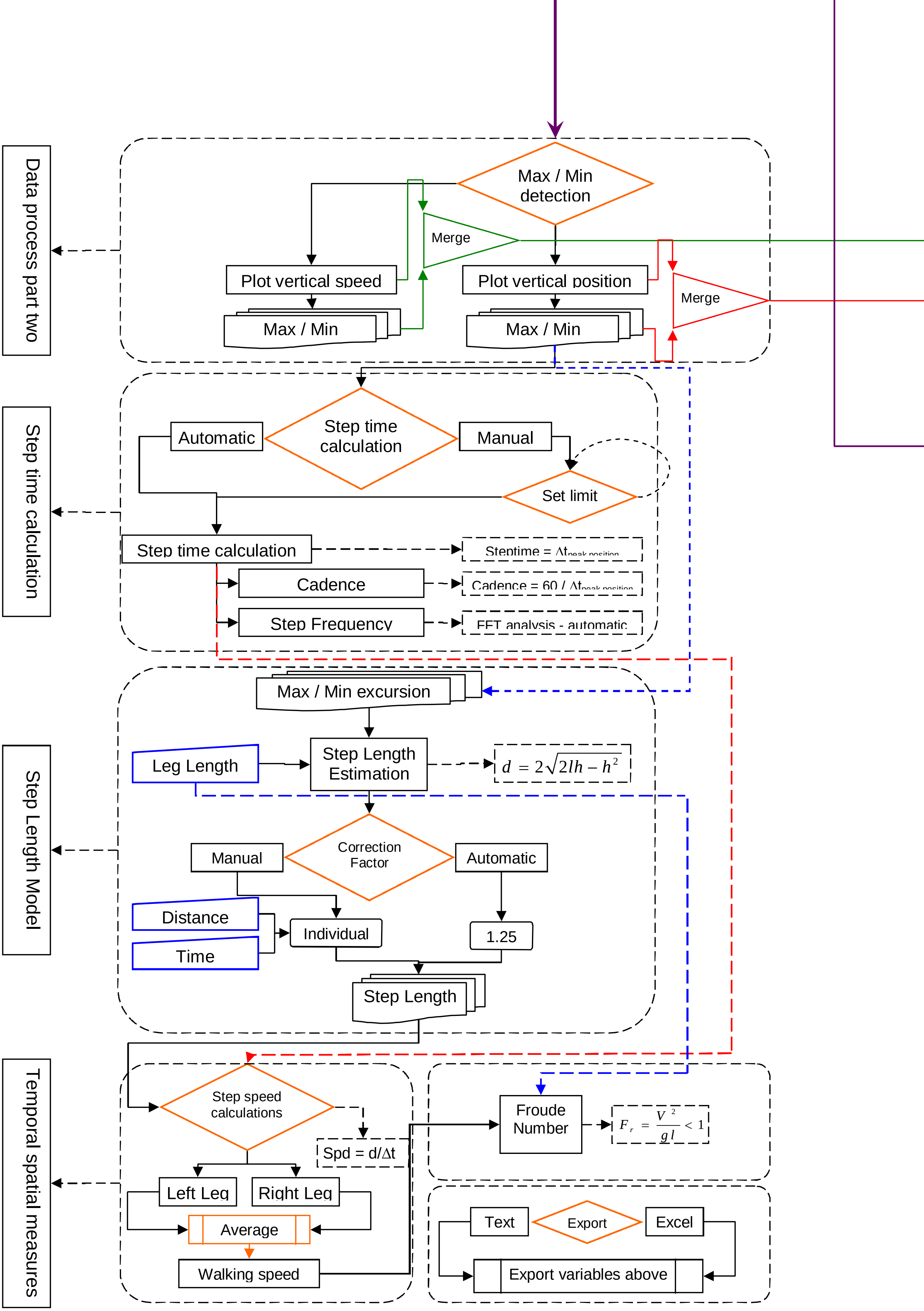
Data process part two
Max / Min detection
Merge
Plot vertical speed
Plot vertical position
Merge
Max / Min
Max / Min
Step time calculation
Automatic
Step time calculation
Manual
Set limit
Step time calculation
Steptime = Δt peak position
Cadence
Cadence = 60 / Δt peak position
Step Frequency
FFT analysis - automatic
Step Length Model
Max / Min excursion
Leg Length
Step Length Estimation
$d = 2\sqrt{2lh - h^2}$
Manual
Correction Factor
Automatic
Distance
Time
Individual
1.25
Step Length
Temporal spatial measures
Step speed calculations
Spd = d/Δt
Left Leg
Right Leg
Average
Walking speed
Froude Number
$F_r = \frac{V^2}{gl} < 1$
Text
Export
Excel
Export variables above

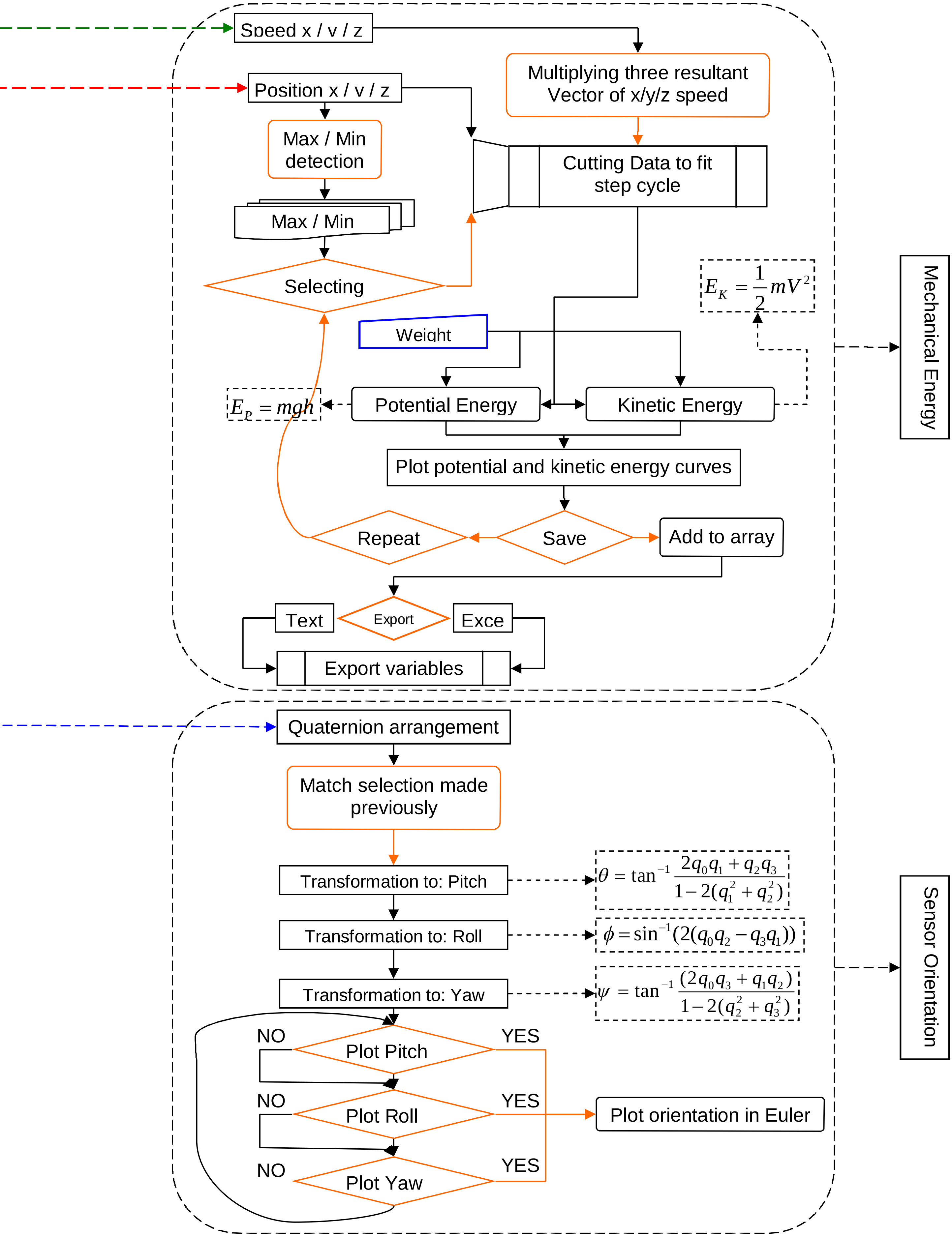
Speed x / v / z
Multiplying three resultant Vector of x/y/z speed
Position x / v / z
Max / Min detection
Cutting Data to fit step cycle
Max / Min
Selecting
$E_K = \frac{1}{2} mV^2$
Weight
$E_p = mgh$
Potential Energy
Kinetic Energy
Plot potential and kinetic energy curves
Repeat
Save
Add to array
Text
Export
Exce
Export variables
Mechanical Energy
Quaternion arrangement
Match selection made previously
Transformation to: Pitch
$\theta = \tan^{-1} \frac{2q_0q_1 + q_2q_3}{1-2(q_1^2+q_2^2)}$
Transformation to: Roll
$\phi = \sin^{-1}(2(q_0q_2 - q_3q_1))$
Transformation to: Yaw
$\psi = \tan^{-1} \frac{(2q_0q_3 + q_1q_2)}{1-2(q_2^2+q_3^2)}$
NO
Plot Pitch
YES
NO
Plot Roll
YES
Plot orientation in Euler
NO
Plot Yaw
YES
Sensor Orientation

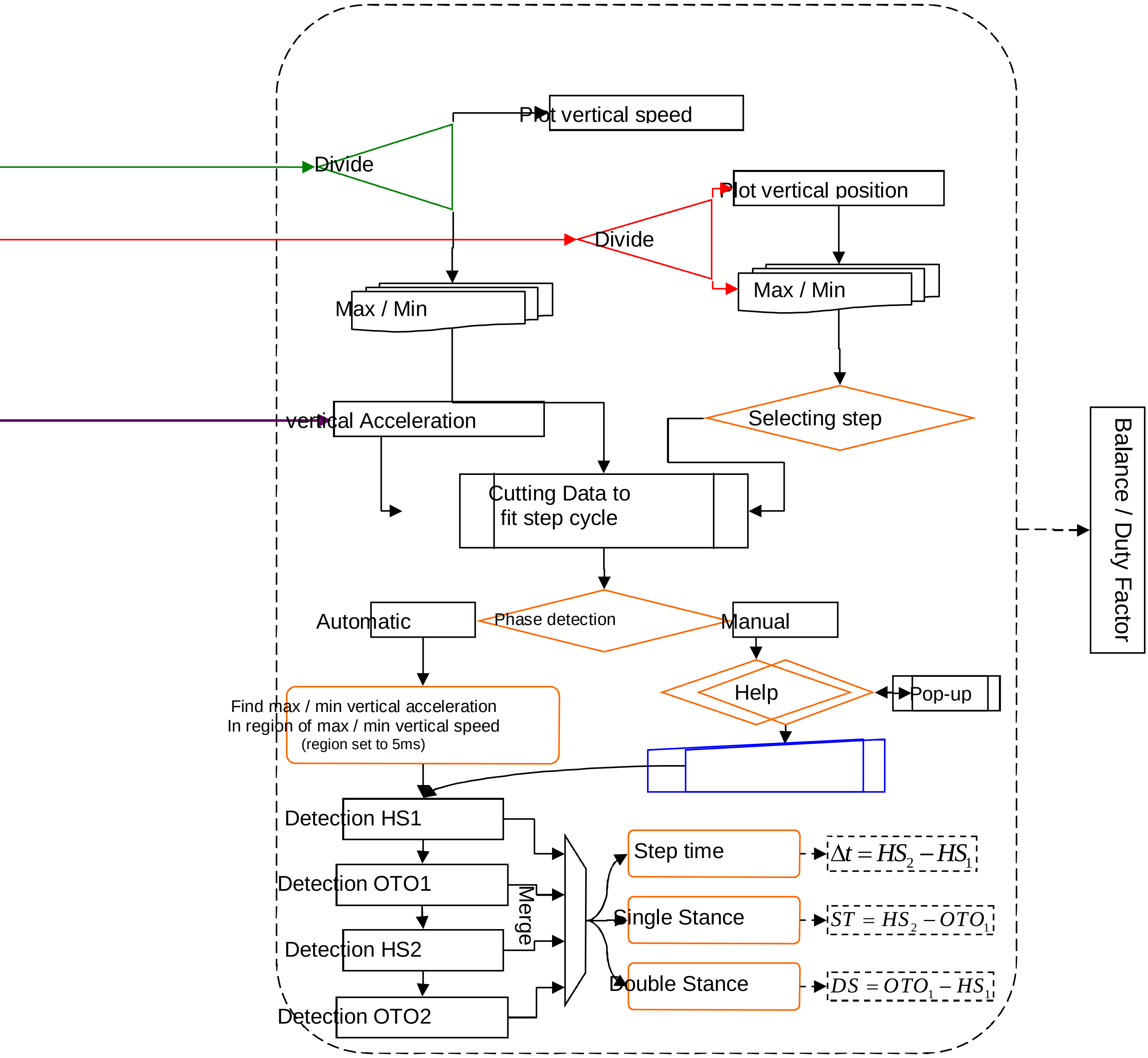

Plot vertical speed
Divide
Plot vertical position
Divide
Max / Min
Max / Min
vertical Acceleration
Selecting step
Cutting Data to
fit step cycle
Balance / Duty Factor
Automatic
Phase detection
Manual
Help
Pop-up
Find max / min vertical acceleration
In region of max / min vertical speed
(region set to 5ms)
Detection HS1
Detection OTO1
Detection HS2
Detection OTO2
Merge
Step time
Single Stance
Double Stance
$\Delta t = HS_2 - HS_1$
$ST = HS_2 - OTO_1$
$DS = OTO_1 - HS_1$

10.4.2 Output parameters

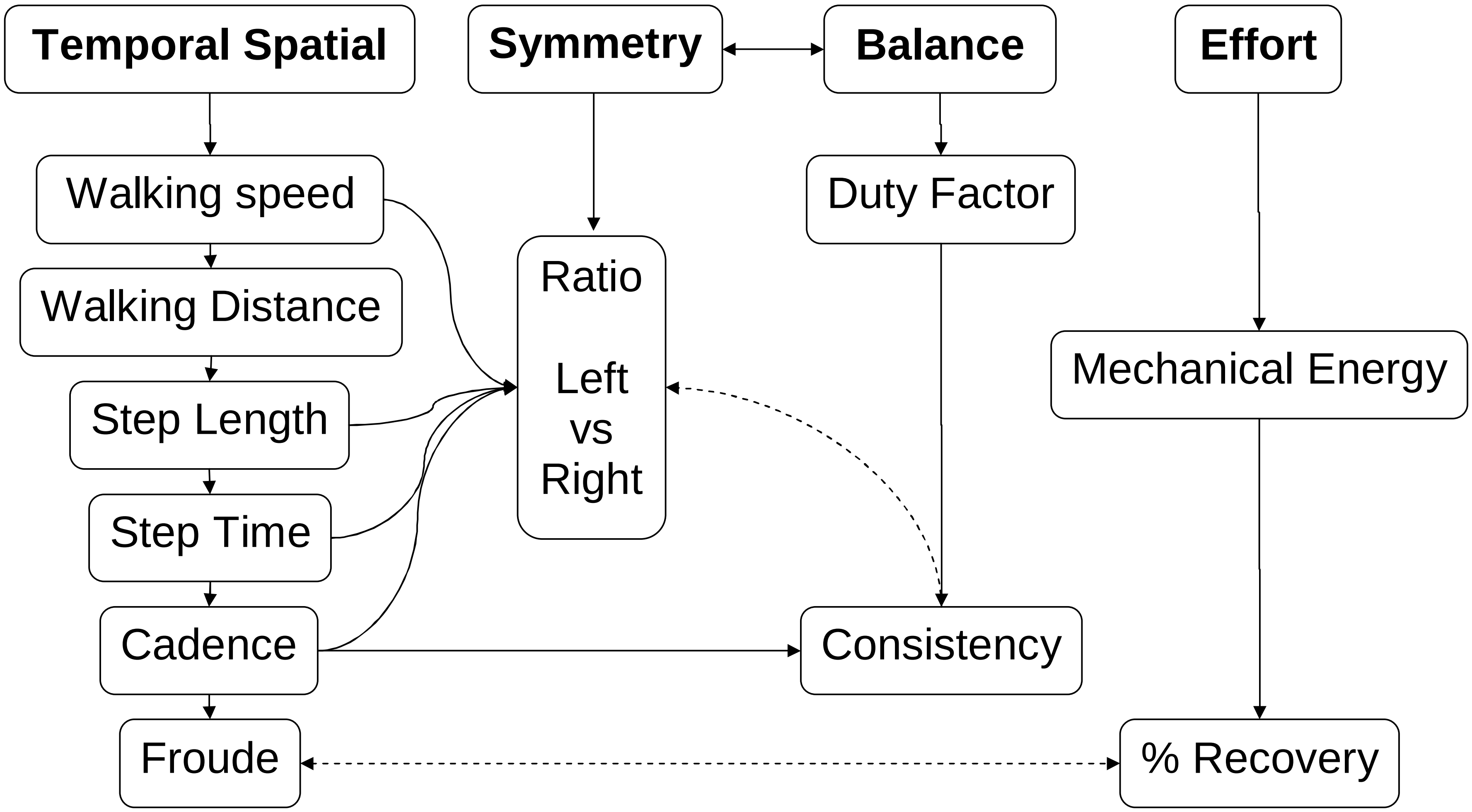

10.5 Relevant Publications

Esser P, Collett J, Dawes H, Howells K. Inertial Sensing of Centre of Mass using Quaternions. *Journal of Sports Science (abstract)* 2008;26:71 - 72.

Esser P, Dawes H, Collett J, Howells K. IMU: Inertial Sensing of Vertical CoM Movement. *Journal of Biomechanics* 2009;42(2009):1578-81.

Elsworth C, Winward C, Sackley C, Meek C, Freebody J, **Esser P**, Soundy A, Barker K, Jones DH, Minns Lowe C, Paget S, Tims M, Parnell R, Patel S, Wade D, Dawes H. Supported community Exercise in people with Long-term Neurological Conditions (long-term neurological conditions): a phase II randomised controlled trial. *Clinical Rehabilitation* IN PRESS

Esser P, Dawes H, Collett J, Howells K, Maynard K. United Kingdom patent UK0823374.4 (*Applied for*)